Cardiovascular Response to Vertebral Osteopathic Manipulative Treatment (OMT), On Asymptomatic Human Subjects

by

Chandhana Pedapati

A Thesis Presented in Partial Fulfillment
of the Requirements for the Degree
Master of Science

Approved November 2014 by the
Graduate Supervisory Committee:

Jitendran Muthuswamy, Chair
Inder Raj Makin, Mentor
David Frakes

ARIZONA STATE UNIVERSITY

December 2014

ABSTRACT

Objective: Examine cardiovascular response to OMT via central and peripheral measurements. Methods: Central and peripheral cardiovascular signals of asymptomatic human subjects were monitored during a procedure with alternating rest and active phases. Active phases included systemic perturbations and application of controlled vertebral pressure (OMT) by an experienced osteopathic physician. Pulse plethysmograph and laser Doppler flow sensors measured peripheral flow from index and middle fingers bilaterally. A three-lead EKG monitored cardiac activity. The biosignals were recorded continuously, in real time, and analyzed in time and frequency domains. Results from the control group (n=11), without OMT, and active group (n=16), with OMT, were compared. Peripheral (n=5) and central responders (n=6), subsets of the active group showing stronger peripheral or central response, were examined. In an additional effort, a modified clinical device recorded spectral Doppler ultrasound signals of the radial and dorsalis pedis arteries of clinically asymptomatic human subjects. Controlled physiologic provocations (limb occlusion and elevation), were performed. Time domain and spectral analyses were completed. Results: In the human subject study, the time wave characteristics and spectral analysis resulted in similar trends. Peripheral blood flow attenuated in the control group over time, while it was maintained in the active group, and increased specifically during OMT in the responder groups. Heart rate remained around 65 BPM in the control group, fluctuated between 64-68 BPM in the active group, and dropped 4 and 3 BPM in the peripheral and central responder groups, respectively. The effect in the OMT group was statistically significant compared to no-OMT, however, was not statistically significant within-groups. For the preliminary spectral ultrasound Doppler study, segmental flow was successfully monitored. A prototype "Quick Assessment"

tool was developed, providing instant post-processing results for clinical use. Conclusions: OMT along the vertebral column may influence autonomic processes that regulate heart rate and peripheral vascular flow.

ACKNOWLEDGMENTS

I want to thank Dr. Inder Makin for all of his efforts and support. Without his undying patience and generosity this project would not be possible. I would like to thank Dr. Deborah Heath, the PI of the project and DO who performed the osteopathic manipulative treatments.

I also want to thank Doug Mast and Dr. Curt Bay for their contributions and collaboration on post processing and statistical analysis on this project.

I would like to acknowledge A.T. Still School of Osteopathic Medicine in Mesa Arizona and Arizona State University School of Biological Health Systems and Engineering.

I want to express my gratitude to my committee members, Dr. Muthuswamy and Dr. Frakes for their support. I would like to acknowledge Laura Hawes for the support and guidance she provided throughout this process.

And finally I would like to thank my son Sanjai for cheering me on.

I am honored and humbled to have had the opportunity to work with such amazing talent. To all those mentioned and not mentioned here, I am indebted to you for your support and kindness during my journey.

TABLE OF CONTENTS

Page

Page

LIST OF TABLES

LIST OF FIGURES

Figure Page

Figure Page

Figure Page

NOMENCLATURE

ABI	Ankle Brachial Index
AM	Amplitude Modulation
ANS	Autonomic Nervous System
ATSU SOMA	Andrew Taylor Still University School of Osteopathic Medicine in Mesa, AZ
ART	Articulatory Treatment
AV	Atrioventricular Node
BPM	Beats Per Minute
BPU	Blood Perfusion Unit
DBF	Digital Blood Flow
DEC	Decrease
DO	Diplomat of Osteopathy
EDV	End Diastolic Volume
ESV	End Systolic Volume
FFT	Fast Fourier Transform
FM	Frequency Modulation
GUI	Graphical User Interface
HF	High Frequency
HVLAT	High Velocity Low Amplitude Thrust
HPF	High Pass Filter
HR	Heart Rate
HRV	Heart Rate Variability
INC	Increase
LDF	Laser Doppler Flowmeter, Laser Doppler Flowmetry
LF	Low Frequency

MV	Mean Value
mV	Millivolts
NC	No Change
OMT	Osteopathic Manipulative Treatment
PAD	Parasympathetic Nervous System
PP	Peak to Peak
PPG	Pulse-plethysmography
PSD	Power Spectral Density
PVOD	Peripheral Vascular Occlusive Disorders
RBC	Red Blood Cell
RMANOVA	Repeated Measures Analysis Of Covariance
RMS	Root Mean Square
SA	Sinoatrial Node
SDS	Suboccipital Dermatomyotomic Stimulation
SNS	Sympathetic Nervous System
TART	Tissue texture changes, Asymmetry, Restricted range of motion, Tenderness
THM	Traub-Hering-Mayer

CHAPTER 1

INTRODUCTION AND BACKGROUND

OMT and the Cardiovascular System

Osteopathic manipulative treatments (OMT) aim to improve and maintain the body's natural abilities to sustain health by balancing the autonomic regulatory processes (sympathetic and parasympathetic activity) (Henley 2008)(Tozzi 2012)(Chila 2010). Skin blood flow and cardiac activity assessments are often used as a measure of autonomic response (Foo 2009) (Grimm 2005) (Shibasaki 2009). In the present study, cardiovascular response to OMT in asymptomatic human subjects was investigated.

Motivation: OMT Function Is Not Clearly Understood

Osteopathic medicine is a well-established modern practice in the US today. Due to over a century of positive clinical outcomes and anecdotal evidence, the practice has maintained its good standing as a mainstream holistic approach to healthcare. However, physiological mechanistic changes induced by the distinct manual techniques, known as OMT, are not well understood. Demand for this understanding is growing in practicing osteopathic physicians, known as diplomats of osteopathy (DO), patients, and the scientific community more and more (Gevitz 2001). As such there is a need for good evidence-based scientific research (Johnson 2001) (Gevitz 2001) (Early 2010).

Rational For Measuring Cardiovascular Response

Irregular or impaired function is referred to as somatic dysfunction in the osteopathic medical field. Somatic dysfunction is evident in tissue texture changes, asymmetry, restricted range of motion and tenderness, or TART (Brolinson 2008).

Sites of somatic dysfunction are identified through palpation and treated with a variety of OMT methods including muscle and joint mobilization, stretching, strain and counter-strain, pressure and resistance techniques (Estrada 2010) (Brolinson 2008).

Somatic dysfunction is a result of an imbalance in the somatovisceral or viscerasomatic neural pathways, whereby an interneuron may become over excitable and negatively impact multiple systems and functions (Chila 2010). This dysfunction causes tissues to swell and leads to TART (Northop 1979). Internal pressures from swelling tissues cause circulatory vessels to be occluded, increasing systemic resistance. An increase in systemic resistance results in poor blood supply whose negative impacts are two fold; first, as lack of nutrients to the tissue and second, as buildup of metabolic waste in the tissue (Chila 2010) (Northop 1979) (Rivers 2007). This combination results in degraded tissue health that can lead to downstream functional impairments. Increased systemic resistance also leads to an increase in heart rate. As such, osteopathic medicine focuses on alleviating systemic resistance so as to "optimize blood circulation to restore and maintain health" (Brolinson 2008). Figure 1 illustrates somatic dysfunction, circulation and OMT in a block diagram. Since optimizing circulation is a focus in osteopathic philosophy, the following hypotheses were studied:

Hypothesis 1: OMT will produce a change from baseline in peripheral flow.

Hypothesis 2: OMT will produce a change from baseline in cardiac activity.

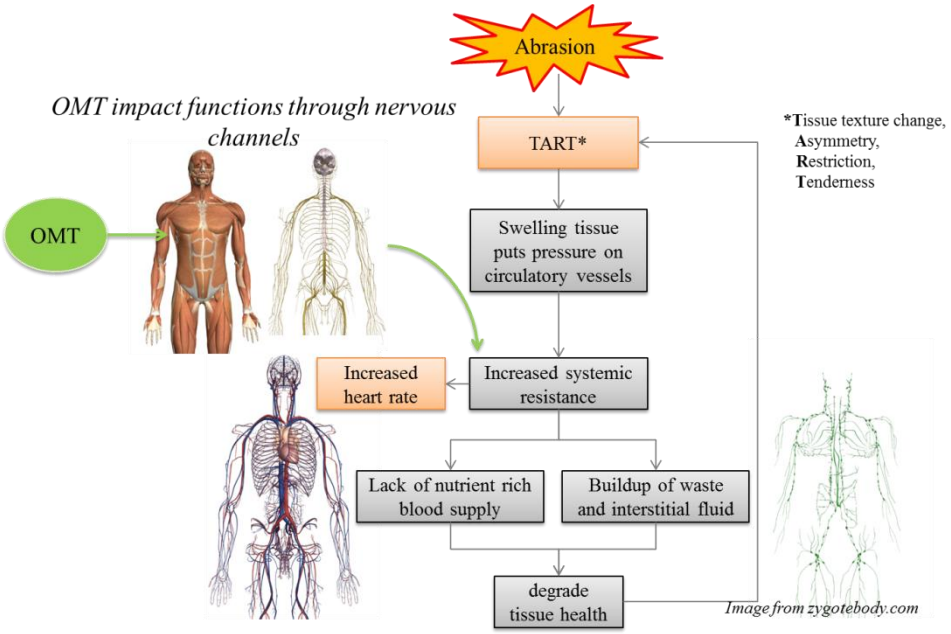

Figure 1: Somatic dysfunction, OMT and circulation

Goals

The goals of this project were as follows:

1. To establish a baseline expectation of physiologic response to OMT: This was achieved by selecting asymptomatic subjects, without tobacco or caffeine use. Also, non-invasive sensors were used to minimize interference. Furthermore, since the systems of the body are highly integrated, and autonomic and non-autonomic processes work in concert, multiple biosignals from central and peripheral perspectives were measured. Data was also acquired bilaterally.

2. To develop a reproducible and reliable test and measurement methodology for future OMT research: This was accomplished in two experiments which are described in proceeding chapters. The first was a quasi-controlled, single blind study in which the subject underwent an OMT protocol. Peripheral blood flow and cardiac activity biosignals were acquired. In the second study, a technique for measuring segmental arterial flow using spectral Doppler ultrasound was developed.

3. Develop physiologic evaluation for clinical procedure assessment: This was achieved by analyzing the biosignals in the time and frequency domain using scripts coded in Matlab.

4. Determine significance of results, if any: This was accomplished with statistical analysis.

Contributions

The contributions of this study were as follows:

- Provided quantitative subjective data to further the understanding of physiologic mechanisms and the role OMT has in it.
- Developed a nascent methodology of test and measurement for furthering osteopathic medical research at A. T. Still University, School of Osteopathic Medicine in Mesa, Arizona
- Demonstrated physiologic asymmetries bilaterally and in the upper and lower extremities.
- Demonstrated blood flow waveform characteristics that have clinical significance.

- CHAPTER 2

- LITERATURE

OMT Development

Osteopathic medicine was developed by Dr. Andrew Taylor Still (1828-1917), a physician, inventor and legislator during Civil War era America, in response to losing his three children to spinal meningitis in 1864. Still devoted his medical practice to better understand the human body as current medical practices proved insufficient. He developed an alternative philosophy to medicine centered on the musculoskeletal system and its interaction with the other body systems. He conjectured that the body's structure impacts the function and vice versa.

Still found that the "musculoskeletal system communicates with the other systems through the nervous and circulatory systems", and conversely, that "disorders reach a patient's awareness through alterations in nervous and circulatory system". Therefore, nervous and circulatory systems were thought of as the "great binders of body unity" (Northup 1979). Still stated in his autobiography that, "all diseases are mere effects, the cause being a partial or complete failure of the nerves to properly conduct the fluids of life". Therefore, homeostasis could be reestablished through precise and direct stimulation of the nervous and circulatory systems. In the 1920's, professors from the first osteopathic medical school in Kirksville, MO, summed up these novel ideas into the four core principles:

1. The body is a unit; the person a unit of body, mind and spirit.
2. The body is capable of self-regulation, self-healing, and health maintenance.
3. Structure and function are reciprocally interrelated.
4- Rational treatment is based on an understanding of the above three principles (Gevitz 2004).

Somatic Dysfunction

Somatic dysfunction, once known as osteopathic lesion, meaning "bone out of place", refers to impaired or irregular function of a system, be that skeletal or myofascial and their related vascular, lymphatic and visceral elements. Other interrelated systems in the body subsequently respond to this disturbance manifesting as pain or degrading function in other areas. A few examples of the interrelated systems response are described by Northup, "rigidity in the muscle over the right side of the abdomen when the appendix is inflamed, muscle involuntarily contracts and is rigid and painful to the touch, stomach ulcers consistently cause areas of spinal irritation just below the shoulders in the back, the radiation of pain to the right shoulder from a diseased gall bladder, and reflection of pain and disability to the left shoulder following heart disease" (Northup 1979).

Somatic dysfunction is treated with a variety of manual techniques that target the specific type of dysfunction in questions. Techniques such as articulatory treatment (ART), myofascial release techniques, lymphatic pump techniques, or Chapman's reflex points, and respiratory maneuvers, are but a few. A manual treatment is applied with the intention of stimulating autonomic nervous processes that ultimately organize efforts to reestablish homeostasis and regain circulation to the specified dysfunctional site. For example, lymphatic pump techniques stimulate "nerve centers that control the vasomotor nerves of the blood vessels in the same region as the lymph blockage" (Millard 1992). The clinician may also survey the patient during the treatment by asking the subject to rate the pain or tenderness of a site being palpated. Once circulation is restored, nutrients and interstitial fluids are also restored to the site and in time, a "release" in the tissue is felt by the DO indicating restoration.

Other signs of treatment efficacy include decreased heart rate and tenderness. In chronic patients, OMT efficacy may be transient, and heart rate often returns to its elevated state post therapy. Thus an extended period of therapy ranging from weeks to years is required to produce a lasting effect.

Anatomy and Physiology

The Nervous System

The nervous system is composed of the central nervous system (CNS) and peripheral nervous systems. These systems have somatic and autonomic nervous divisions. The somatic nervous system, also called the cerebrospinal nervous system, receives input from sensory organs and systems and controls voluntary (skeletal) muscles. The thalamus is the "relay station for the sensory pathways". The autonomic nervous system, or more aptly referred to as the visceral nervous system, controls the involuntary muscles, or smooth muscles and glands. The autonomic nervous system regulates unconscious physiologic processes such as sweating, blood pressure and heart rate. The hypothalamus organizes the autonomic, endocrine and somatic-motor processes. Somatosensory and visceral organs share neural pathways to transmit information to the CNS (Brodal 2010)

The present study is concerned with cardiovascular response, which falls under ANS regulation. The autonomic nervous system is further divided into two divisions, the sympathetic nervous system (SNS) and the parasympathetic nervous system (PNS). The SNS is concerned with mobilizing the body during situations of demand such as stress or emergencies. The PNS is concerned with daily maintenance of the body such as digestion and reproductive behaviors (Brodal 2010) (Rhodes 1996).

The figure below shows the two branches of the ANS and their respective afferent and efferent neural pathways. Most organs are regulated by both branches. The sympathetic chain is lies in the thoracic region, and the parasympathetic nerves initiate in the cervical and sacral regions of the spinal column.

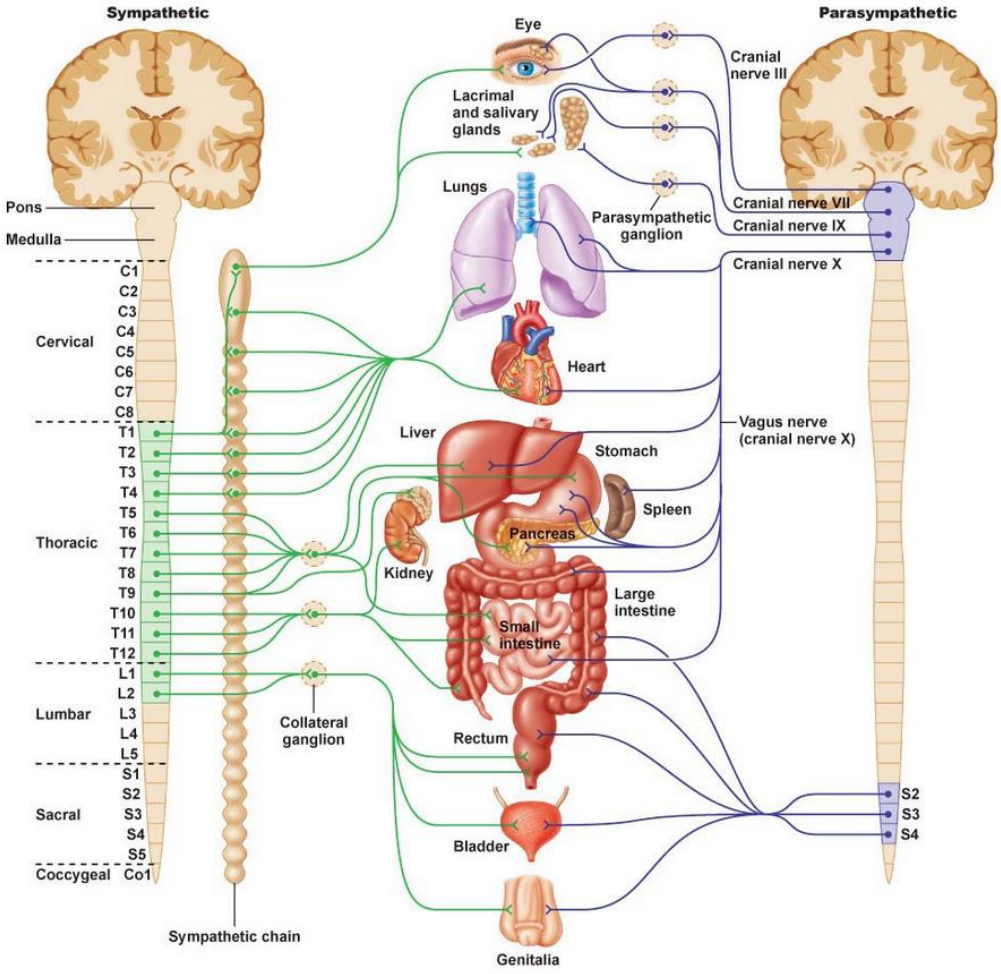

Figure 2: Autonomic Nervous System Branches

Cardiovascular Innervations

The heart is innervated by both branches of the ANS. The vagal nerve is the parasympathetic nerve. Parasympathetic innervations are found only in the

sinoatrial (SA) and atrioventricular (AV) nodes of the cardiac muscle. The denervated heart has an increase in heart rate, and therefore the PNS is the dominant autonomic function in the heart, which serves to slow heart rate (Rhodes 1996). Increased sympathetic activity at the sinoatrial node results in increased heart rate. Increased parasympathetic activity at the SA node results in decreased heart rate. Decreased heart rate allows for more ventricular filling time. Increased stretching of the ventricular wall increases strength of contraction. Therefore, the cardiac output is increased and more blood with greater pressure is output into the systemic arteries. A greater blood pulse wave results in alleviating systemic resistance issues (Rhodes 1996) (Hall 2011).

SNS innervates the endothelial cells which are continuous from the heart and throughout the vascular system. As such, vascular functions are under sympathetic control, as distribution of blood is the key function. The function of larger vessels, arteries and segmental arteries, is to transport blood. As such the vasomotion in these vessels are mainly due to blood pressure waves. The main function of the smaller vessels, capillaries and arterioles, is to regulate the distribution of blood flow. An increase in sympathetic activity in these blood vessels results in vasodilation (Kierszenbaum 2012). More details are found in the supplemental chapter in the appendix.

Key literature

Non-evidence based OMT research.

Numerous non-evidence based clinical studies provided the positive clinical outcomes that back these osteopathic philosophies. For example, Voight et al. (2011) demonstrated that the OMT therapy reduced pain and duration of migraine in

females. Other studies have shown reductions in length of hospitalization and improvements in symptoms of neonatal infants with use of OMT on gastrointestinal function (Pizzolorousso 2011) or pneumonia with use of OMT added to regular treatments (Noll 2010). However, data from these studies are based upon subjective feedback to questionnaires and non-qualitative data. Good evidence-based research is required to solidify these claims.

Evidence Based OMT Research

Invasive Techniques. Recent evidence based investigations on hematologic changes in blood and lymph have been conducted. Walkowski et al. "investigated the effect of OMT on the level of circulating metabolites and leukocytes in healthy volunteers" concluding that OMT influenced release of molecules that contribute to improved health. Rivers et al measured albumin, hematocrit, hemoglobin, platelet count, total protein, and white blood cell count and systolic and diastolic blood pressure at intervals of 20, 50 and 80 min after a 10 minute lymphatic pump technique in a group of healthy men. The results showed statistically significant platelet count reduction and increased diastolic pressure at 80min post therapy, suggesting sympathoexitetory responses. However these two studies involved invasive methods.

Cardiovascular responses. Cardiovascular responses to OMT have been previously investigated. The findings of these studies vary. Purdy et al. (1996) measured digital blood flow (DBF) as a measure of sympathetic activity. and demonstrated that suboccipital dermatomyotomic stimulation (SDS), placing of fingers in the suboccipital region bilaterally and perform slow circular kneading for 120 seconds, did alter the strain gauge plethysmograph blood flow amplitude and the height from dichroitic notch to peak, using 25 healthy subjects. A touch only

protocol, or sham, was found to induce changes in DBF as well, however, to a lesser degree compared to OMT. The study also grouped the subjects by comfort level, and found that different groups experienced different degrees of changes. The group reporting comfort during the session had the greatest improvements in DBF. The group reporting most discomfort during the session had a greater response to the sham than the OMT. The report findings suggest that both sham and OMT have influences on digital blood flow. In this study, the analysis was completed on a five cycle averaged waveform. The amplitude was interpreted as "vasomotor tone of the dermal vessels", and the height from dichroitic notch to peak was interpreted as "resistance vessel activity, where an "elevation of the dichroitic notch implies a relatively vasoconstrictive state, whereas depression suggests vasodilation.

The study suggested that there were responders and non-responders to OMT treatment. Also from this study it is apparent that subject comfort may be of importance in OMT efficacy. However, one weakness in this study may be the dataset length used in analysis. In a highly variable data set, it is possible that 5 waveforms may not be representative of the subtle changes that OMT may produce.

Karason (2001) examined digital blood flow (DBF) with laser Doppler flowmeter (LDF) .in 20 healthy males, grouped by smoker and non-smoker, in response to sham and high-velocity low-amplitude thrust (HVLAT) to the lumbosacral joint. DBF was monitored in the dorsum of the foot over the L5 dermatome. This study found that the sham treatment produced similar results as no touch. And that the HVLAT produced statistically significant increases in cutaneous blood flow in non-smokers. For the purpose of vascular and microvascular research, it is widely accepted that smoking negatively effects the compliance of arterial and pulmonary vessels. As such, Tabaco use is nominally included in the exclusion criteria. So the

use of the term asymptomatic in this study may be considered a misnomer. The results from the study also suggest that this may be true. The aim of the study was to "evaluate the short-term effects of a thorough lymphatic treatment protocol and designed to include techniques to influence sympathetic tone, the thoracic inlet, the thoracic diaphragm, and the lymphatics", the inclusion of a smoker group would serve the purpose of a symptomatic population. The interesting aspect of this study is that the subjects control session occurred a week prior to the active OMT session. The duration between rest and OMT is one to be considered.

Henley et al. (2008) examined a myofascial release technique and its effect on heart rate variability. The 17 subjects acted as their own control, and a sham procedure was also included in the protocol. The control, sham and active sessions were completed in three separate sessions. Each subject participated in each type of session, to achieve a repeated measures study. Additionally, a head-tilt was employed to induce sympathetic tone. The time series analysis used 300 seconds of continuous data, sampled from the final portion of each phase. The heart rate increased in all three sessions, and the heart rate variability suppression was demonstrated during the OMT but not in control or sham. This served as an indicator that the OMT successfully inhibited sympathoexitetory response.

On the other hand, Milnes et al. (2007) failed to support the theory that C4 technique lowers sympathetic tone as hypothesized. In this study a cranial technique was applied to C4 in ten healthy subjects. A sham procedure was also used. In addition to heart rate variability, respiration rate, galvanic skin resistance and skin temperature were monitored, yet the heart rate variability proved to be the best measure for sympathetic tone. Only the last five minutes of each phase was used in analysis. The heart rate variability data suggested increases in

parasympathetic activity and also provided evidence that there are responders and non-responders to the cranial OMT.

Challenges in OMT Research.

OMT is often investigated as though it were a drug, and treatment efficacy outcomes have shown to be as effective in reducing pain as a drug (Brolinson 2008). However, because it is not a drug, and due to complexity and interrelated systems and high degree of variability research of osteopathic manipulative treatments face challenges in adhering to the scientific method of allopathic medical research. Early et al. (2010) raised some important questions regarding the OMT research fitting the scientific research model. For one, a double blind and controlled studies is difficult to achieve logistically. The reason is simply that clinician cannot be made unaware of the treatment that is being applied.

Another method common to allopathic medical research is the placebo. In OMT research however, the placebo, or sham procedure, has proven to be a controversial topic. In a sham procedure the subject receives a non-therapeutic touch or touch only (a standardized sham procedure has not yet been established). Skin blood flow has been shown to be responsive even to light touch, gentle message or small changes in body temperature (Hisu 2012). This is especially so if the area has been exposed to a manipulative treatment prior to touch as the body has the capability of learning and adapting, thereby producing an anticipatory response (Early 2010). For these reasons sham can yield false positive results.

Another issue arises in standardization in treatment application. Some studies overcome this barrier by monitoring applied pressure at the site of OMT with strain gauges. Others have attempted position tracking techniques. However,

subject to subject variability demands varying application of pressures and symmetry of applications to achieve homeostasis (Brolinson 2008).

In addition to test methodology, measurement methodology is also not standardized. Interpretation of data, for one varies from study to study. Zeggarra, et al. (2014) reviewed hundreds of manual therapy studies in a systematic approach, where 20 articles met the criteria. Their study identified a hand full of techniques that are commonly used in OMT research. Of these many have relative units of measure. Evaluation, therefore, hinges on interpretation of waveform characteristics, and mapping that understanding to physiology and clinical outcomes. Among the studies surveyed it is evident that the mapping of outcome measures to physiologic mechanisms varies and further demonstrates that interpretation of data is not a trivial exercise.

Project Overview

In consideration of the above, the following approach was taken in this study. Central and peripheral vascular changes in response to systemic tests and OMT were studied. This was accomplished in two efforts. The first effort was a human study that used standard photon based sensors operating in the red to infrared wavelength regime to measure blood flow in the upper extremities at the arteriole and capillary level. In addition EKG to measure cardiac electrical activity. In this study an OMT protocol on asymptomatic human subjects was followed. Inclusion criteria were no history of cardiovascular disease, and no significant neuro-muscular trauma. Tobacco and caffeine use was also prohibited. Biopac DAQ systems and instrumentation, a commercially available product used in medical education and research, was used. As such, this project will hereafter be referred to as the "Biopac study".

The second effort was a technique development study. This study was conducted to develop a long-term peripheral vascular data logging capability using a sound wave based technology, namely spectral Doppler ultrasound technology. In this study the segmental arteries of the upper and lower extremities were measured were monitored during a reactivity test protocol on asymptomatic human subjects. No OMT were performed. This project will hereafter be referred to as the "spectral Doppler ultrasound study". The matrix below lists the specifications for both studies, and the figure to the right identifies the sites of bio data acquisition. The future development of this work is intended to combine the capabilities in these two studies to provide a detailed cardiovascular profile. The chapters 3 and 4 will discuss the methods and theory of the Biopac study and the spectral Doppler ultrasound study, respectively.

	STUDY 1: *"Biopac Study"* ○	STUDY 2: *"Spectral Doppler Ultrasound"* ◇
STUDY TYPE	Quasi controlled, single blind study	Technique development
NUMBER OF SESSIONS	27	5
OMT PROTOCOL	Yes	No
MEASUREMENT SITE	Upper extremity, bilateral	Upper and lower extremity, Unilateral
VASCULATURE MEASURED	Microvasculature (skin blood flow)	Segmental Artery (radial, dorsalis pedis)
NON-INVASIVE SENSOR TYPE	Fiber optic (PPG and LDF)	Spectral Doppler ultrasound
EKG	Yes	No
GROUPING	Control (n=11) Active (n=16) Peripheral Responder (n=5) Central Responder (n=6)	Radial artery (n=5) Dorsalis Pedis artery (n=5)
POST PROCESSING	Yes	Yes
STATISTICAL ANALYSIS	Yes	No

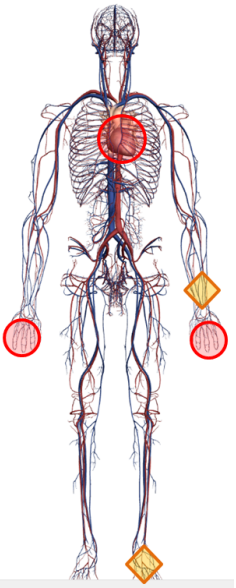

Image from zygotebody.com

Figure 3: Project Description

CHAPTER 3

METHODS AND THEORY: BIOPAC STUDY

The principal investigators of this pilot study were Dr. Deborah Heath and Dr. Inder Makin of A.T. Still University, School of Osteopathic Medicine, in Mesa Arizona (ATSU SOMA). This study was IRB approved and consent of the volunteer subjects was obtained prior to the experiment. The IRB approval form is in the appendix.

The Biopac study non-invasively monitored peripheral flow and electrical cardiac activity. Pulse plethysmography (PPG) and laser Doppler flow (LDF) sensors were used to monitor the peripheral vasculature in the upper extremity, at the finger tips, bilaterally. A three-lead EKG was used to monitor the electrical activity of the heart. Room temperature was also monitored throughout each session. In a session, a seasoned clinician administered treatments on a supine subject while a separate operator conducted the DAQ and instrumentation.

Two experimental conditions were examined, a purely baseline session, used as a control, and an active session, where OMTs were administered. In the control session the subject lay undisturbed in the supine position for approximately 1 hour. In the active session a 15 phase protocol was followed, which included two reactivity tests and 5 OMT's alternating with quiescent phases. Table 1 shows the sequence of events in active session protocol. The duration of the active session was approximately 1.5-2 hours. 36 sessions were recorded in all. Of these 27 were usable for post processing and analysis, where 11 were control sessions.

Active Session Protocol.

The active session has 15 phases including reactivity tests and OMT alternating with rest phases. The table below describes active protocol chronology with phase durations.

Table 1:
Active Session Protocol.

	Active Session Protocol [~120 min]														
Phase	1	**2**	3	**4**	5	**6***	7	**8***	9	**10***	11	**12***	13	**14***	15
Phase Name	Baseline start (Bo)	**Occlusion of left arm (Occl.)**	Quiescent Phase 1 (Q1)	**Hyperthermia Wrap of left arm (HW)**	Quiescent Phase 2 (Q2)	**Respiratory Maneuver (RM)**	Quiescent Phase 3 (Q3)	**OA-C2**	Quiescent Phase 4 (Q4)	**T1-T4**	Quiescent Phase 5 (Q5)	**T8-L2**	Quiescent Phase 6 (Q6)	**L5-S**	Baseline End (Bf)
Duration approx.. [min]	10	**<5**	10	**<5**	10	**<5**	10	**5**	10	**5**	10	**5**	10	**5**	10

'' = OMT phase*

Baseline. In the baseline phase (~ 12 minutes) the subject is allowed to rest come to rest. No provocations are performed by the clinician. The subject is encouraged not to speak or move unless to adjust for comfort. In the cases where movement did occur, the time was noted and then the noisy data was later parsed out.

Systemic Provocation. The systemic tests were occlusion and hyperthermia wrap of the left arm. The occlusion was accomplished with an inflatable cuff on the upper arm held above 60 mmHg for the duration (3.7 ± 0.3 minutes) of the phase. The circulation is should decrease in the occluded arm, while the circulation is maintained in the other arm. Post-occlusive hyperemic reaction was observed (Allen 2007) (Fullerton 2002) (Bergstrand 2009) (Roustit 2010).

The hyperthermia wrap (6.8 ± 1.9 minutes) was accomplished with an electrical heated pad wrapped around the upper arm at 38-42 degrees Celsius. This increase in temperature would induce vasodilation in the peripheral vasculature. However, during this study the wrap was not consistently effective.

OMT. OMT's used in this study were digital pressure along the vertebral column. The pressure is sustained with minimal tension at the segment until a change in tissue texture or temperature was noted. For this study, five OMTs were selected. These include one maneuver applied to the sternum and four applied to the vertebral column as follows:

Respiratory Maneuver
OA-C2
T1-T4
T8-L2
L5-S

Respiratory Maneuver (RM) (0.9 ± 0.3 minutes) was accomplished by applying light pressure on the linea alba, located just below the sternum until texture change has been noted (Heath 2011). Data from this phase was noisy, and due to the short duration usable data was very limited. For these reasons the results from this phase are not accurate.

For *OA-C2* treatment (5.8 ± 2.4 minutes), pressure was applied to the vagal nerve, which runs through a cavity in the spinus process. The largest space between the vertebrae that allows access to the vagal nerve is near the C2 vertebra. Pressure along OA-C2 stimulates the vagus nerve inducing a parasympathetic excitatory response. The expected result is a decrease in heart rate.

For the *T1-T4* treatment (8.4 ± 3.1 minutes) light pressure was applied to the vertebral column along the T1 through the T4 digits. The nerves innervated in this region include the arms, lungs, heart, and gall bladder.

For the *T8-L2* treatment (5.0 ± 2.3 minutes), light pressure was applied to the vertebral column along the T8-L2 digits. The nerves that innervate these vertebrae include the spleen, adrenal glands, kidneys, small intestine and lymph circulation.

For the *L5-S* treatment (3.6 ± 1.3 minutes), light pressure was applied to the vertebral column along the L5-S digits. The nerves innervating this region of the spinal column include those from the lower legs, ankles, feet, hip bone and buttocks.

Subject Data

A total of 20 subjects, 15 female and 5 male, between the ages of 19 and 58 with a median age of 34 were used in 36 sessions. Of the 36 sessions recorded 27 were usable, reducing the sample population to 13 female and maintaining the 5 male. A total of 11 control and 16 active sessions with durations of 1±0.2 hours and 2.1±0.3 hours respectively were included in the final analysis. Rational for omission of sessions is provided in the appendix.

Subjects were asymptomatic with no prior history of cardiovascular disease and no significant neuro-muscular trauma. Although the subjects selected for study were asymptomatic, the clinician identified somatic dysfunction. These observed dysfunctions contributed to the subject-specific responses, where some subject displayed an enhanced response, while others had a more subtle response. A group of subjects had an increase in blood flow during OMT, and were subsequently termed the peripheral responders. Another group of subjects had a decrease in heart rate during OMT, and were subsequently termed the central responders.

Instrumentation, Data Acquisition Setup and Procedure

Instrumentation and data acquisition

Biopac is a commercially available data acquisition system primarily used in medical education and clinical research applications. Central and peripheral vasculature data were recorded simultaneously using two Biopac data acquisition systems. The PPG and LDF sensors were selected to measure peripheral flow, bilaterally. The PPG and LDF sensors were fixed to the index and middle fingers respectively, on both hands. The PPG and LDF sensors were fastened to the fingers with double sided tape and Velcro to maintain sensor placement. A three-lead EKG measured the electrical activity of the heart. Conducting gel was used on the EKG leads to maintain electrode to skin contact and ensure clean signal acquisition. A room temperature sensor was fixed to the table adjacent to the subject.

Two Biopac units were used for data acquisition. One Biopac unit had the EKG and room temperature electrodes, and was configured as the master box. The second, or slave, Biopac unit had four peripheral flow sensors in the following order: Chanel1) left hand PPG, Chanel2) left hand LDF, Chanel 3) right hand PPG, and Channel 4) right hand LDF. With this setup, the operator could manually trigger the slave data logger after with the master. Also, a tagging feature used in the master would automatically apply the tag in the slave. The clinician would inform the operator the point in time a new phase began and the operator would manually apply a tag in the raw data using a Biopac software function as well as note it in a separate tracking sheet. Two '.acq' data files were produced for each session, one file per Biopac box. The master file contained the EKG and room temperature data and the slave file contained the PPG-LDF data. Tracking sheets were used during the session to record in post processing for data parsing. The tags in the software were

not available in the raw data file output. The EKG and room temperature sensors - were on the master data acquisition box on Channels 1 and 2, respectively. The PPG and LDF sensors were on a second slave data acquisition box, where Channels 1 and 3 were PPG left and right side, and Channels 2 and 4 were the LDF left and right side, respectively. The master box was configured to manually trigger the slave box. The output '.acq' files were converted to a '.mat' file for post processing in Matlab. Room temperature was also monitored throughout the session. Details on the Biopac hardware, instrumentation and software settings are documented in the appendix.

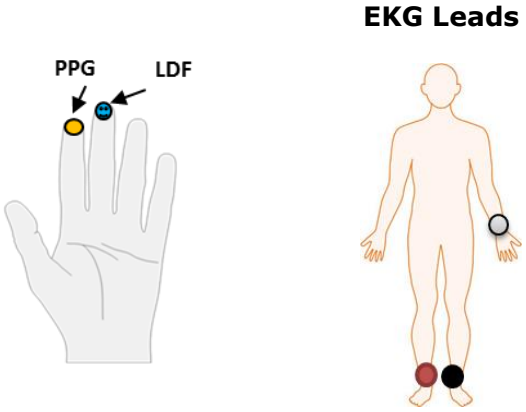

Figure 4: Sensor Locations: on both right and left hand, PPG on index figure, LDF on middle finger (left). EKG Lead placement: White on right forearm, Black on right leg, Red on left leg (right).

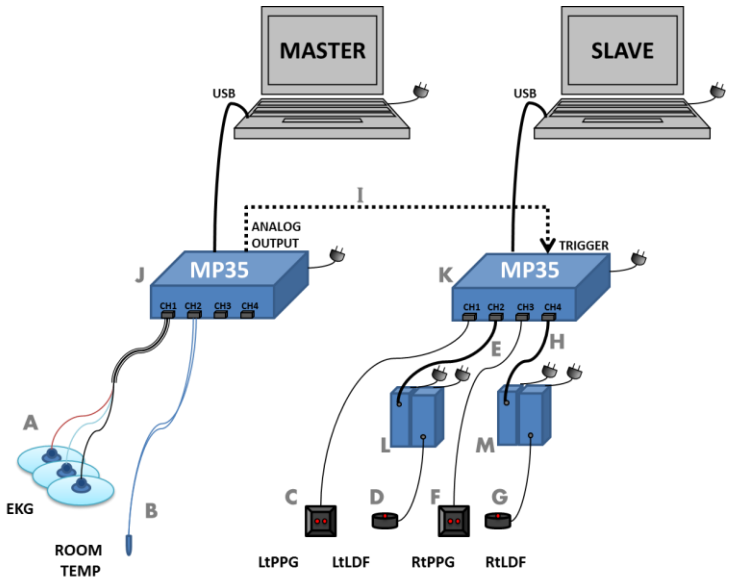

Figure 5: Biopac DAQ Connection Diagram

Procedure

Clinician's procedure. The clinician initiated and terminated the session by measuring the sitting and resting blood pressure of the subject. During the "control" session the subject lay supine and at rest. During the active session, the clinician followed the active session previously described. The clinician would ask the subject to assess the pain or tenderness at the selected site on a scale from 0 to 3, 0 being no tenderness. The clinician's aim was to reduce the rating to zero with treatment. These pain ratings were recorded both pre and post therapy. The clinician also noted the level of effort required for reducing pain rating. The clinician used these indices to later assess and classify those subjects with most improvement as clinical responders.

Operator's Procedure. A separate operator managed the instrumentation and data acquisition and, subject comfort. The sensors were calibrated, and gains adjusted per session. The available options for gain settings in the version of Biopac used were the default 5000 and 2000. The master box acquisitioning was initiated

and when the clinician was ready to start the procedure. When the master data settled to a clean signal, the operator hit a manual trigger on the master GUI to initiate the slave box acquisition. Adjustments were made to the sensor position and fastening and subject position on table to ensure optimal signal acquisition. The procedure could begin when clean signals were noted.

The operator noted change of phase using a tagging feature on the software as well as recorded the time on a separate tracking sheet. The tracking sheet was also used to record the blood pressures, room temperatures and any other notes throughout the session. At the end of the session, the data logs were saved and the subject was allowed to sit up.

Sources of Variability

Data contained a large amount of variability. For one, the vasculature of human subjects presents a large degree of variability, both from subject to subject as well as within one subject from day to day, minute to minute. Changes in blood flow and cardiac rhythms stem from physiologic adaptations to external environments such as room temperature and altitude change, to internal environments such as mental state or disease. These factors drive autonomic processes, heart rate variability, and metabolic changes. These changes can be observed in biophysical signals.

Room temperature during the study was source of variability. The room temperature within the room where the sessions took place fluctuated within 3 to 4 degrees Celsius. This could have an effect on the peripheral vasculature as it adapts to temperature changes, therefore the measurements will express this variability.

Sensor positioning and fastening were another source of variability. If the PPG or LDF sensor was fastened too loose on the finger the detected signal would be weak. Also, a loose contact between the sensor and finger might introduce other light artifacts. If the sensor was fastened too tight on the finger the vessels would be compressed, and the signal output would be distorted and noisy. During one session, the subjects hands were face down, such that the table added pressure on the sensor and finger. The signal was not usable and the session data was omitted from analysis. Thereafter, the position of the hands was standardized to be palm up, and the fastenings of the sensors were adjusted until maximum signals were obtained. Sensor position was not changed during the session, unless the sensor was displaced.

The duration of the OMT was another variable. Early on in the program, the sessions had shorter duration OMTs. The resulting raw data had a similar result as the control sessions, showing a decaying trend. Subsequently, the clinician increased the duration and intensity of the treatment to increase the effect of OMT. These sessions were termed "long duration" sessions. The short duration sessions were excluded from final analysis.

The duration of the manipulations during the long duration sessions was also variable OMT application is subject specific. The standardization factor in this study was the subject feedback of tenderness rating (0-no tenderness, to 3-maximum tenderness) before and after treatment. Subject perception of tenderness is subjective and not quantitative.

Subject comfort was suggested by Purdy et al. (1996) as a variable in OMT efficacy. During the control sessions the subject discomfort and movement was minimal, but during the active sessions the subject tended to readjust for comfort

more as a result of the interaction with the clinician. A blanket was provided per subject request. Pillows for under the head and knees were also provided to assist in a more relaxed posture. Because the table was narrow, arm rests used to ensure a relaxed position of arms naturally and slightly away from the body, without the arms falling off of the table. Without the boards the subject would need to expend effort holding the arms close to the body. Even this amount of effort from the subject could lead to distortion and possible false positives. It is important that the subject is made comfortable prior to beginning any readings, as any major postural changes would result in increased circulation. Subject 26 is an example of this. Towards the end of the session the subject requested a pillow for the under the knees which resulted in increased blood flow in the upper extremities as well as changes in heart rate. This portion of the session had to be parsed out from the processed data.

The subjects' state of mind, i.e. stress and anxiety levels, is another source of variability which was not accounted for. The state of mind of the subject may influence autonomic processes that regulate blood distribution (Bordal 2010). This variable was not monitored, measured or controlled.

Validation of Raw Data

Pulsatile Waveform

The raw data from the PPG, LDF and EKG signals were validated. The blood flow waveforms are pulsatile in nature based upon cardiac activity and vasomotion, displaying systolic and diastolic peaks and dichroitic notch (Allen 2007) (Bergstrand 2009) (Chu 2009) (Nitzan 1998). The raw data from the PPG and LDF signals displayed this characteristic. Figure 6 below is an excerpt of the raw data from Biopac, PPG (trace 1 and 3) and LDF (trace 2 and 4), of the session with Subject 5. The waveform from both sensors have the pulsatile nature of the cardiac rhythm, and furthermore shows a slow wave, or varying low frequency baseline that may be attributed to respiration, sympathetic nervous system activity and thermal regulation (Allen 2007).

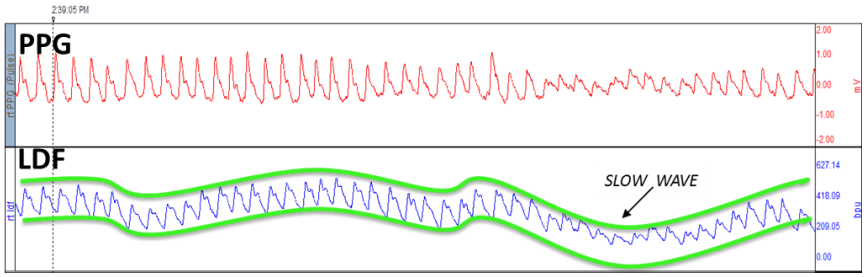

Figure 6: **Peripheral Flow Raw Data**: blood flow data from Biopac DAQ of Subject 17 session shows pulsatile behavior of volume (PPG) and flow (LDF) signals, as seen in the cardiac pulse. The slow wave in LDF signal is due to a DC shift caused by variations in sinoatrial node depolarization. The PPG signal does not have this slow wave due to a high pass filter in the software.

Post-Occlusive Reactive Hyperemia.

A post occlusive reactive hyperemic response was seen in all of the subjects. During occlusion the blood flow signals flatten out, indicating reduced flow and blood volume. During this time of zero blood flow, metabolic waste builds up in the tissue including vasodilators, which decreases systemic resistance. After the pressure in

the cuff is released there is a transient surge of blood flow due to lowered systemic resistance (Rhodes 1996). At the same time there was an observed decrease in flow in the right hand, indicating regulatory mechanisms maintaining equilibrium in systemic circulation. The figure below shows the release of occlusion the left arm followed by a reactive hyperemic response, shown by an immediate increase in signals. This agrees with literature suggesting an appropriate systemic response of the subject as well as data acquisition system (Freccero 2003) (Eun 1995) (Knotzer 2007).

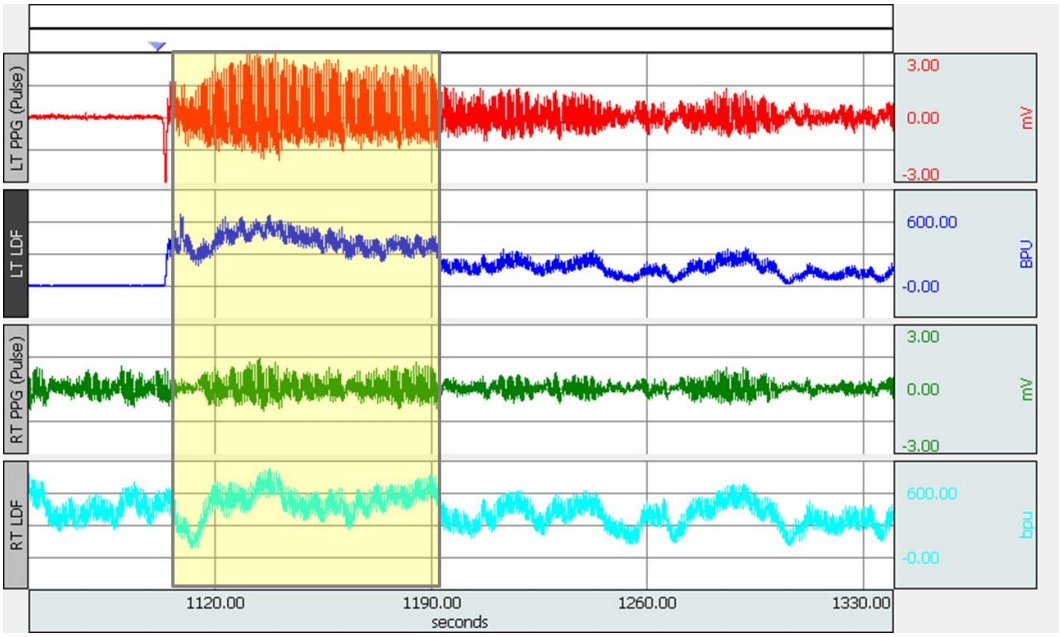

Figure 7: Post-Occlusive Reactive Hyperemia

Bilateral measurements

In this study bilateral measurements were taken from the upper extremities. During occlusive and hyperthermia wrap of the left arm phases we were able to verify that the data acquisition system was operating appropriately. Bilateral differences observed in the peripheral blood signals are agree with literature, Allen (2007), Asymmetry of the body is well documented in literature, for example, metabolism of dominant arm during drug uptake and corresponding contralateral side of the brain (Simonsen 2008) (Korf 1980), neurochemical bilateralism, nerve innervation, and cerebral bilaterality, and local vascular and lymphatic circulation asymmetries. Bilateral measurements are clinically significant in diagnosing peripheral vascular occlusive disorders (PVOD), (Chang 2001).

The sensors were switched to the opposite hands to ensure that no bias was present. Subjects 05 and 16 are examples of sessions where the sensors were switched. The data shows that in swapped and non-swapped sessions the right hand data had greater magnitudes than the left hand. The system test for this validation effort is found in the appendix.

Posture change

Another observation that validated the raw data was the increase in upper extremity blood flow after the legs were elevated. A lower extremity posture change should lead to a decreased peripheral flow the lower extremities. This results in upper extremity blood flow increase to maintain balanced systemic pressure. To facilitate the investigation of the reflex responses, a change in posture is regarded as one of the commonly used convenient tests (Foo 2009). In the Figure 5 subject 26 changed the posture of the lower extremities resulting in an increased peripheral blood volume and flow to the upper extremities, both right and left side.

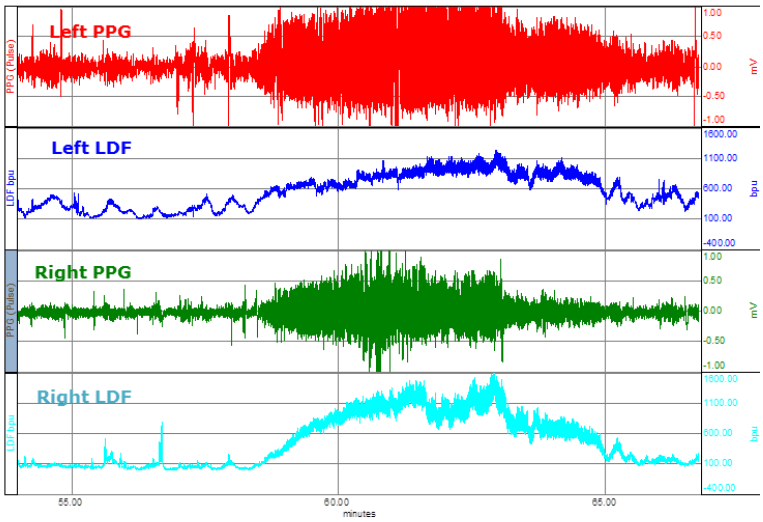

Figure 8: Posture Change. Subject 26 blood flow increased in upper extremity due at 58min when supine subject raised legs and placed a pillow under knees for support and added comfort.

Simulation

Simulation of the PPG and LDF blood flow waveforms in Matlab were completed in order to better understand the components of the signals. Three sinusoids were summed to simulate the signals:

Figure 9 shows the results of the PPG and LDF simulation. The top plot shows the simple summation of three sinusoids to obtain the PPG and LDF waveforms. The PPG signal had a high pass filter (HPF) at 0.5 Hz. As such the DC shift and slow wave components were absent for the waveform. The LDF signal did have these components. This simulation is shown in the Figure 9 (a). Figure 9 (b) and (c) shows the PPG and LDF waveforms, respectively, with added random noise. The resultant power spectral density estimation (PSD) is shown below the simulated noisy waveform. These figures are compared to the raw data waveforms and their respective PSD estimation on the right. In the PPG signal the peaks at 1 and 2 Hz are seen. In the LDF signal the peaks a DC component and peaks at 0.1, 1 and 2 Hz are seen.

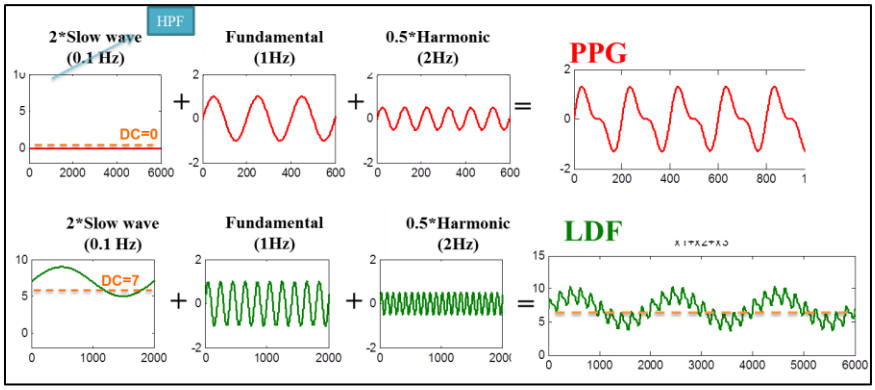

(a)

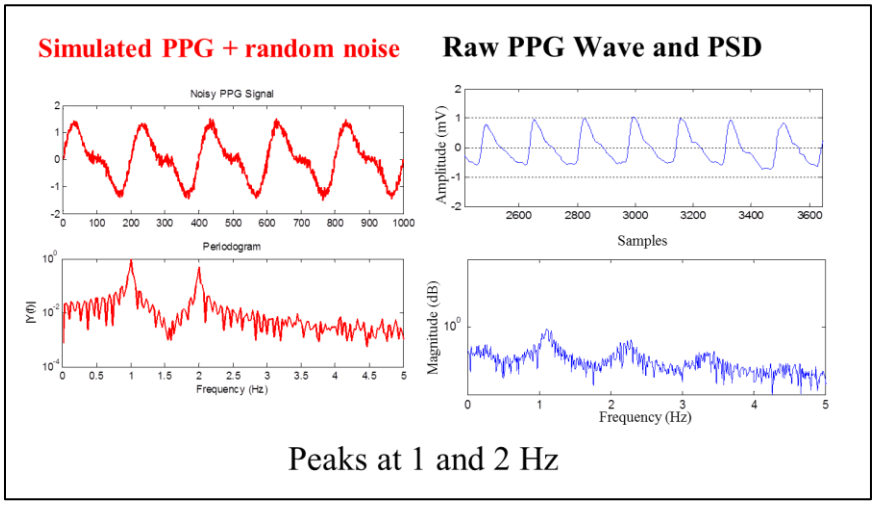

(b)

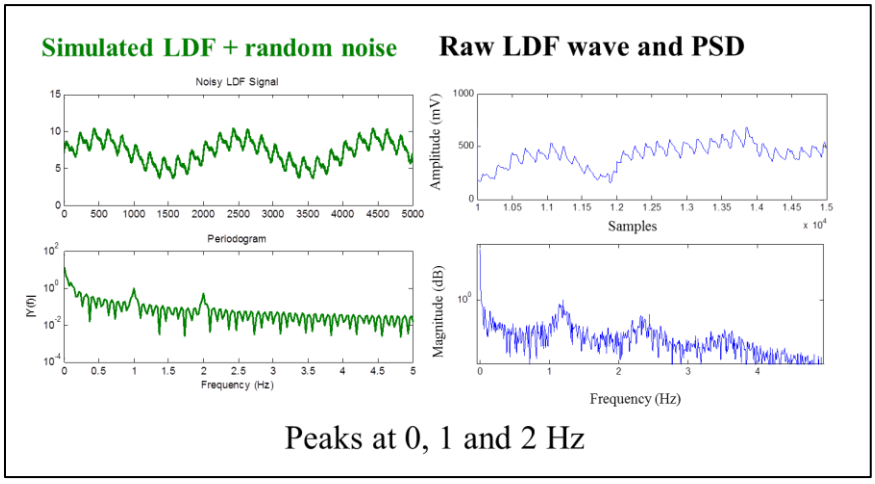

(c)

Figure 9: PPG and LDF simulation

Pulse Plethysmograph

Sensor Introduction and Applications

The plethysmography technology has been in use in the medical field for over 80 years. The PPG is a non-invasive sensor that is attached to a thin area of the body such as the ear, fingertip or toe to measure skin blood flow.

Because it is customizable to many applications, the PPG sensor is used to monitor a variety of biophysical signals. Applications range from monitoring air volume in lungs, to blood flow in organs such as kidneys, genitals, and cerebrum, and oxygen saturation of blood. Anything that may affect peripheral blood flow can be monitored by the PPG sensor. Respiration, for example, can be monitored. Since respiration acts as a cardiac pump, a decrease in respiratory rate results in a decrease in cardiac volume, leading to a decrease in peripheral flow.

The PPG sensor is also used during surgery to monitor anesthesia depth. If a patient has a response to an incision the PPG will shows as an increase in amplitude indicating sympathetic response to the pain. A pulse oximeter monitors the oxygen saturation in blood at the fingertip by using a specific wavelength that is absorbed by hemoglobin, a protein that carries oxygen in blood (Shelley 2007). The features on a PPG waveform can be used in diagnostics. A study in 1940 compared the crest time from the peak of a PPG waveform normalized to the heart rate with normal and hypertensive subjects. The hypertensive subjects showed an increase in crest time (Allen 2007) (Foo 2009). Recent interests have turned to using the PPG to monitor sympathetic activity via hemodynamic responses. Sleep apnea causes sympathetic vasoconstriction responses which increase blood pressure during sleep. The PPG waveforms are used to assess ANS reflex response (Foo 2009).

The advantage of using the PPG sensor is that it is versatile, low cost, non-invasive and is suitable for long-term measurements. The photo pulse plethysmograph used in this study measures blood volume changes in the microvascular bed.

PPG Sensor Operation

The PPG sensor is composed of photo emitter and a photo detector. It uses infrared light to illuminate the skin and the detector to catch the reflected light off of the blood vessel wall. Depending on the application, a specified wavelength, within the red and near infrared light range is used. The wavelength of the light emitted is generally between 600 and 700, or the near red region because skin pigments, oxyhemoglobin, hemoglobin and bilirubin minimally absorb the light, and optical density of skin due to erythema is negligible (Kamal 1989). Green light at around 800 nm has been used to reduce the penetration depth (Bergstrand 2009).

Because there is no calibration procedure available to standardize the PPG voltage reading between subjects the signal can only have a relative unit, where "the value of the plethysmography comes from an analysis over time, as opposed to an absolute number" (Shelley 2007). As such sensor provides a signal where the absolute value is not known (Kamal 1989) (Shelley 2007).

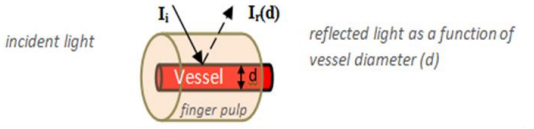

Modified Beer-Lambert Law

$$A = \alpha \times \Delta V \quad (1)$$

A = Absorption
α = absorption coefficient of blood
ΔV = volume of blood

Figure 10: PPG diagram and equations

Penetration Depth. Light is absorbed by water, the major component of the tissue, and transmitted, reflected, and back scattered by the vascular structures in the finger pulp Bergstrand et al demonstrated that the penetration depth of the PPG light source depends upon the wavelength of the light source and the distance between the light source and the photo detector (Bergstrand 2009) (Allen 2007). A green light wave length of 560 nm will provide a measurement depth of 2 mm with a 5 mm distance from the photo detector, and a near-infra red light at 810 nm can provide a deeper measurement depth at approximately 8 to 20 mm with a distance of 5 and 10 mm from the photo detector respectively (Bergstrand 2009). Roberts reports of a study conducted in 1979 by Challenor "who compared outputs operating at 805 and 650 nm and found their outputs to be substantially the same" (Roberts 1982). Per the Biopac documentation, the PPG sensor TSD200 measures changes in the blood volume in the capillary bed.

Configurations. There are two main configurations, the transmitted and reflectance PPG sensor. In the transmitted configuration the finger is placed between the emitter and detector and the light transmitted through the tissue is detected. The transmitted light is measured so that the peak light transmitted is at diastole when blood volume is low. The resulting signal is usually inverted so that systole is the peak, and diastole is the minimum. In the reflectance configuration the emitter and detector are adjacent and placed on the same side of the finger. The reflected, or back scattered, light is detected. The resulting signal shows the systolic peak as the maximum intensity and diastole is the minimum intensity. The PPG sensor would also detect prominent levels of venous return (Shelley 2007) (Nitzan1989) (Kamal) Pulse pressure is attenuated as it propagate from the heart to the systemic vessels. But the cardiac rhythms due to heart rate and heart rate variability are present in the flow and are captured in the PPG signal. Roberts states

that transmitted PPG sensors contain more artifacts due to sensor detector and emitter alignment and fastening, and increased artifact light sources detected. This project uses a reflectance PPG.

Waveform. Steady blood flow appears as a constant volume. When blood pulses through the arteriole and capillary beds, the vessels dilate and tissue blood volume increases and the intensity of reflected light increases (Allen 2007) (Nitzan 1998). Similarly, when the pulse diminishes the vessel constricts and there is less tissue blood volume, and more light is absorbed into the tissue back, resulting in a decreased reflected light intensity. The light intensity is then converted to a voltage. Nijboer et al. (1981) found that the relationship between light intensity detected and voltage produced by it are not linear. They also reported that the light emitted by the reflectance sensor was stronger compared to the transmittance.

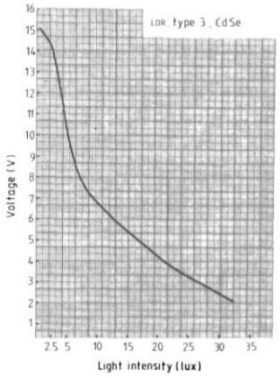

Figure 11: PPG sensor Light intensity vs. voltage relationship (Nijboer 1981)

PPG Raw Data and Time Characterization.

The PPG waveform represents the cardiac cycle showing systole, diastole and dichroitic notch. In a compliant vessel, pulsing waves of blood distend the vessel walls. The endothelial cells lining the vessel walls also respond to this stretching. When a vessel wall is stretched, the endothelial cells also stretch causing increased depolarization. As the membrane rate of depolarization increases, the amount of constriction increases. This response to vessel wall stretching is also known as myogenic activity (Rhodes 1996). Autonomic activity also regulates vasomotion, by shunting capillary vessels diverting blood to and from neighboring tissues and organs upon demand. The PPG sensor measures these changes in vessel wall distention.

The PPG waveform has an AC component and a DC component (Kamal 1989). These components are caused by the cardiac pulse pressure and changes vascular resistance (Allen 2007). The DC component represents the non-pulsing arterial blood and venous blood, and the AC component represents the pulsing arterial flow (Abdollahi, 2013). The DC component therefore represents the resting tone of the vessel wall, and the AC component represents the changes in vessel diameter due to pulsing fluid.

The PPG waveform is often used as a measure of blood volume based upon the rational that as the amount of blood in the tissue increases PPG signal increases. However, in this project, the PPG waveform only shows the AC component, the pulse pressure changes. The DC component, or the mean value (MV), was removed by the high pass filter (HPR) in the software. As such, the PPG signal does not provide a complete measure of blood volume. To have an increase in blood volume over time, both area and blood velocity must increase.

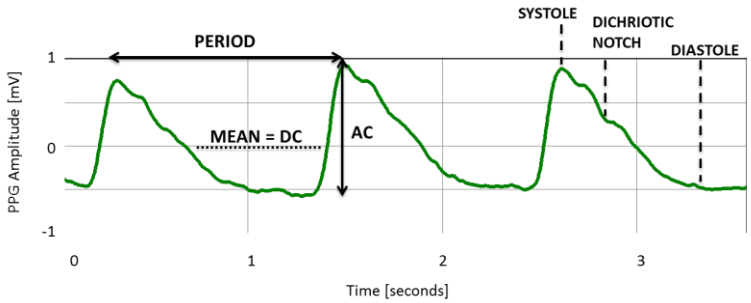

Figure 12: PPG waveform from the Biopac DAQ

The signal strength varies from subject to subject mainly due to varying physiologies; as such the gain was adjusted in the software per subject to produce a yield an optimal signal without clipping or data loss. A high pass filter was applied in the software at approximately 0.5 Hz. Due to the high pass filter the DC component was filtered out and waveform shows as distributed about an approximate zero mean. Vasomotion, provide by AC and DC components, are the low frequency components in the spectral domain, and are mediated by sympathetic activity (Nitzan 1998) (Allen 2007) (Shelley 2007) (Kamal 1989) (Foo 2009). Low frequency range is 0.04-0.4 Hz and higher frequency ranges from 0.5-2Hz. The period of the PPG signal represents the cardiac cycle and is used as a measure of heart rate (Nitzan 1998) (Allen 2007). The PPG waveform was characterized with three estimators. These were the peak-to-peak value (PP) or AC component, the root mean square (RMS) value providing the average diameter over a cardiac pulse, and the mean value (MV) or DC component, which was approximately zero due validating the effect of the HPF.

Laser Doppler Flowmeter

LDF Introduction and Applications

The LDF sensor is a non-invasive fiber optic sensor that measures blood flow over time. The LDF sensor emerged in early 1970's, and was first used to measure blood flow of retinal vessels in rabbits. Shortly after its use was extended to human skin blood flow (EUN 1995) (Humeau 2010). Because of its low cost, non-invasive method of monitoring microvascular blood flow the LDF sensor is used in many fields and applications. It is used extensively in the field of dermatology for determining pathologies of the microvessels such as diabetes or Raynaud's phenomenon, to pharmacological research measuring effects of vasodilators (Eun 1995)(Humeau 2010). It is also used in therapeutic applications such as diabetes therapy, plastic surgery. It is also used in many tissues aside from epidermis, such as studying ischemia in brain, liver and kidney tissues (Bergstrand 2009) (Fredriksson 2009). Esen et al. describes how the LDF output is also used for examining responsiveness of blood flow control mechanisms to understand endothelial function and dysfunction, for vascular disease diagnosis and prediction (Esen 2009). The sensor can be placed on the ear, forearm, finger and toe, each providing a slightly different waveform. (Roustit 2010) (Allen 2007). In this project, the LDF measurements are taken from the middle fingers of the right and left hand.

LDF Sensor Operation

The laser Doppler flow meter is comprised of a helium-neon light source and two fiber optic cables, one that delivers light, and one that detects light, measuring cutaneous blood flow (Eun 1995) (Fredricksson 2009)(Kvernmo 1999). A signal conditioner is connected to the sensor band pass filtering the signal prior to output.

For the moor instruments LDF sensor the cut off angular frequencies are generally 20 Hz to 3-22 KHz depending on the laser wavelength and blood cell speeds (Moor Instruments). The LDF sensor uses a specific wavelength of light to illuminate the skin, and detect the change in the wavelength reflected back to determine changes in blood flow. Compared to the PPG sensor where the vasomotion contributes to the signal output, the LDF sensor output is yielded from the blood cells movement only (Fredriksson 2009).

The LDF sensor uses the Doppler shift of the red blood cells to determine velocity of blood in the capillary bed. LDF provides a measurement of blood flow by detecting the first power spectral moment of the reflected light containing the Doppler-shifted content. The backscattered light detected by the photodiode is amplified and processed resulting in an analog output signal in millivolts [mV]. The output, however, is expressed as relative unit called blood perfusion unit [BPU], where 1 BPU is a "pre-defined electrical signal in mV" (Knotzer 2007). The LDF output plots the Doppler shift as a perfusion measurement. This shift is mathematically a change in position over time, which gives a measure of velocity. The greater the velocity of the RBC the greater the Doppler shift, therefore showing an increased signal.

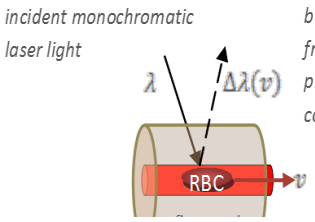

$$BPU = v_{RBC} \times c_{RBC} \qquad (2)$$

$$v_{RBC} = \frac{k f_D}{\cos\theta}, \quad f_D = f_t - f_r$$

Figure 13: LDF Diagram and Equations

Penetration Depth. The penetration depth is dependent on the optical properties of the tissue and the probe geometry (Fullerton 2002). From subject to subject, the vasculature within the sampling volume varies in "size, function, tension, tonicity and microanatomical orientation relative to the incident and reflected laser light" (Fullerton 2002), and the skin varies in thickness and pigmentation (Freccero 2003) and effect the interaction with the light. Light wavelengths of the LDF probe range from green light to near infrared light, 540nm to 780nm, and shallow to deep, respectively (Fredriksson 2009), where near infrared lights are found more prevalently in modern LDF sensors. With the above factors considered, the sample size depth can range from 0.25-1.5 mm, where the blood flow values represent the flow in the capillaries and smaller vessels (Fullerton 2002) (Fredricksson 2009) (Knotzer 2007).

Configurations: The LDF is used as a fiber optic device. A modification of the LDF sensor is found in scanners, or perfusion imagers (Bergstrand 2009), where the moving mirrors are used in place of fiber optics (Eun 1995), creating a two dimensional flow map (Fullerton 2002).

Waveform. Steady blood flow appears as a constant velocity. When blood pulses through the arteriole and capillary beds the red blood cells (RBC) accelerate. The detected shifted frequency of the RBC therefore increases. Similarly, when the pulse diminishes the RBC decelerates, the shift is smaller and the light intensity decreases. The light intensity is converted to a voltage output. The voltage is related to velocity using the Doppler shift equation.

LDF raw data and time characterization

The LDF waveform shows the pulsatile cardiac cycle as the change in RBC velocity over time. In a vessel with non-compliant walls, the change in blood velocity would be due to blood pressure from ventricular contractions. An increase in heart rate would allow less time for ventricular filling and therefore require a weaker ventricular contraction would eject that smaller amount of blood into the systemic arteries. A decreased heart rate would allow more time for ventricular filling and produce a stronger contraction in order to eject the greater amount of fluid into the systemic arteries. The resulting blood pressures would cause a wave to propagate through the vessels, thus altering the RBC velocity. The RBC velocity is also influenced by the frictional resistance between the RBC and vessel wall. As the wall constricts friction increases causing the blood flow to slow. A dilated vessel would decrease resistance by increase the cross-sectional area for blood to flow freely. The LDF signal provides a measure of the changes in RBC velocity over time.

The LDF waveform has an AC component and a DC component. The AC component is the amplitude of the wave, measured as a PP value. The DC component is the shift above zero mean, measured as a MV. The average value of a pulsatile signal can best be determined by the RMS value. The LDF RMS measure provides average velocity of the RBC. The PP, MV and RMS values were measured for each cardiac cycle.

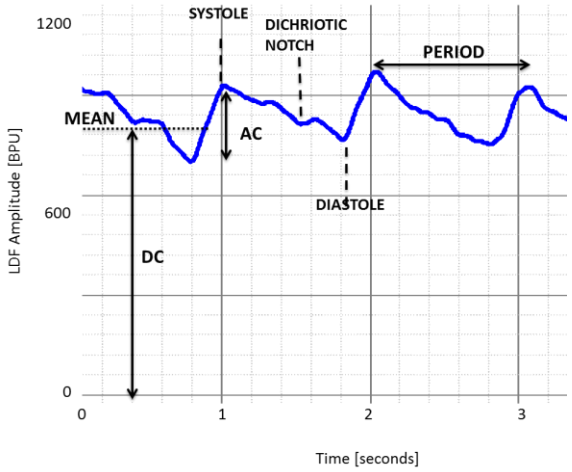

Figure 14: LDF Waveform from Biopac DAQ

Frequency Components of PPG and LDF Signals

The dc component relates to the gross amount of blood pooling in the tissue (Kamal 1989). The ac components of the signals are from 0.01-6Hz.Sympathetic activity is related to components from 0.01-0.5 Hz. Murthy et. al. (2001) describes spectral analysis techniques which identify atrial flutter as components at 0.6 and 0.8 Hz corresponding to two and three flutter waves. Post MI subjects showed frequencies between 0.2 and 0.3 Hz corresponding to loss of "sympathetic pacing of the heart". Lower frequency components, below 0.1 Hz of the PPG signal correspond to physiologic activity: myogenic, neurogenic and endothelial, related metabolic activities correspond to intervals 0.052–0.145 Hz, 0.021–0.052 Hz, 0.0095–0.021 Hz respectively (Humeau 2004) (Bracic 1999). These low frequency spectra were not analyzed in this project

The modulated heart rate is found between 0.5-2Hz. A normal heart rate is between 55-70 BPM, corresponding to peaks at 0.9-1.17 Hz, respectively (Murthy 2001) (Humeau 2004) (Kamal 1989). The heart rate is modulated by the sympathetic components found below 0.5 Hz. The sidebands found around the heart rate, or carrier frequency, occur as those below 0.5 Hz. The amplitude modulation of the heart rate is due to variation in systemic resistance. The frequency modulation of the heart rate is due to the variation in sympathetic activity in the myocardium, due to vagal response or respiration, for example. A Traub-Hering-Mayer (THM) frequency produced by the ANS at 0.1 Hz is produced both at the SA node and by the vascular tree to push blood through. The SA node 0.1 Hz component is due to parasympathetic activity, and FM modulates the HR. The vasculature 0.1Hz component is produced by sympathetic activity and AM modulates the HR. This is seen in the time wave as a dichroitic notch. An amplitude modulated carrier frequency has a spectrum with a large carrier frequency and lower magnitude sidebands. A frequency modulated carrier frequency has a greater magnitude sidebands, and lower magnitude carrier frequency. Similarly, heart rate variability (HRV) is inversely related to heart rate. The HRV is a result of SA node activity. The HRV therefore FM modulates the HR. When HRV increases, HR decreases. And if HR increases, HRV decreases. HRV is more and more being used as indicator of cardiovascular health. Decreases in HRV predict mortality following myocardial infarction. Changes in HRV are found in diseases ranging from congestive heart failure to diabetes to depression (Heitmann 2011).

Higher frequency components, greater than 2 Hz correspond to harmonics (Kamal 1989). Kamal et. al. describes the fate of the harmonics from heart to capillary bed. In the aorta harmonic components spread up to the up to the 20th harmonic. Blood pressure and flow attenuate as blood travels away from the heart. The number of harmonics increases as blood flows away from the heart. The higher harmonics, above 3 Hz, are attenuated by the precapillary sphincter. At the site of the PPG sensor, the fundamental was attenuated, the harmonics were amplified, and the higher harmonics were filtered. The harmonics do not have a clinical significance.

Electrocardiography

EKG Introduction and applications

Electrocardiography (ECG or EKG for the German term elektrokardiogramm), is a non-invasive method of measuring electrical activity of the heart. The electrical activity from a depolarizing cardiac muscle is a dominant and pervasive signal that can be detected in many ways, including as electrical activity on the skin. Three electrodes, a positive, negative and ground, placed on an area of the body will detect the electrical activity central to that site. When the three leads are placed on the extremities of the body the central activity that is detected is the sinoatrial depolarization.

A twelve lead EKG is used in clinical diagnostics. The three-lead EKG is not useful for diagnostic purposes, but was sufficient for the purpose of this study, which was to obtain heart rate and heart rate variability.

EKG Raw Data and Time Characterization

The raw EKG data clearly shows the QRS complex, describing electrical depolarization and repolarization of ventricles. The greatest electrical activity occurs at ventricle depolarization (between R and S), where contraction of muscle ejects blood into the systemic arteries. The interval between subsequent R waves, called the inter-beat interval or RR interval, was used to calculate heart rate:

$$HR = \frac{60}{RR} = \frac{sec*min^{-1}}{\text{sec}*beat^{-1}} = \frac{beat}{min} = [bpm] \quad (3)$$

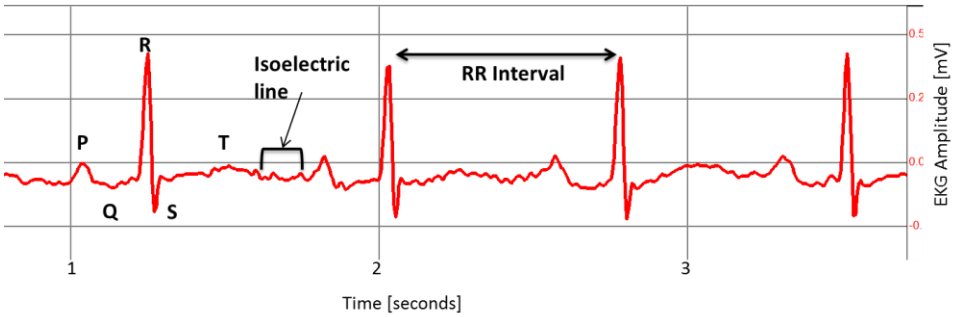

Figure 15: EKG output from Biopac DAQ

Post Processing

Data Parsing

One hundred seconds of clean data were parsed out from each phase. Ideally the data was taken in ten second sections evenly spread throughout the phase. The data was processed in ten second patches at a time.

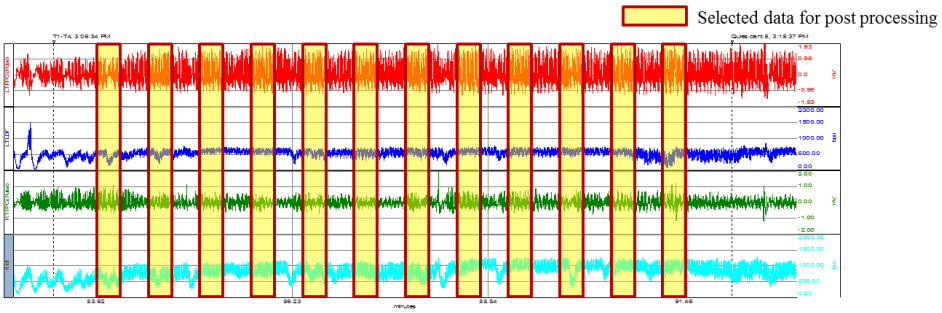

Figure 16: Data Parsed from PPG and LDF data.

Time Domain Analysis

PPG and LDF. For the PPG and LDF data each cardiac cycle was isolated and characterized individually. A peak detector was developed to isolate each cardiac cycle. The peak detector was customized for each subject based upon their resting heart rate. The peaks were used to identify an average time step, or heart rate, within the ten second patch of data. The data was stepped through using this calculated average cycle time. The time characteristics were calculated for each cardiac cycle. The mean estimator was calculated for each phase. And a cumulative estimator was calculated with all trials.

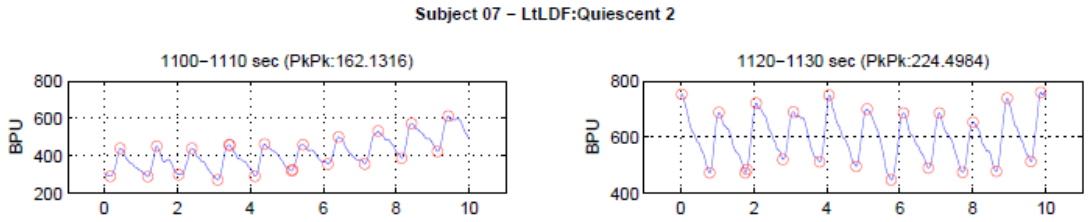

Figure 17: PPG and LDF Peak to Peak Detector output for LtLDF signal at two different 10 second segments in Subject 07 Quiescent phase 2

EKG. A peak detector was also created for the EKG data as well. Heart rate was calculated from the interbeat interval. The mean was calculated for each phase. And a cumulative mean was calculated with all trials.

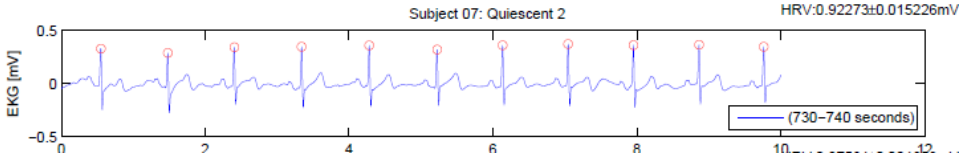

Figure 18: EKG Peak detector output for Subject 07 Quiescent phase 2

Volume Flow. The concept of volume flow is used in fields varying from medical to industrial, in order to determine flow through a tube, or vessel. Abdollahi, et. al proposed a novel method of combining the PPG and LDF sensors into a single unit in effort to "indicate the presence and magnitude of blood flow". This technique was developed for the purpose of providing an early warning of ischemia during bowel surgery. In their study the sensors were adjoined to obtain readings from the same site simultaneously. The waveforms were output as two separate data sets.

In this project, volume is also valuable. The flow may not necessarily be improved if only vessel diameter increases or only blood flow increases. Velocity of fluid slows through a widening pipe, and increases through a narrowing pipe, but flow in either case is conserved due to continuity and conservation of mass. To obtain improved peripheral flow both measures must increase. The following is proposed to identify increase in velocity coincident with increase in vessel cross sectional area to serve as an indicator of peripheral flow enhancement.

It was not feasible to adjoin the two peripheral sensors in the same finger due to sensor size and positioning/fastening requirements. Instead, a numerical representation of the presence and magnitude of flow was proposed. This was obtained by taking the dot product of the PPG and LDF signals. The rational for this mathematical representation is as follows. The PPG signal provides measure of vessel diameter, or an area ($A = \pi r^2$) of the vessel, and the LDF signal provides the velocity of the RBC within the vessel. The volume can then be found by multiplying the area times the volume. Blood flow is defined by the volume of blood over per unit area per unit time (Rhodes 1996).

$$\frac{\boldsymbol{Volume}}{\boldsymbol{Time}} = \boldsymbol{Area} * \boldsymbol{velocity} \quad (4)$$

The figure below shows the PPG and LDF waveforms from both hands and their resultant volume. At the 10 second mark and the 47 second mark we can see that the volume-flow increasing and decreasing, respectively.

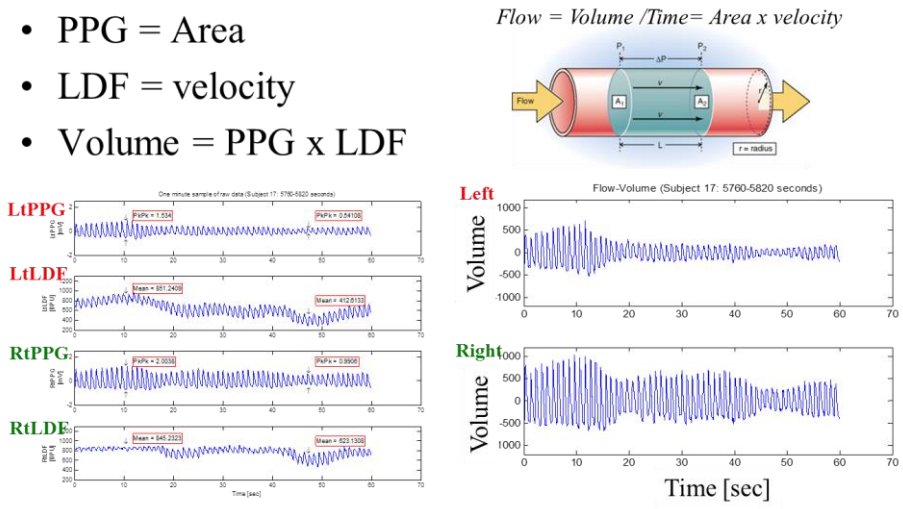

Figure 19: Volume-Flow. PPG, LDF (Left) and Volume (right) waveforms. of excerpt from Subject 17.

From this plot we can observe that that the PPG PP and LDF MV contribute to the volume. An increase in velocity, seen as LDF MV, occurs with decrease in vascular resistance, seen as increase in PPG PP. The figures above show an increase (or decrease) in the LDF MV and the PPG PP on the left and corresponding increase (or decrease) in the volume on the right. The LDF PP, or ventricular contraction, does not show any dominant effects on the volume PP. The PPG MV has the effect of a HPF, so that the LDF MV only modulates the PPG amplitude. Nevertheless, we can see enhanced volume from 0 to 20 seconds, and diminished volume from 40 to 50 seconds. Also we can note that the volume in the right hand has greater amplitudes than the left hand. The volumes for right and left hand were calculated and characterized in with the same manner as the PPG and LDF waveforms, with PP, RMS and MV.

The limitation of this method is that the two data sets are from different vessels (different fingers and different depths of the skin). Also, the high-pass filter on the PPG signal also limits the output. If the slow wave component were available,

volume MV calculation could provide a representation of volume when the heart is not depolarizing, or at rest. This volume calculation with the addition of the PPG slow wave component could merit further examination in future work.

The table below provides a summary of the time domain characterizations and interpretations.

Table 2
Summary of Blood Flow Outcome Measures

	PPG	***LDF***	***Volume*** *[PPG*LDF]*
Raw Data point	Diameter (d) of vessel at that point, or area, ($A=\pi[½ *d]^2$)	Velocity of RBCs in vessel (v)	Volume of blood in vessel (V)
Raw Data over time	diameter over time=vasomotion	Velocity over time = rate of change of velocity ($v/time$), or acceleration of blood (a)	Change in Volume of blood over time = blood flow (Q)
Peak to Peak (PP) peak systole – peak diastole	AC component change in vessel area over cardiac cycle(ΔA)	AC component: Change in velocity over a cardiac cycle (Δv) due to pulse pressure created by ventricular contraction	Change in volume over a cardiac cycle (ΔV)
RMS $rms^2 = \bar{x}^2 + \sigma^2$ root mean square of all points in one cardiac cycle - provides average value of pulsatile signal	average area of blood vessel	average velocity of RBC in cardiac pulse	average volume of blood in vessel
Mean Value (MV) ½ *(peak systole+peak diastole)	DC component of signal≈ 0, tone of vessel when heart is not depolarizing (heart at rest)resting phase of heart	DC component of signal, velocity of blood when heart is not depolarizing (heart at rest)	DC component of signal ≈ 0, volume of blood when heart is not depolarizing (heart at rest)

Frequency Domain Analysis

PPG and LDF. The same 100 seconds of data parsed for the time domain calculations were contacted into one data set per phase. The data set was multiplied by a hanning window function. The power was calculated to yield the power spectrum. The first 5Hz of data were reviewed. After this point the spectral content decays.

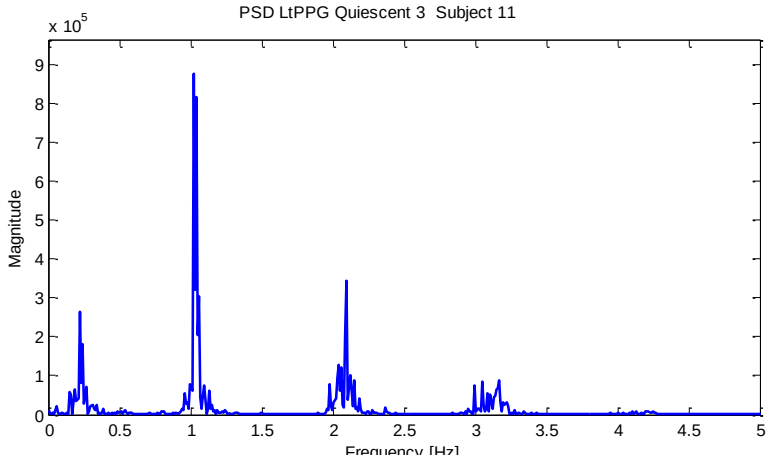

Figure 20: Non-normalized PSD of LtPPG: Subject 11 Quiescent Phase 3

Normalization Approach. For each subject a normalization factor was calculated by taking the peak heart rate of the entire session. In this way the change in spectral content throughout the session can be observed in relation to that peak. For the LDF signal, the peak occurs in the DC component of the signal. The algorithm to find the peak was altered for the LDF signal to only detect the peak at the heart rate, and ignore the peak from the DC component.

The PSD data assembled in a Matlab image, with phases in the x-axis and frequency in the y-axis. The color scale provides the normalized magnitude of the signal. See figure below.

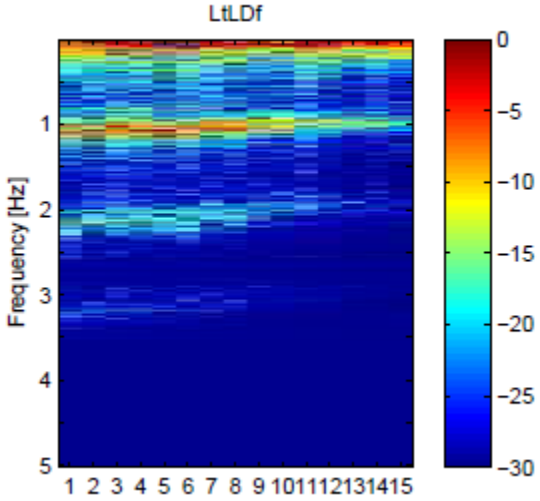

Figure 21: PSD Estimate Image: Subject 07 LtLDF.

Hsiu et al. (2012) suggested that harmonics can be used to quantify microcirculatory responses and provide information on pulse transmission of frequency components. The frequency spectrum either bandwidth either increases or decreases during a phase. To spectral broadening was quantified. First the spectrum was split into three ranges of interest:

Table 3
Frequency Components of PPG, LDF and EKG Signals

Component	PPG	LDF	EKG
Slow wave (0-0.5 Hz)	**sympathetic activity that modulates heart rate(0.01-0.5 HZ):** -endothelial activity (0.0095-0.021 Hz), -neurogenic activity (0.021-0.052 Hz), -myogenic activity (0.052-0.145 Hz), - respiration (0.03 Hz), - THM frequency to pulse blood in both SA node and vasculature (0.1 HZ), (Humeau 2004, Kamal 1989, Murthy 2001)	**sympathetic activity that modulates heart rate(0.01-0.5 HZ):** - respiration (0.3 Hz), -myogenic activity, blood pressure regulation (0.10; 0.06-0.2 Hz), -neurogenic activity(0.04 Hz), -vascular endothelium, metabolic activity—the rhythmic regulation of vessel resistance to the blood flow initiated by concentrations of metabolic substances in the blood (0.01 Hz), (Bracic 1998, Rossi 2008)	**Low frequency due to sympathetic activity** (0.04-0.15 Hz) **High frequency due to parasympathetic activity** (0.15-0.4 Hz). **LF/HF ratio provides the heart rate variability (HRV**) (Henley 2008)(Lewis 2005)(Delaney 2001)
Fundamental (0.5-1.5 Hz)	**heart rate** (Humeau 2004, Kamal 1989, Murthy 2001)	**heart rate**(Bracic 1998, Rossi 2008)	**Heart rate** (Kilpatrick 1994)
Harmonics (1.5-3 Hz)	**Blood pressure waveform** directly proportional to blood supply (Hsiu 2012)	--	--

The magnitude from these spectral ranges was obtained for each phase and compared. The mean estimator was calculated for each phase. And a cumulative estimator was calculated with all trials.

EKG. The spectral estimation of the EKG was performed as above with the PPG and LDF data. However, the estimators were of different ranges and the LF/HF ratio was used to provide a measure of heart rate variability (Henley 2008)(Lewis 2005) (Delaney 2001).

- Low Frequency (LF) [0.04-0.15 Hz]. : sympathetic activity
- High Frequency (HF) [0.15-0.4 Hz] : parasympathetic activity

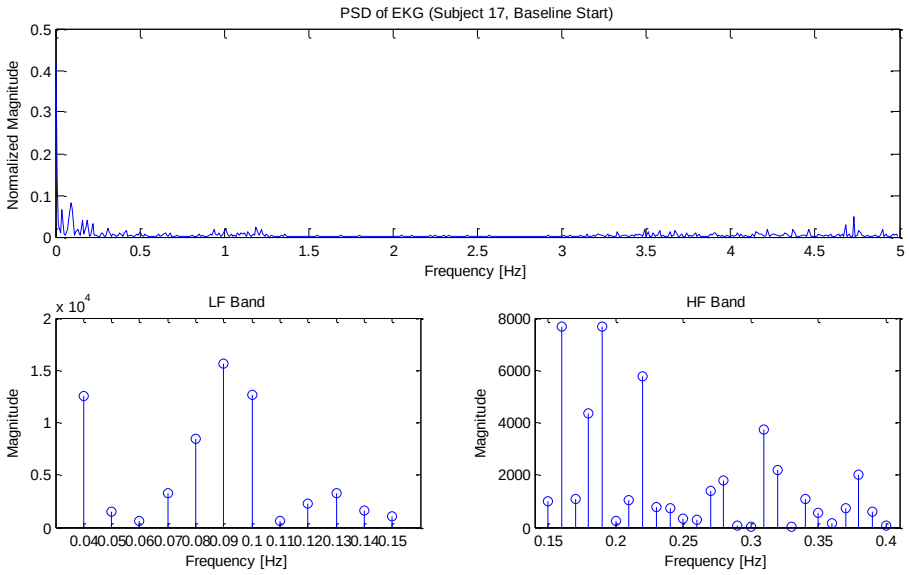

Figure 22: LFHF Ratio

The following calculations were completed for Low Frequency (sympathetics) and High Frequency (parasympathetics). This method was validated with the Biopac ACQKnowledge software HRV function, documented in the appendix.

Statistical Analysis

Group Stratification

The raw data showed a decaying trend in blood flow in the control group. The active group did not display a decline; rather the signals maintained a PPG PP value and fluctuating LDF MV. A subset of the active group displayed enhanced responses during OMT. This subset was termed the Peripheral Responders. The figure below*Figure 23* shows a representative PPG waveform from each group.

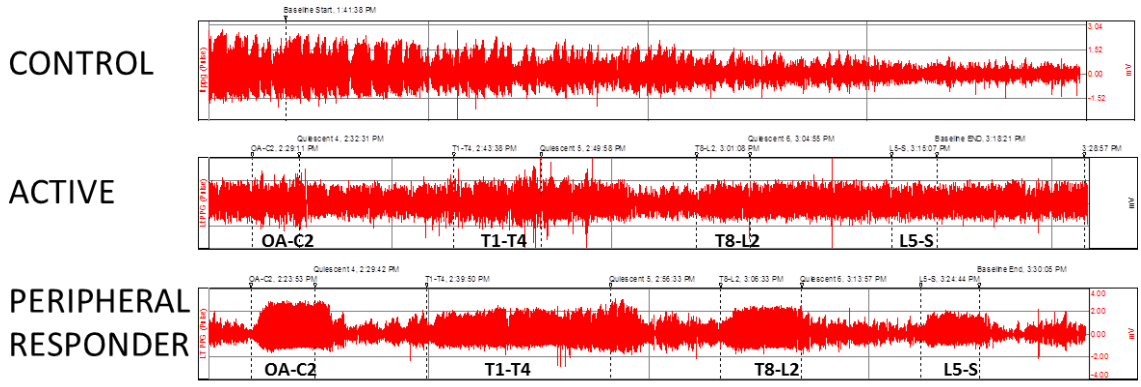

Figure 23: Peripheral Responder - Comparison Left PPG data sets showing control (Subject 07), active (Subject 18) and peripheral responder (Subject 14).

Similarly, the heart rate calculations showed varied responses among subjects. The control group showed little change in heart rate throughout the session, the Active group heart rate fluctuated throughout the session. And a subset of the Active group showed a decrease in heart rate during OMT. This subset was termed the Central Responder group.

The Control group results were compared to the Active, Peripheral Responder and Central Responder groups to determine statistical significance.

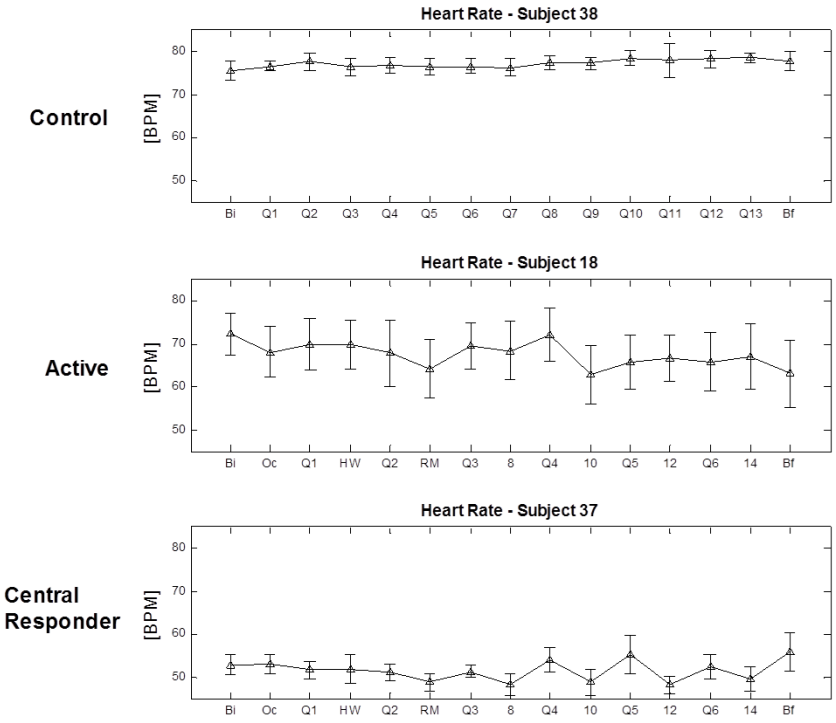

Figure 24: Central Responder. Comparison of Control (top), Active (middle) and Central Responder (bottom) Groups

Mann-Whitney U Test

A parametric and a non-parametric statistical analysis technique were used. The non-parametric method was used due to the sample size (less than 20 samples per group). The Mann-Whitney U test is a conservative approach as it has no assumptions regarding dependency and data (the rank order) is ordinal. It also used because the data was not always normally distributed. The Mann-Whitney U test ranks the means in an order and calculates the mean of the rank order. Significance between the mean rank orders is determined.

Repeated Measures Analysis of Covariance (RMANOVA)

A RMANOVA between-group test was completed for the mean trend of phases 7-15 on the spectral estimation results. Assumptions to use this statistical analysis were ignored; the analysis was completed with the intent that this is an exploratory study only. Statistical analysis descriptions are found in the appendix.

Percent Change Assessment

Because the variability between subjects was so high the treatment effect could be masked. For example, during a treatment Subject A may have an increase in a biophysical measure, Subject B may also have an increase but to a lesser degree, and Subject C may have a decrease in response to the treatment that is greater in magnitude than subject A and B. In this illustration two out of the three subjects experienced an increase; however, the calculated mean of the three may show that there was no effect. The treatment effect could be masked due to physiologic differences rather than therapeutic intervention. To address this issue, another assessment of treatment efficacy was completed by showing the percent of subjects with a change. The percent change for a measure described above was calculated per subject. Any change less than ± 5% was considered as no change (NC), otherwise it was reported as increase (INC) or decrease (DEC). The total number of subjects with an increase, decrease or no change was tabulated and reported as a percentage of the group. Percent change assessment was completed for all results.

Error

The parsed data from the master and slave were not extracted from the exact times. One reason for this was because it was difficult to match up the data sets. One reason was due to noise and disturbance from different sources. The peripheral sensors may have had noise interference from subject movement and the EKG data would not have any noise interference at that same time, and vice versa. Also, it was difficult to match the EKG and PPG/LDF data due to the fact that the recorded time stamps were not the same. First, the start times of the two data sets were different so the time delay between start and a certain phase was slightly off. Second, the clocks on the computers were not set to the same time, so that the recorded time of day between the two datasets was off. Mid-way through the study the clocks on the two computers were synchronized so that the exact time of data capture would be known. However, the difficulty remained due to the fact that there is a very slight delay on the trigger between the master and the slave. Also, it is known that the electrical activity of the heart and the mechanical activity of the peripheral vasculature have a delay, due latency period between electrical impulse and myocardium activation and to wave propagation through resistive systemic vasculature *(Rhodes 1996)*. Attempts to align the data to the 0.01 second became a best guess. It was decided that having the data match exactly would not add necessary information to the study at this point. For the purpose of this study it was sufficient that the data from master and slave were taken from the same phase, but not at the exact times.

CHAPTER 4

METHODS AND THEORY: SPECTRAL DOPPLER ULTRASOUND STUDY

A capability was developed at ASTU SOMA, for acquiring long term data from a L500A Vista AVS unit from Summit Doppler System (Makin and Hope 2012). The purpose of the spectral Doppler ultrasound study was to perform a reliability and feasibility test. This chapter describes the device and post processing algorithms.

Setup and Procedure

The modified Vista unit fed the raw data into a LabVIEW based data acquisition program, which then output the data as text file format. The data was post processed with Matlab scripts. A probe positioner was designed to hold the Doppler probe at a 60 degree angle to facilitate continuous measurements. In this experiment a subject lay supine as the facilitator performed systemic perturbation, and an operator conducted the data acquisition. No OMTs were performed. Blood flow from radial and the dorsalis pedis arteries were monitored in individual tests, as only one modified Doppler unit was available.

Figure 25: Spectral Doppler Ultrasound Study Setup (top), probe holder (bottom left), radial artery probe position (bottom middle), and dorsalis pedis artery probel position (bottom right)

The protocol for this study included two reactivity tests, namely occlusion and limb elevation. The occlusive phase used a cuff around the limb proximal to the probe, where the cuff was inflated to above 60 mmHg for 90 seconds. In the posture phase, the aim was to elevate the artery above the level of the heart. For the radial artery test the arm was raised vertically, and perpendicular to the body. For the dorsalis pedis artery test a modified Trendelenburg position was used, where the legs were raised bending only at the hip. A cushion and block were placed under the subjects' calves to assist the subject in maintaining position without exerting effort. This also helped to prevent bending at the knee which might cause occlusion of the vessels. Each test was approximately 20 minutes in duration, with three minute rest phases and 1.5 minute active phases. The table below shows the procedure order.

Table 4
Spectral Doppler Ultrasound Protocol

	Active Session [~20 min]				
Phase	1	**2**	3	**4**	5
Phase Name	Rest 01	**Occlusion**	Rest 02	**Posture**	Rest 03
Duration approx.. [min]	3	**1.5**	3	**1.5**	10

A total of 5 sessions, with 3 male and 1 female, asymptomatic subjects were conducted. The table below contains the session data. The first two sessions were experimental informal procedures and were not included in the final analysis.

Table 5:
Doppler Ultrasound Project - Subject Data Table

Subject No.	Date/Time	Initials	Gender	Notes	Active Length [min]		
					Radial	Dorsalis Pedis	Total
*Subject 01**	*07-Sept-13*	*JM*	*M*	*Informal Procedure – omitted from overall analysis*	*14.58*	*20.97*	*35.55*
*Subject 02**	*11-Feb-14*	*AC*	*M*	*Informal Procedure: subject sitting upright on table, probe alternates between radial and dorsalis pedis arteries – omitted from overall analysis*	*52.02*	*(combined)*	*52.02*
Subject 03	25-Feb-14	AC	M	Formal Procedure	12.26	15.13	27.39
Subject 04	05-Mar-14	DL	M	Formal Procedure	19.96	19.33	39.29
Subject 05	05-Mar-14	AC	M	Formal Procedure	21.20	22.28	43.48
Subject 06	11-Mar-14	JV	F	Formal Procedure. Occlusion phase and posture phase is reversed. The first occlusion test was omitted due to probe uncoupling and was redone after post posture rest phase.	30.51	23.20	53.71
Subject 07	02-May-14	JM	M	Formal Procedure	23.90	23.73	47.63
n=5				**Total Active Length**	**21.57±6.6**	**20.73±3.56**	**42.30±9.89**

Spectral Doppler Ultrasound and Applications

The Vista AVS is a commercial, point of use diagnostic tool that is used for assessing peripheral arterial disease (PAD). The devices measures the ankle brachial index (ABI), or ankle brachial pressure index (ABPI), to diagnose PAD. The ABI is the ratio between the ankle pressure and the brachial pressure. A normal circulation will have a higher pressure in the ankle. The ratio provides an index of peripheral health, where ABI >=1 is normal, and ABI <=0.8 signifies arterial impairment, and ABI< 0.5 indicates severe PAD.

The pressure from an artery is obtained by inflating a cuff proximal of the probe until the arterial pulse is zeroed. The cuff is slowly deflated releasing pressure. The cuff pressure at first return flow is defined as the arterial pressure. The pressure in the Dorsalis pedis can be difficult to obtain. In the presence of PAD dorsalis pedis pressure can even be confused with the clinician's finger pulse when palpating. Several pedal arteries can be used to for the ankle pressure. These are

the Dorsalis pedis, peroneal, anterior tibial and posterior tibial arteries, for example (Eagle 2006).

This ABI method does have limitations in that it is operating under the assumption that the upper extremity circulation is normal. This assumption is due to the fact that PAD generally occurs in the lower limbs first. False positives may arise if PAD is present in the upper limb. The upper limbs circulation could be poor yet the ABI ratio would show as normal. Also, it is often the case that the brachial arteries on either arm have different pressures. A false positive may result in the event that pressures from both arms are not measured.

Sensor Operation

The Doppler ultrasound device uses the Doppler Effect to detect the velocity of the red blood cells, providing a measure of blood flow. The probe emits an ultrasonic wave, a sound wave above >20,000 Hz, into the tissue. The incident beam hits red blood cells suspended in plasma and the sound is scattered radially from the particle. The scattered wave from the RBC in motion changes frequency in proportion to the speed of the RBC. The ultrasonic wave incident on this frequency produces a beat frequency whose amplitude and frequency also change with respect to speed of RBC. This beat frequency produces a sound wave whose pressure causes a piezoelectric element in the Doppler ultrasound probe to distort. The piezoelectric element thus converts the frequency to a voltage. The ratio of the speed of sound in through the medium and the thickness of the element determine resonance.

The resonance of the element is defined as the "Q" factor. The Q factor is determined by the manufacturer.

$$Q = \frac{f_o}{\Delta f} \tag{5}$$

where, $\Delta f$is the full width half bandwidth value of the spectrum.(Azhari 2010)

The unit provides audible and a quantitative plot outputs. The echoes normal1 to RBC velocity are within human hearing range and are therefore amplified and output from the unit. The audible sound wave indicating blood flow changes are used by the clinician to adjust probe position and used in subsequent clinical diagnostics. A visual output is also provided by the device. The echoes collected by the probe transducer are amplified and mixed at 90^o phase change with the incident beam. The phase change, rather than the magnitude of the frequency, of the amplified echoes are used to obtain the velocity.

The Doppler shift equation is used to relate the shifted frequency to the velocity of the particle. An equation for the Doppler frequency related to velocity was provided (Reid 1987):

$$vcos\theta = Kf_d, \tag{6}$$

where, $f_d = f_t - f_r$, $K = 0.5 * c * f_t^{-1}$

And v = radial velocity of incident object, f_d = Doppler shifted frequency, f_t= transmitted frequency, f_r = received frequency, c = speed of the incident beam through the tissue, θ = angle between the forward velocity and line of sight between the probe and the incident object.

The ultrasonic interaction with the tissue and RBC is much more involved, as waves reflect and scatter off stationary tissues, fluids and multiple cells traveling at different velocities. Different devices use different techniques to account for all of these. To simplify, the circuit design uses a high pass filter to remove the input from the tissues and slower moving cells at the vessel wall. A low pass filter is used to detect the difference between the incident and reflected waves. The two filter outputs provide a real and imaginary component of a signal when mixed in quadrature. The signal is Fourier transformed to provide the output displayed on the screen. The value of the output, however, is in arbitrary units of mV. A scaling feature on the unit allows the signal to be viewed optimally.

Spectral Doppler Ultrasound waveform and Characterization

The peak velocity in the Doppler waveform is due to ventricular systole and the minimum velocity is due to ventricular diastole. The phasic characteristic of the signal is indicative of arterial dysfunction. A normal artery will have a triphasic waveform with forward, then reverse then forward signal. A biphasic signal has forward and reverse signal, and a monophasic signal has forward only, indicating loss of arterial compliance. The raw Doppler data from the LabVIEW output was separated into the forward and reverse Doppler components. These were determined by the direction of blood flow with respect to the probe, where forward represents flow towards the probe and reverse represents flow away from the probe.

Differences were noted between the radial and dorsalis pedis artery data. The radial arterial flow was DC shifted in 5 out of 6 subjects, such that the reverse component was lost, yet the entire triphasic waveform was represented. The dorsalis pedis waveform was entirely distributed about the zero axis such that there was no loss of reverse of forward flow at any time. Only one subject showed a loss of

reverse flow in dorsalis Pedis, which only lasted for a few seconds, and was thus considered an outlier. The dorsalis pedis artery also had biphasic waveforms, whereas the radial artery did not.

Post Processing

The Doppler ultrasound data was analyzed in the time and frequency domain. The forward and reverse Doppler signals were combined into one signal. This was completed by a point by point addition of the two signals. The figure below illustrates the separate and combined signal for both arteries showing no loss of waveform.

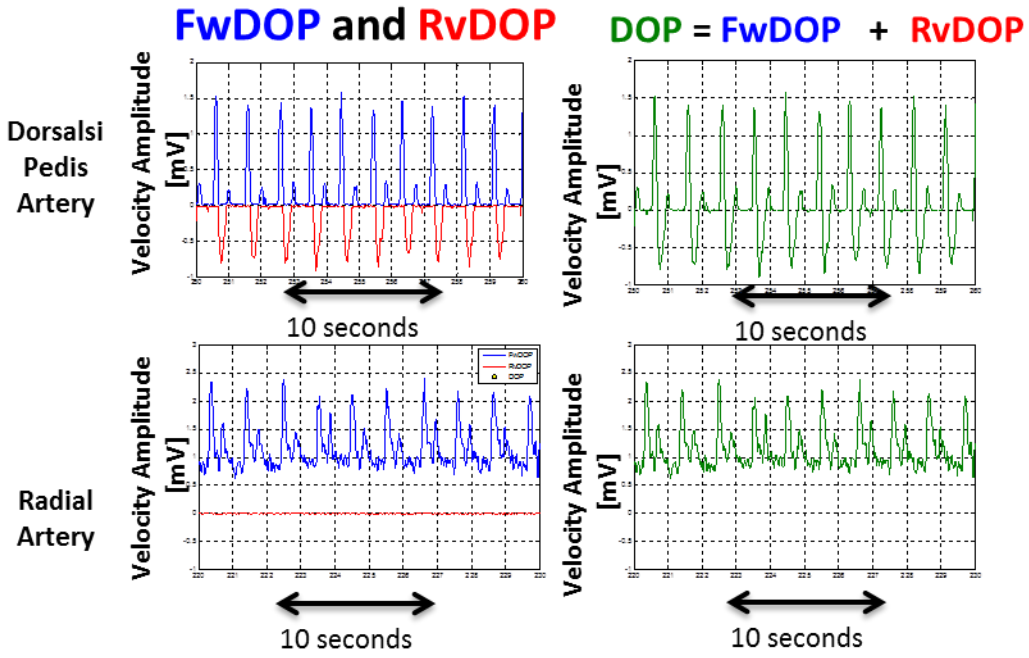

Figure 26: Combined Doppler Signal. Forward Doppler (FwDOP) + Reverse Doppler (RvDOP). (Top) Dorsalis Pedis shows no loss of reverse flow. (Bottom) Radial artery shows loss of reverse flow.

Data parsing

The first and last 5% of data was excluded to avoid periods of subject movement between phases, so only 90% of the data in the phase was analyzed.

Time Domain Analysis

Signal characterization. A peak detector was developed to isolate the cardiac cycles. A histogram of the combined Doppler signal showed that the peaks were located in the upper 10% of the data. This figure was used as a cutoff to refine the peak detector. The cardiac cycle was then identified as the time between two peaks and the start of the cycle was set to the twenty points before the first peak. The peak systolic and peak diastolic velocity, average velocity, mean velocity (time averaged), pulsatility index, resistivity index, forward and reverse velocity and peak to peak (pp) were calculated for each cardiac cycle. The mean was calculated for each phase. And a cumulative estimator was calculated with all trials.

Estimator	Abbreviation	Calculation	Units
Peak Systolic Velocity	S	Maximum (velocity)	mV
Peak Diastole Velocity	D	Minimum (velocity)	mV
Peak to Peak Velocity	S-D	S-D	mV
Average Velocity	AV	$\frac{S+D}{2}$	mV
Mean Velocity Time averaged value	MV	$\frac{\sum \text{velocity}}{\text{length(velocity)}}$	mV
Forward Peak Velocity	FwP	S-MV	mV
Reverse Peak Velocity	RvP	D-MV	mV
Pulsatility Index	PI	$\frac{S-D}{MV}$	[none]
Resistivity Index	RI	$\frac{S-D}{S}$	[none]

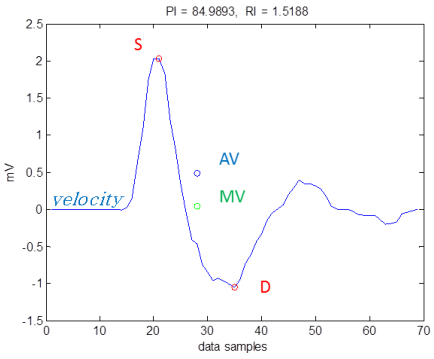

Figure 27: Spectral Doppler Ultrasound Indices

Frequency Domain Analysis

Doppler ultrasound waveform is composed of multiple frequency components. A DC shift was expected to be prominent in the radial artery. Low frequency components from slow wave were also expected to be more prominent in radial artery, based upon a slow wave observed in the raw data. A frequency component due to cardiac rhythm and higher frequencies resulting from heart rate variability and cardiac activity are also expected, and observed within a cardiac cycle as time between peak systole and dichroitic notch for example. Harmonics due to effects of local regulation on blood flow which increase with distance away from heart are also expected. Spurious peaks due to noise and filter leakage were also expected.

The sampling time of the Vista AVS-LabVIEW setup was reported to be "40Hz with a noise floor of 8 mV_{rms}" (Makin and Hope 2012). For the following spectral analysis the sampling time from all sessions was calculated. The mean sampling time was found to be 0.013 seconds per sample, with a sampling frequency of 74.6 Hz. The sampling frequency used in the subsequent analysis was 75Hz.

Based upon the available length of data sets, the highest achievable frequency resolution was 0.01 Hz. This requires which needs 109.2 seconds of data, or 8192 samples, providing an FFT size of 2^13. Since the experiments were of only 20 minutes in duration subject movement was minimal and noisy data sets were not an issue. Therefore, data parsing was not necessary and 10.92 seconds of continuous data was selected. Several preset transform windows in Matlab were compared and a Chebyshev filter with lobe attenuation of 300dB was selected. The windowed data was zero padded as necessary. The power of the FFT was calculated to obtain the final PSD. The max peak at 1 Hz (heart rate) from the entire session

was selected as the normalizing factor. The change in spectral content can then be viewed with respect to the peak within the session.

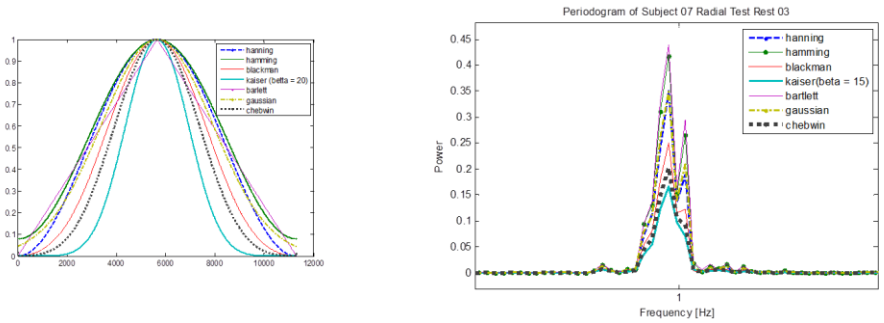

Figure 28: FFT Filters. Chebyshev window with r=300 dB lobe attenuation shown in black dashed line

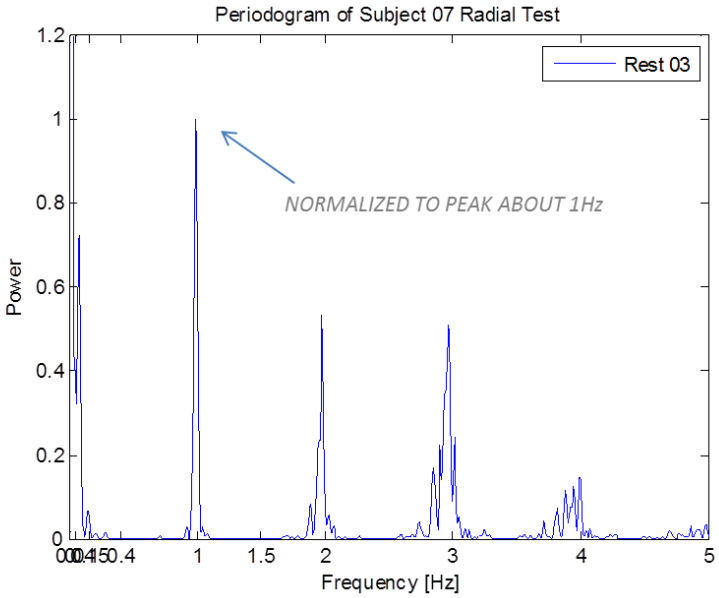

Figure 29: Normalized PSD of final rest phase of Subject 07 Radial Test, normalized to 1Hz peak.

CHAPTER 5

RESULTS

The results from the Biopac project and Doppler ultrasound project are reported in this chapter. Further discussion and interpretation of results is found in Chapter 6.

Peripheral Flow Results

Bilateral Response

The blood flow signals showed a bilateral response in the raw data. A test on the data acquisition system was performed and concluded that this was not a systemic error. The results of this test are documented in the appendix. **Figure 30** shows raw data from Subject 25 resting phase where the PPG signal amplitude and LDF MV and PP were greater in the right hand compared to the left hand. The right hand blood flow parameters were greater in the right hand in most subjects.

The cumulative time and frequency domain results showed similar bilateral responses, where right hand flow parameters were greater in the right hand compared to the left. The figure below shows the time domain RMS calculations for the LDF signal (left) and the frequency magnitude of the LDF signal (right).

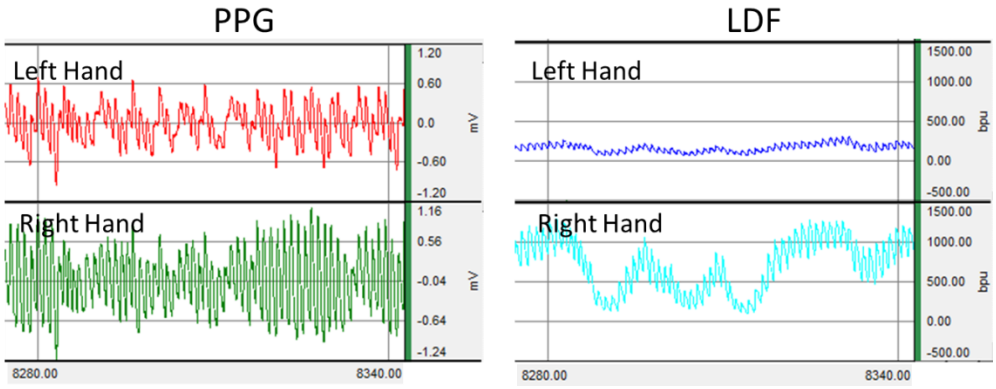

Figure 30: Bilateral response in Subject 25 Rest 6 Phase 60 seconds of data. The PPG and LDF plots have the same y-axis scales. The right hand PPG is centered at -0.04 rather than 0.

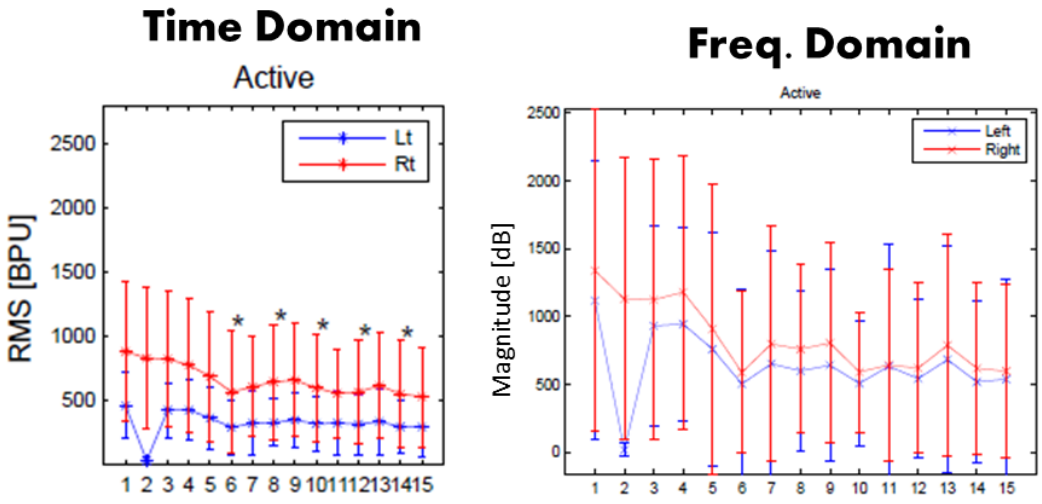

Figure 31: Bilateral response was seen in the cumulative results of the time domain analysis and frequency domain analysis (Left) LDF RMS values. (x-axis) phase in session, (y-axis) RMS value in blood perfusion units (BPU), '*' items denote OMT phases. (Right) LDF Frequency Magnitude of plot from 0-10 Hz. (x-axis) phase in session, (y-axis) frequency magnitude in dB.

Trends

Control Group. For the control group, the time and frequency domain analysis of the blood flow parameters resulted in a similar asymptotic decaying trend. The difference in flow parameters between the left and right hand diminished as the control session progressed. The variability in the calculations also decayed. The figure below shows the PPG RMS calculations and the frequency magnitude from 0-10 Hz of the control group.

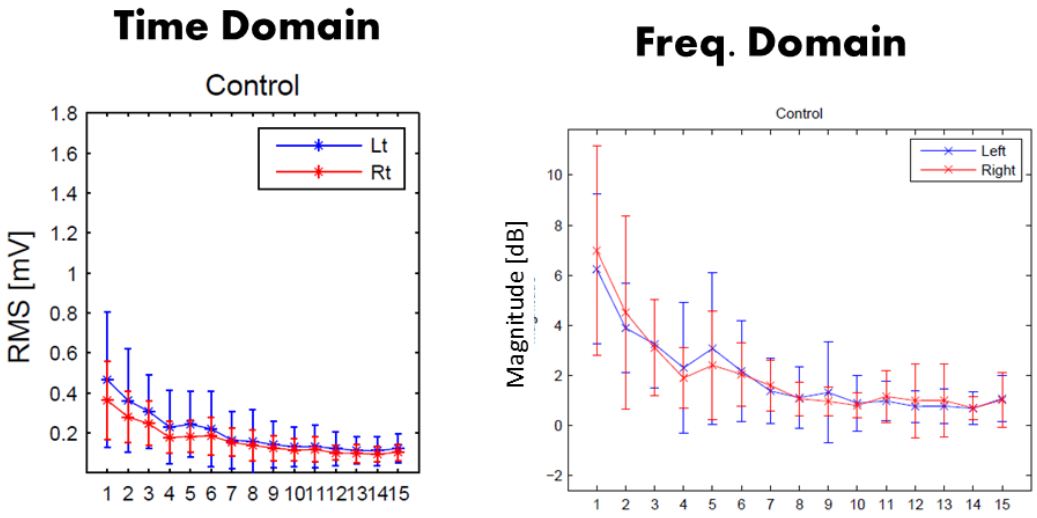

Figure 32: Control Group Trend. Asymptotic decaying trend in the time and frequency domain analysis.(left) left and right PPG RMS time domain analysis of control group; (right) frequency magnitude plot of left and right PPG of the control group.

Active Group. The time and frequency analysis results of the active group showed that the blood flow parameters maintained signal strength as the session progressed. A light decay in signal is observed from initial to final phase; however this trend shows less decay than the control group. The active group also showed an increasing bilateral response during some OMT. The variability in the data does not decrease it did with the control group. The figure below shows the PPG time (RMS) and frequency domain (0-10 Hz) analysis. The right hand shows increases during from T8-L2 (phase 12) till the end of the session.

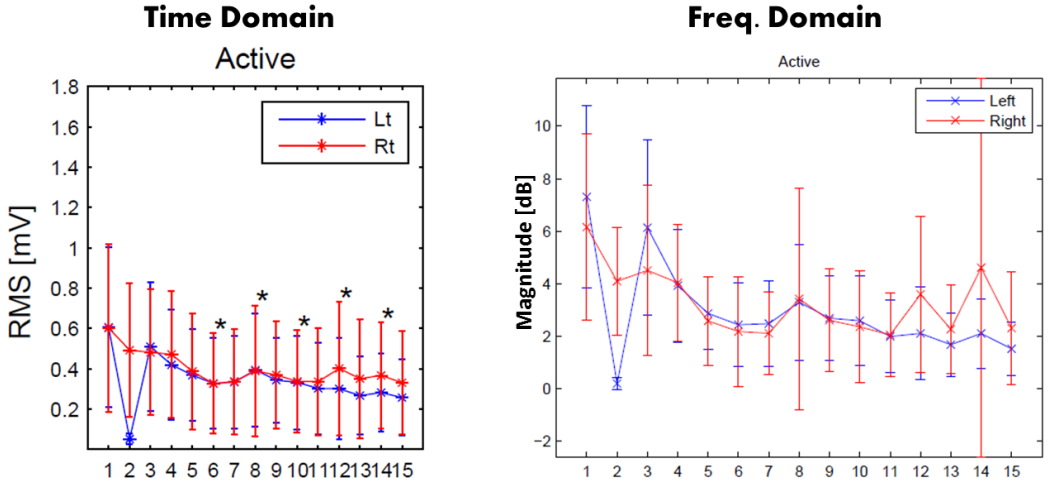

Figure 33: Active Group Trend. (left) PPG RMS time domain analysis of active group; (right) PPG frequency magnitude plot of the active group.

Peripheral Responder Group. The peripheral responder group trend did not decay as did the control group active group. The signal was maintained, as seen in the time and frequency domain analysis results below. The values during OMT (phase 8, 10, 12, 14).

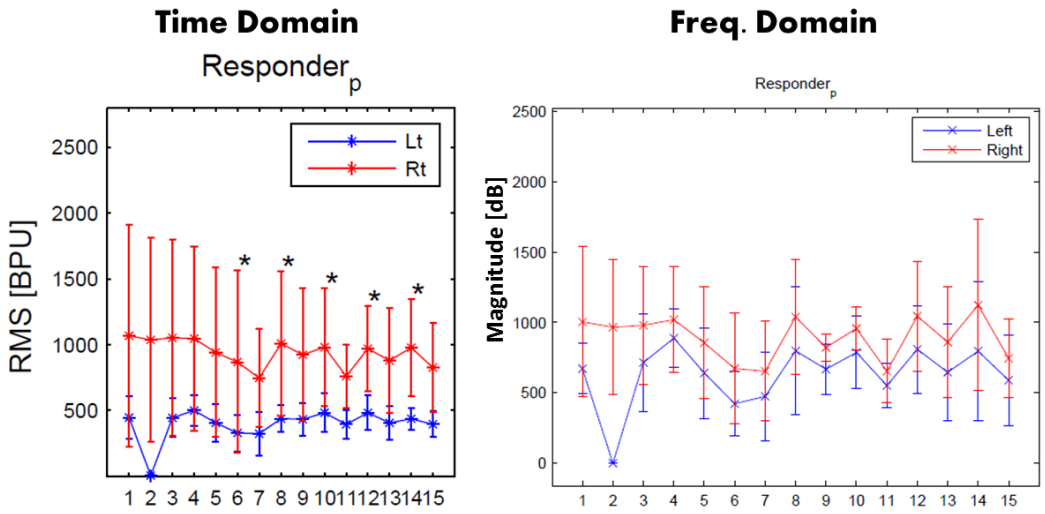

Figure 34: Peripheral Responder group trend. left) LDF RMS time domain analysis; (right) LDF frequency magnitude plot.

There was no statistical significance within group trends for any group.

Percent Change.

The number of subjects that showed an increase or decrease from rest to active phase is shown in **Table 18**, where of the signal characteristic changed by at least 5% to be considered an increase or decrease.

In all groups a majority of subjects experienced a decline in blood flow signal from initial to final phase of session, excluding the peripheral responder group where 60% had an increase in PPG and Volume RMS in the right hand.

During OA-C2, the majority in all active groups had an increase in PPG, LDF and Volume RMS, excluding the right hand volume RMS where 50% of active group decreased, and half of the central responders increased and half decreased.

During T1-T4 the active group has a decrease in both hands in all blood flow signal characteristics. The responder group's percent of increases and decreases varied across signal characteristics.

During T8-L2 a majority of active subjects increase in all blood flow signal characteristics. The majority of peripheral responders did as well. The majority of central responders showed increases in all signal characteristics excluding LDF RMS where the majority decrease in the left hand, and half increase and half decrease the right hand.

During L5-S all active subjects have a majority of subjects that have increased PPG RMS and decrease in LDF RMS. The majority of active subjects have a resulting decrease in Volume RMS for both hands. The majority of peripheral responders had increases in PPG, LDF and Volume RMS in both hands. The majority of central responders had increases in all blood flow characteristics excluding right hand LDR RMS, where majority of the group decreased.

Statistical Analysis

Responses also varied from subject to subject. The PPG and LDF and Volume PP, RMS and MV values had a large degree of variability. The variability was much smaller in the control group. The Control group's blood flow trends decreased steadily throughout the session on both sides of the body. The flow signals decrease by about 50% in both PP and RMS values. For Active groups the decay in blood flow was to a lesser degree. Instead, the flow was maintained throughout the session.

The Peripheral Responder group had enhanced responses during OMT. The Central Responder group showed no decay, and had enhanced response in the PPG results during three OMTs. A statistical analysis of the RMS values for all groups showed that the mean slope of the Active compared to the Control group, from phase 7 and on, was statistically significant.

Table 6
Mann-Whitney U statistical analysis results, comparing phases between groups.

LtPPG RMS	Control vs. Active	Control vs. Peripheral Responder	Control vs. Central Responder
OA-C2	0.006**	0.004**	0.035*
T1-T4	0.014*	0.015*	0.056
T8-L2	0.026*	0.020*	0.027*
L5-S	0.007**	0.003**	0.016*

RtPPG RMS	Control vs. Active	Control vs. Peripheral Responder	Control vs. Central Responder
OA-C2	0.007**	0.036*	0.009**
T1-T4	0.009**	0.020*	0.021*
T8-L2	0.000**	0.003**	0.002**
L5-S	0.000**	0.002**	0.001**

LtLDF RMS	Control vs. Active	Control vs. Peripheral Responder	Control vs. Central Responder
OA-C2	0.044*	0.012*	0.006**
T1-T4	0.018*	0.003**	0.159
T8-L2	0.020*	0.002**	0.366
L5-S	0.009**	0.002**	0.228

RtLDF RMS	Control vs. Active	Control vs. Peripheral Responder	Control vs. Central Responder
OA-C2	0.003**	0.002**	0.007**
T1-T4	0.003**	0.002**	0.016*
T8-L2	0.000**	0.002**	0.012*
L5-S	0.001**	0.002**	0.012*

HR	Control vs. Active	Control vs. Peripheral Responder	Control vs. Central Responder
OA-C2	0.490	0.062ǂ	0.763
T1-T4	0.622	0.100ǂ	0.922
T8-L2	0.521	0.079ǂ	0.688
L5-S	0.374	0.079ǂ	0.841

HRV	Control vs. Active	Control vs. Peripheral Responder	Control vs. Central Responder
OA-C2	0.587	0.865	0.763
T1-T4	0.402	0.533	0.228
T8-L2	0.490	0.336	0.191
L5-S	0.490	0.692	0.615

Frequency Components

Overview. The PSD of the PPG and LDF signal shows peaks within 0 to 4 Hz. After 4 Hz the spectra attenuate. The PPG signal had the greatest magnitude around 1 Hz, and the LDF signal had the greatest magnitude around 0 Hz. For the control group, the peaks beyond the 1.5Hz fundamental decayed as the session progressed. In the Active group, the frequency components above 1.5 Hz did not decay

throughout the session. The peripheral and central responders showed increases in bandwidth of the frequency components above 1.5 Hz during OMT.

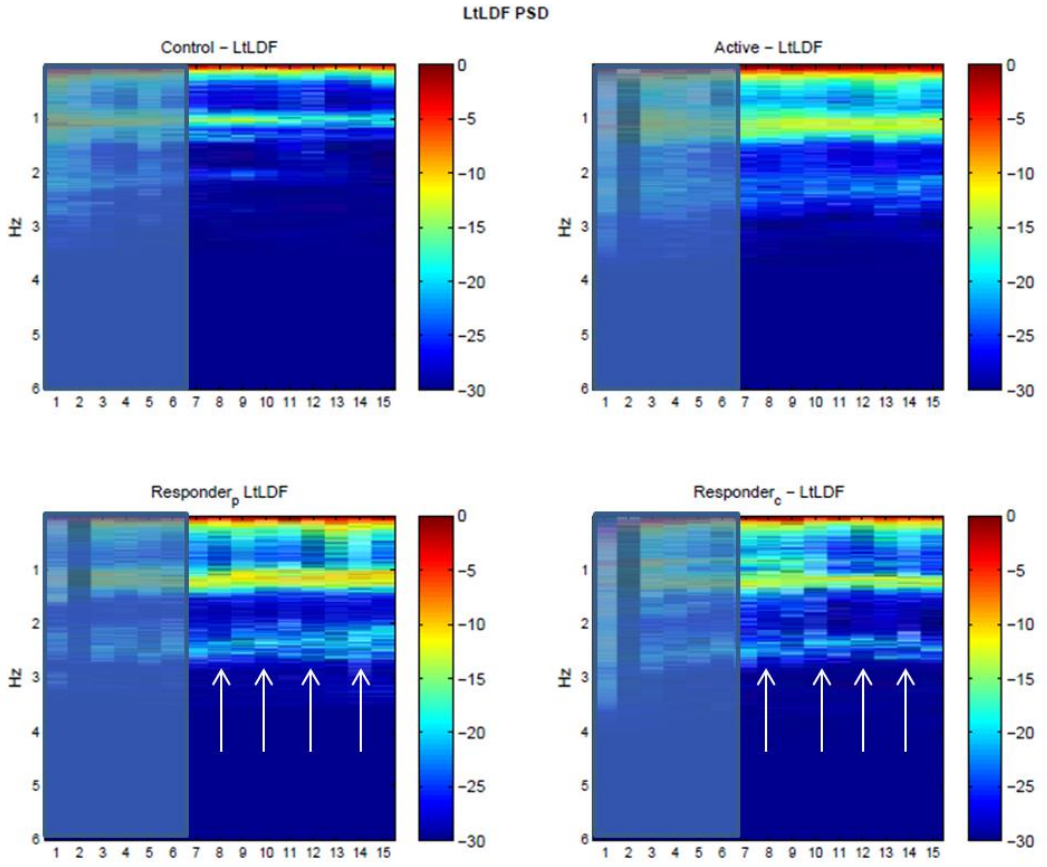

Figure 35: PSD results for left LDF, showing all groups. , x-axis shows time in phases, y-axis is frequency in Hz, and color scale shows intensity of spectral density in db. Control Group (top left) , Active group (top right), Peripheral Responder group (bottom left), central responder group (bottom right)

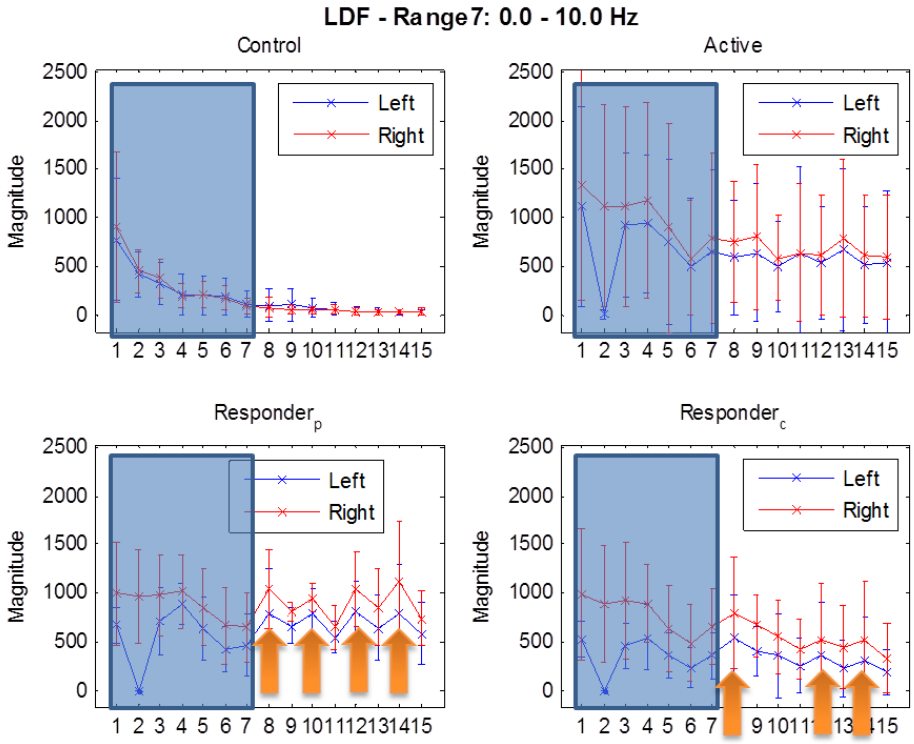

Figure 36: LDF Frequency magnitude from 0-10 Hz

Components. The frequency components of interest occurred in three ranges, 0-0.5 Hz, 0.5-1.5 Hz, and 1.5-3 Hz. .

Figure 37 and Figure 38 show the results of the PPG and LDF frequency component analysis, respectively. For these plots the right and left hand trials were combined for ease of viewing. But the analysis and statistics were calculated separately for each hand.

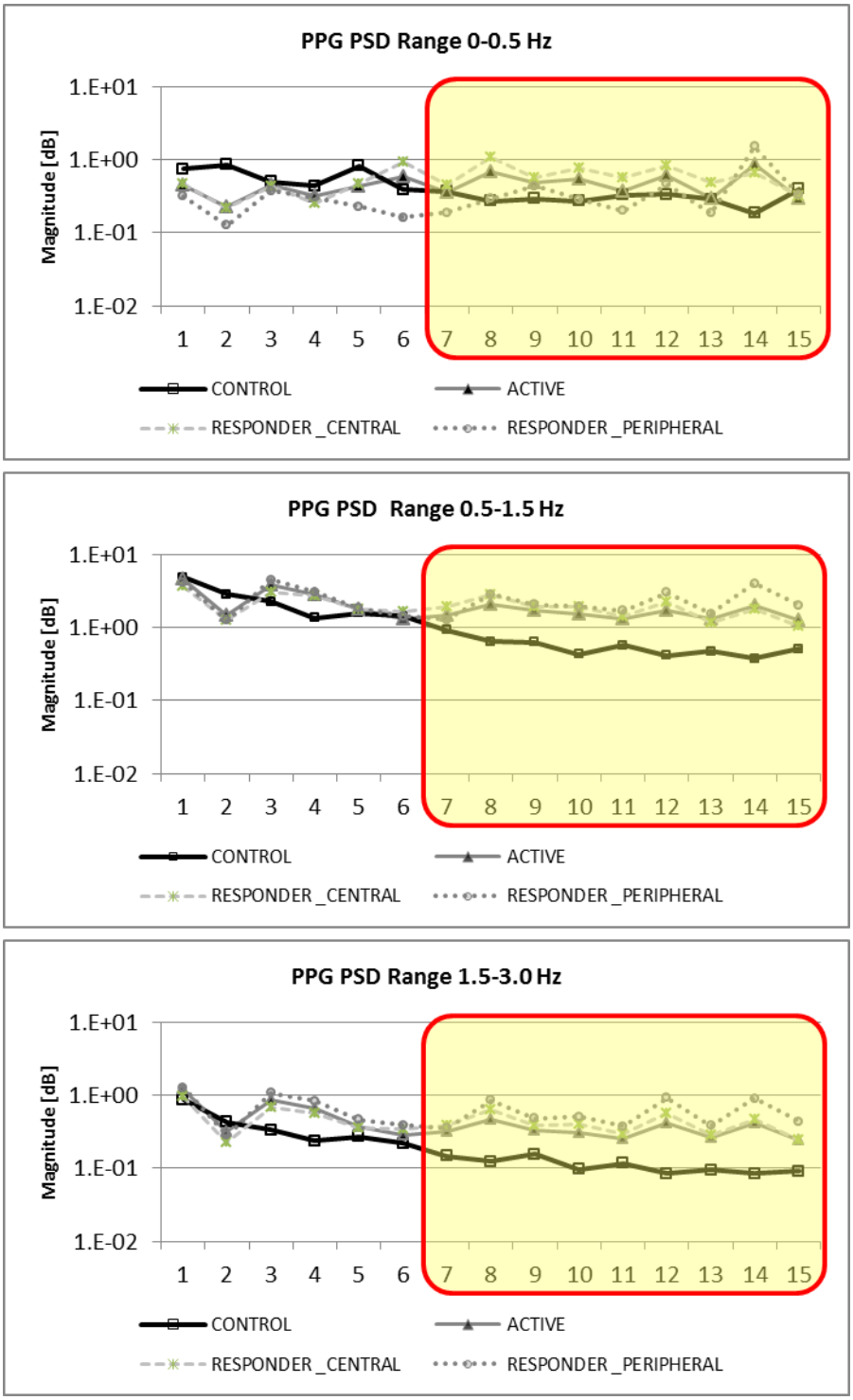

Figure 37: PPG Frequency Magnitude (left and right hands combined) of range 0-0.5 Hz, 0.5-1.5 Hz, and 1.5-3.0 Hz.

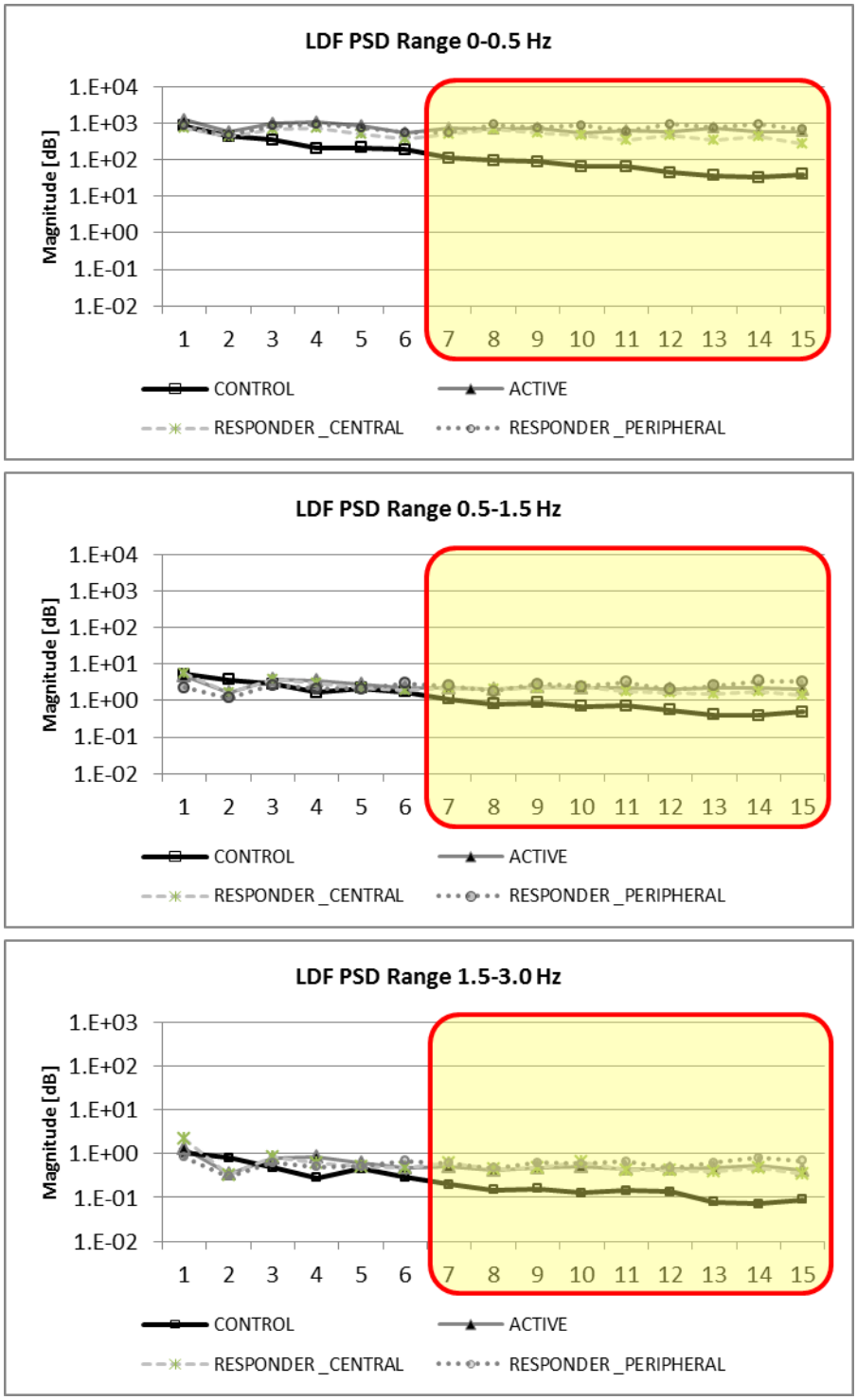

Figure 38: LDF Frequency Magnitude (left and right hand combined)of range 0-0.5 Hz, 0.5-1.5 Hz, and 1.5-3.0 Hz.

Table 7
RMANOVA analysis of Frequency Magnitude, Active compared to Control group

Frequency Magnitudes

Active compared to Control

p-values RMANOVA analysis

	Left	Right
PPG [0-0.5 Hz]	0.170	0.550
PPG [0.5-1.5 Hz]	0.004**	0.048
PPG [1.5-3 Hz]	0.001**	0.03*
LDF [0-0.5 Hz]	0.001**	0.006**
LDF [0.5-1.5 Hz]	0.010**	0.003**
LDF [1.5-3 Hz]	0.014*	0.003**

**p<0.05, **p<0.01*

The magnitude of the PPG signal in this range from 0-5 Hz showed that the control and the active group had approximately the same mean throughout the session. The responder groups had increased magnitudes during the OMT phases. Central responder group had a greater magnitudes throughout the session compared to other groups only in this range, in this signal, during OA-C2, T1-T4 and T8-L2. For all other OMT and frequency ranges, both LDF and PPG, the peripheral responders had the greatest magnitudes.

The LDF results were 3 orders of magnitude greater than the PPG results in this range. Also, LDF frequency components above 0.5 Hz are three orders of magnitude lower than the slow wave component (0-0.5 Hz). This is due to the DC shift in the signal.

PPG frequency components above 0.5 Hz and all frequency components for LDF showed that the control group magnitudes attenuated as the session progressed. The active group maintained a mean spectral content and the responder

groups had increased magnitudes in the OMT phases. Also, for these the group with the greatest magnitudes was the peripheral responder group.

The spectrum from 1.5 to 3Hz had a greater magnitude in PPG compared to LDF, where the active group mean from phase 7-15 for PPG =3.38e-1±0.1 and LDF =4.68e-1±0.05, and peripheral responder group mean from phase 7-15 was PPG=5.89e-1±0.29 and LDF= 6.12e-1±0.12.

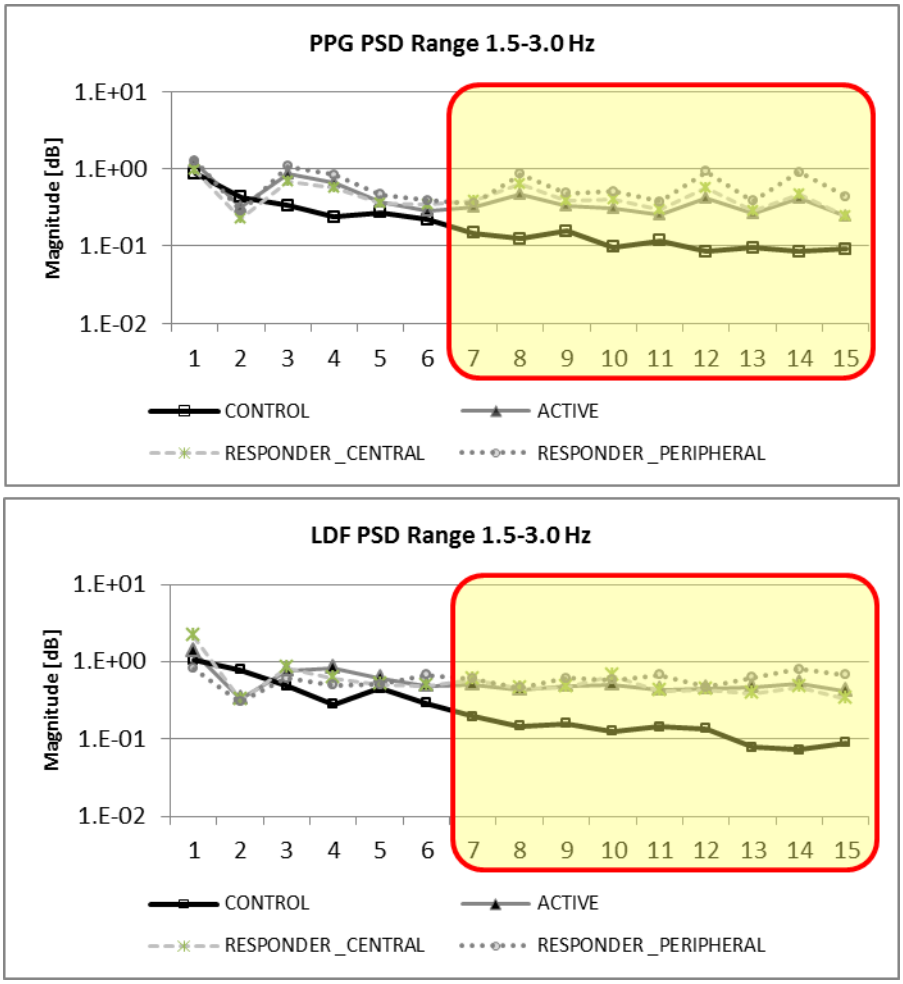

Figure 39: PPG and LDF frequency magnitude from 1.5-30 Hz.

EKG Results

Heart Rate

The heart rate in the control group was about 65 BPM throughout the session. The active group showed some fluctuations as the session progressed. A slight decrease was noted in OA-C2 (phase 8) and T1-T4 (phase 10). The responder groups showed greater fluctuations during the session. The central group showed the greatest decreases in heart rate during OMT, with T1-T4 showing the greatest decrease of 5BPM. The central responders' heart rate returned to the initial heart rate by the end of the session. The peripheral responder group showed the greatest decrease in heart rate from start to end of session, at about 4BPM. This group also started out with the highest heart rate at 74 BPM.

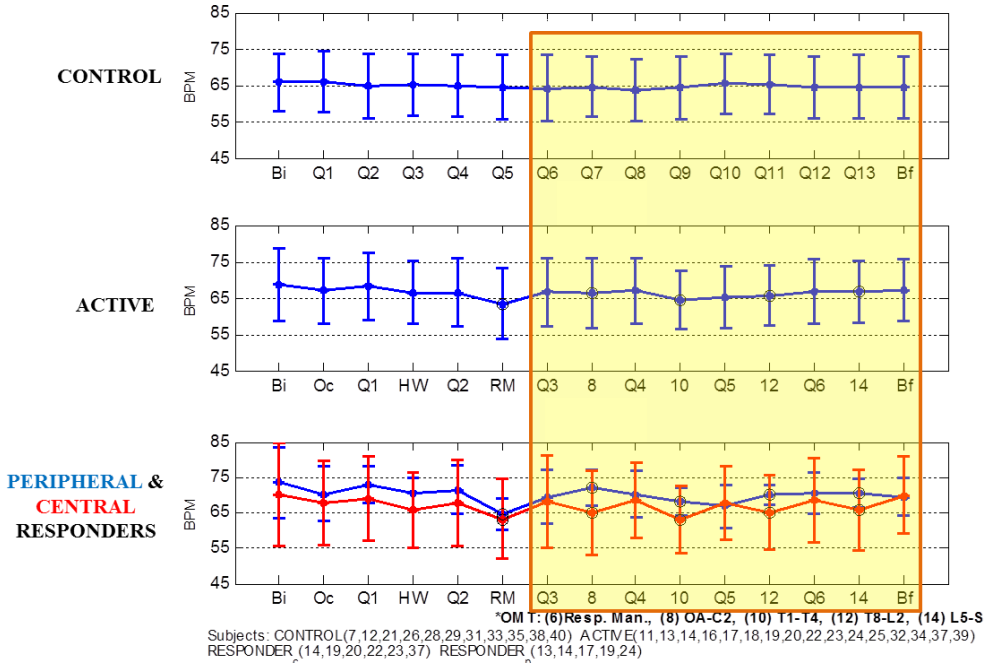

Figure 40: Heart Rate [BPM] of control, active and responder groups.

Table 8
Change in heart rate [BPM] from prior quiescent phase.

	Control n=11	Active n=16	Peripheral Responder n=5	Central Responder n=6
Initial to Final delta	-1.33 ± 3.01	-1.63 ± 5.72	-4.03 ± 6.51	-0.16 ± 7.13
OA-C2 delta	0.49 ± 3.03	-0.30 ± 5.04	2.41 ± 8.63	-3.12 ± 1.82
T1-T4 delta	0.71 ± 2.74	-2.57 ± 4.33	-1.94 ± 6.03	-5.59 ± 1.60
T8-L2 delta	-0.39 ± 1.30	0.54 ± 4.31	3.34 ± 5.30	-2.77 ± 3.39
L5-S delta	-0.09 ± 0.88	-0.01 ± 3.05	0.10 ± 4.05	-2.59 ± 1.27

The number of subjects per group that had an increase, decrease, or no change (less than 0.5 BPM increase or decrease) is shown in **Table 9**. The control group showed no dominant trend throughout the session. The number of increases, decreases or no change was spread throughout the subjects. The dominant trend in the Active group was a decrease in three of the four OMTs. 60% of the Peripheral Responder group showed decrease from start to end of the session. All of the subjects in the Central responder group showed a decrease in heart rate in all OMTs excluding T8-L2 where 83% decreased. The Central Responders had an increase in heart rate from start to end of the session.

Table 9
Heart Rate Percent Change: Subjects with Decrease, Increase or No change (<0.5 BPM) in heart rate from initial to final phase and from rest to active phase.

	Control (n=11)			Active (n=16)			P. Resp (n=5)			C. Resp (n=6)		
	Dec	**Inc**	**NC**	**Dec**	**Inc**	**NC**	**Dec**	**Inc**	**NC**	**Dec**	**Inc**	**NC**
Initial to Final	36%	36%	27%	44%	50%	6%	60%	40%	0%	17%	83%	0%
OA-C2	27%	27%	45%	75%	25%	0%	60%	40%	0%	100%	0%	0%
T1-T4	36%	36%	27%	69%	19%	13%	80%	20%	0%	100%	0%	0%
T8-L2	64%	27%	9%	38%	44%	19%	40%	60%	0%	83%	0%	17%
L5-S	36%	27%	36%	50%	31%	19%	40%	40%	20%	100%	0%	0%

The mean heart rate of the control group was approximately 65 BPM throughout the session. The active group's heart rate increased and decreased throughout the session, between 65 and 70 BPM. The overall change in heart rate reduced nearly 2 BPM. The central Responder group had a reduction of 3BPM during each OMT, from approximately 68 to 65BMP each OMT. The starting and ending

heart rate was 70 BPM for this central responder group. The peripheral responder group had changes in heart rate throughout the session, with an overall decrease from start of session at 74 BPM down to 70 BPM by the end of the session. This was the greatest decrease in heart rate of all the groups. The central responders showed the greatest decrease in heart rate during all OMTs, with the greatest reduction occurring in the OA-C2 treatment.

Heart Rate Variability

The heart rate variability was assessed by calculating the normalized frequency magnitudes of low and high frequency. The heart rate variability is the ratio of low to high frequency magnitudes.

Low frequency 0.04-0.15 Hz. The active group showed a decreased magnitude for all OMTs, except for T8-L2; however the variability did increase during this phase. Both responder groups decreased during OMT phases. From phase 9 and on the Peripheral Responder group had greater frequency magnitude compared to the Central Responder. This range is associated with the sympathetic activity, and this decreased during OMT for active and responder groups, excluding T8-L2.

High frequency – 0.15-0.4 Hz. The Active group had increased magnitudes for all OMT except T8-L2 where the magnitude did not change from the prior rest phase. The variability did increase during this phase. The central responder had a greater magnitude than the peripheral responder from phase 9 and on. This range is associated with parasympathetic activity, and this increased during OMT, excluding T8-L2.

LFHF Ratio. LFHF ratio increased during OA-C2 and T8-L2, and decreased during, T1-T4 and L5-S. In the peripheral responder group the ratio decreased during all OMT phases. In the central responder group the ratio decreased for all OMT phases excluding T8-L2. The peripheral responder group had a higher ratio from phase 9 and onward.

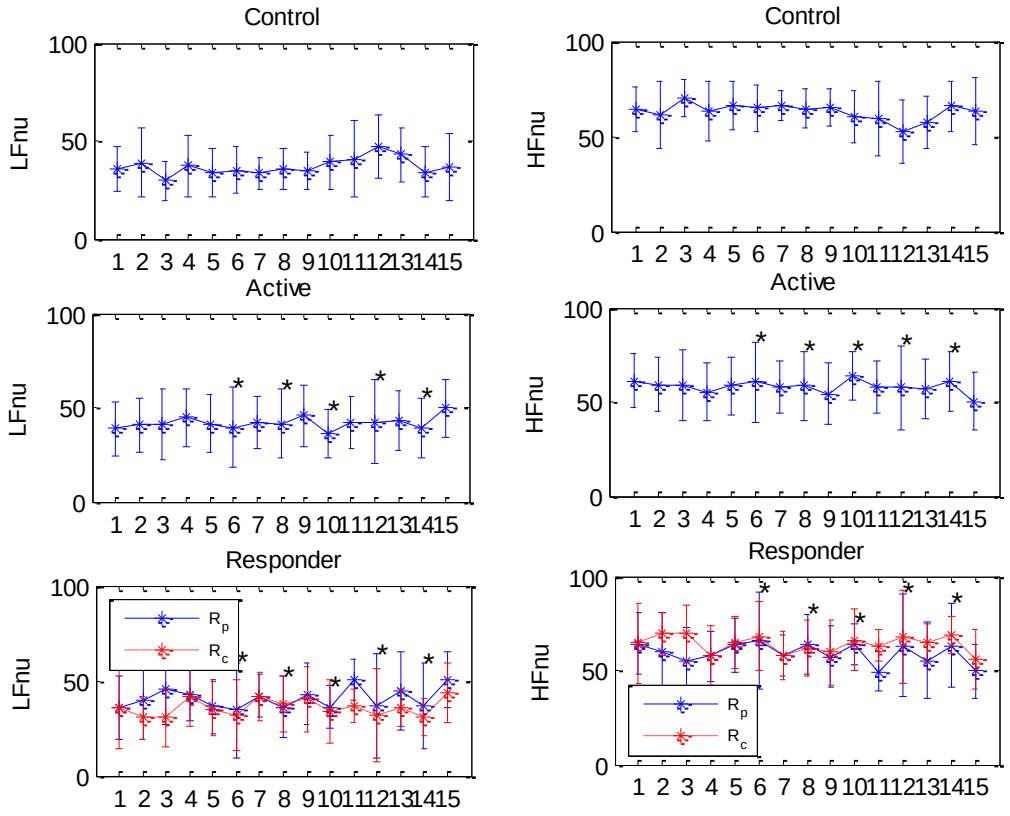

Figure 41: LF and HF of EKG. Low frequency (sympathetic) and high frequency (parasympathetic).

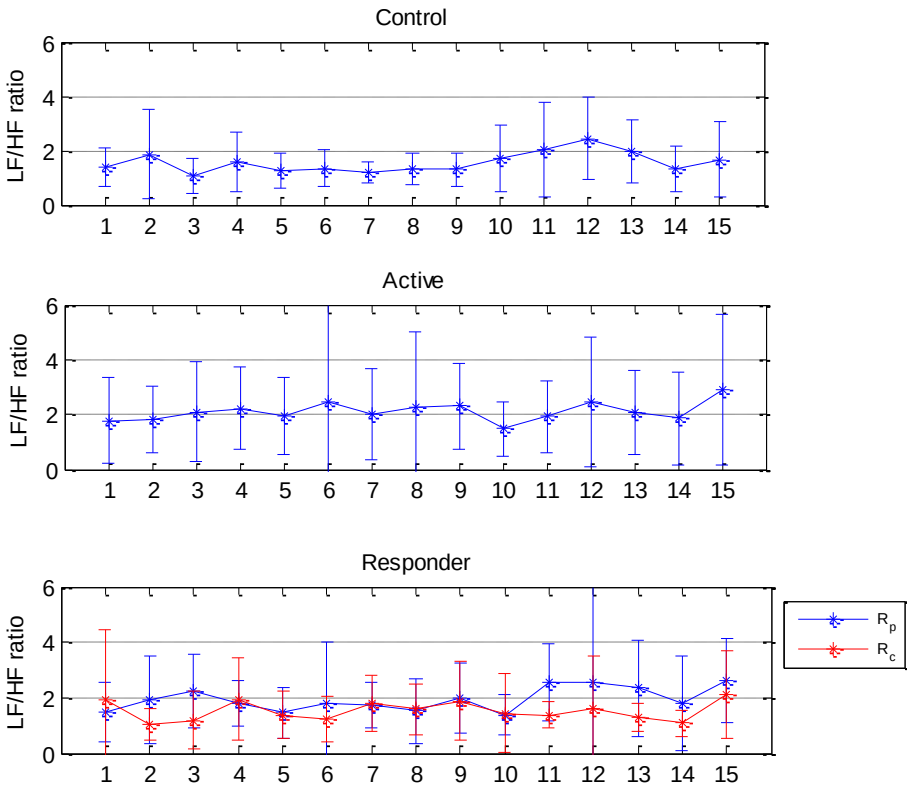

Figure 42: Heart Rate Variability

Summary of Biopac Study Results

The table below summarizes the results from the Biopac study.

Table 10
Summary of Results Table

	Blood Flow Parameters	**Central Activity**
Time Domain *time wave characteristics are used widely in medicine for diagnostics and prognosis (Hsiu 2012)*	PPG /LDF showed statistically increasing trends compared to control groups	EKG showed decreasing trends but were statistically insignificant
Frequency Domain *blood pulse contains harmonics starting in the heart and aorta. Frequency components are amplified and attenuated as blood travels through arteries, arterioles and capillary beds (Kamal 1989)*	Spectral strength statistically increased compared to control group in all three ranges *Slow wave (<0.5 Hz)* *Fundamental (0.5-2 Hz)* *Harmonics (>2Hz)*	changes were noted during OMT but were statistically insignificant

Spectral Doppler Ultrasound Results

The radial artery and dorsalis pedis artery test were conducted separately. The figure below shows the raw data sets from test subject 03.

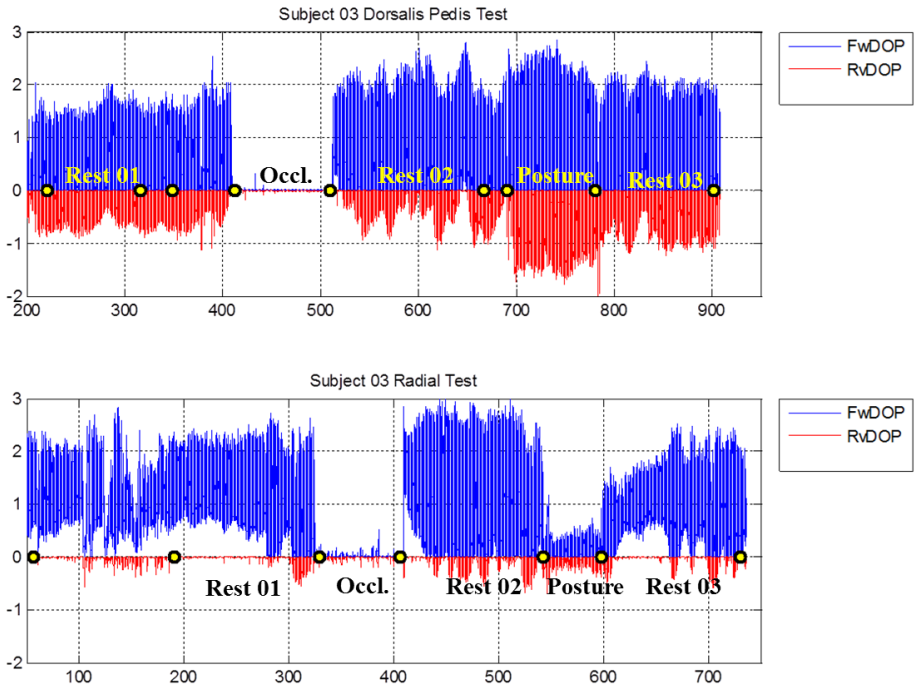

Figure 43: Subject 03 spectral Doppler Ultrasound dorsalis pedis (top) and radial artery (bottom) test. The y-axis is in units of mV. The x-axis is time in seconds.

Upper and Lower Extremity Differences

The output from the upper and lower extremity arteries showed different physiologic output. **Figure 44** illustrates this. The radial artery has greater amplitude than the dorsalis pedis artery. In this example, the radial artery is triphasic and the dorsalis pedis artery is biphasic.

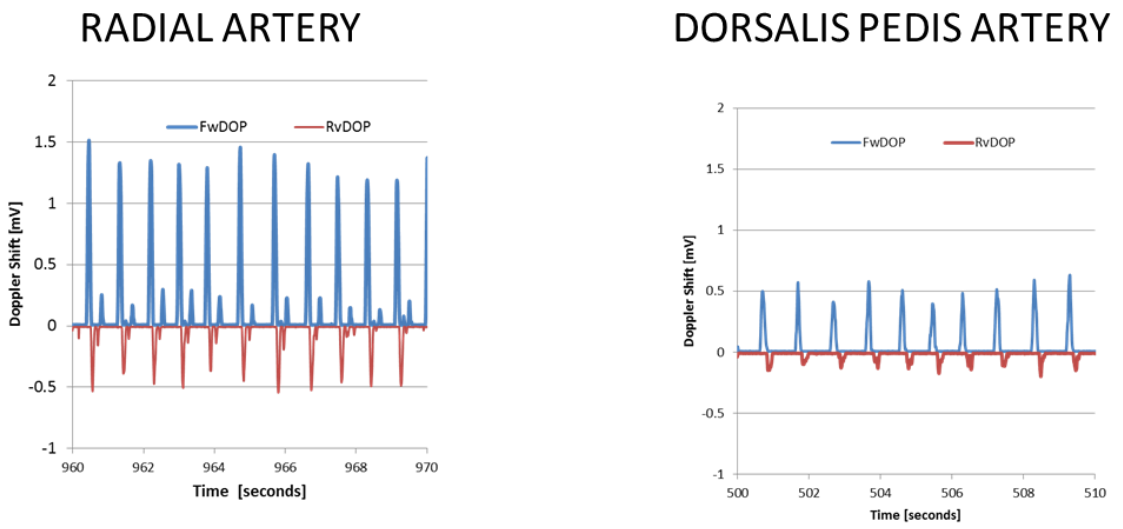

Figure 44: Radial and Dorsalis Waveform Comparison. Subject 6 rest phase, radial artery test (left) with a triphasic waveform, dorsalis pedis artery test (right) with a biphasic waveform

Furthermore, during the sessions, the radial artery data intermittently displayed loss of reverse flow in all but one subject. The triphasic waveform was still present indicating no loss in vascular function The dorsalis pedis artery data did not show any loss in reverse flow during the experiments. . During the occlusive phase all subjects experienced a near zero blood velocity in both extremities. The posture change resulted in an increased velocity in the lower extremity, but a decrease in the upper extremity.

Time Domain Analysis

Figure 45, in the appendix, provides the cumulative peak to peak measurements of the forward, reverse and combined Doppler waves. Variability increased during the lower extremity posture change. Also during the posture change in the dorsalis pedis tests the peak diastolic velocity decreased more than the peak systolic velocity increased. The change in diastole contributed to the combined Doppler peak to peak increase. During the posture change in the radial artery tests

both peak systolic and diastolic velocities decreased. The overall peak to peak velocity decreased was due to changes in both systole and diastole.

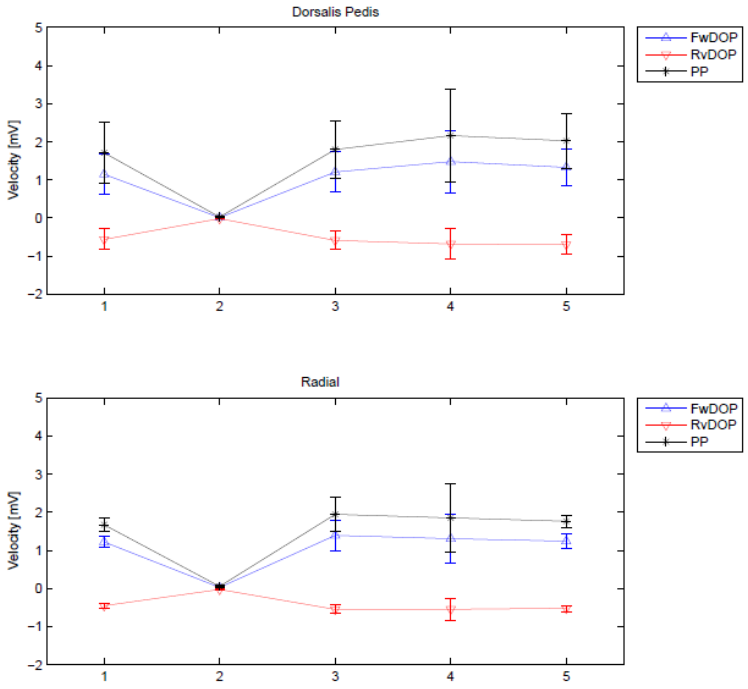

Figure 45: Peak to Peak Results. Dorsalis Pedis test (top), Radial Artery test (bottom). The x=axis shows the phases in the session: 1=Rest1, 2=Occlusion, 3=Rest2, 4=Posture Change, 5=Rest. Y-axis is the velocity in mV.

Frequency Domain Analysis

PSD results also varied from subject to subject. Some subjects showed greater spectral strength in the radial artery while other had a greater spectral strength in the dorsalis pedis artery. This could be due to physiologic differences between subjects. It may also be artifact of sensor position and contact. **Figure 46** compared PSD results of subjects 4 and 6. Subject 4 had a greater spectral content in the lower extremity while Subject 6 had greater spectral content in the upper extremity.

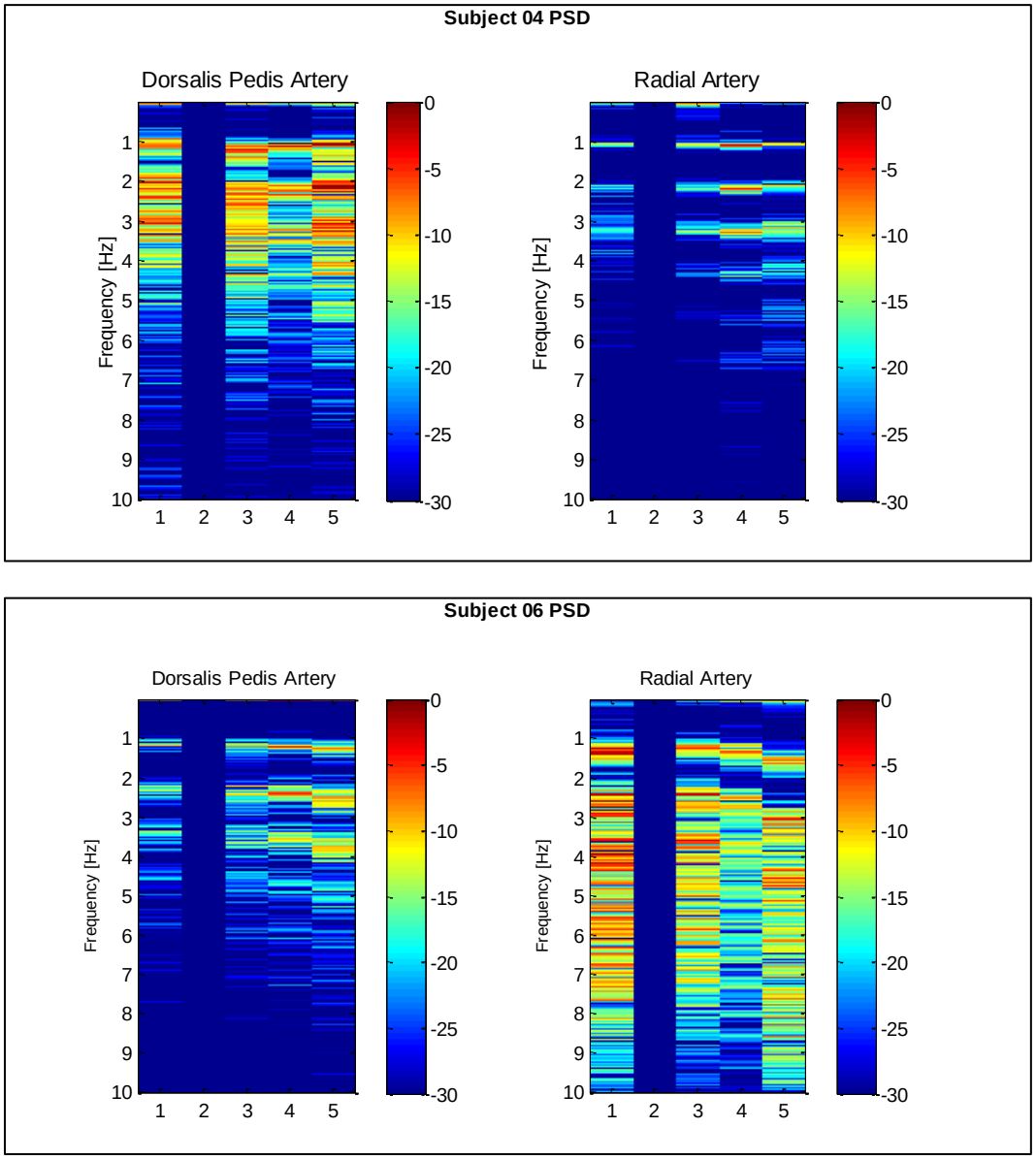

Figure 46: PSD Comparison between two subjects. These subjects show spectral content differences between extremities. (top) Subject 4 dorsalis pedis and radial artery PSD, (bottom) Subject 6 dorsalis pedis and radial artery PSD.

Cumulative Results. The radial artery had a wider spectral content spread compared to the dorsalis pedis artery. The spectra started to attenuate at 6 Hz in the dorsalis pedis artery and started to attenuate after 10 Hz in the radial artery. The magnitude of the frequency in the initial rest phase was three times greater in the radial artery than the dorsalis pedis artery. See

Figure *47* and Figure 48 for the PSD images and Magnitudes respectively.

The spectral content attenuated during the occlusive and posture change phases for both arteries. The dorsalis pedis artery showed less change from phase to phase compared to the radial artery.

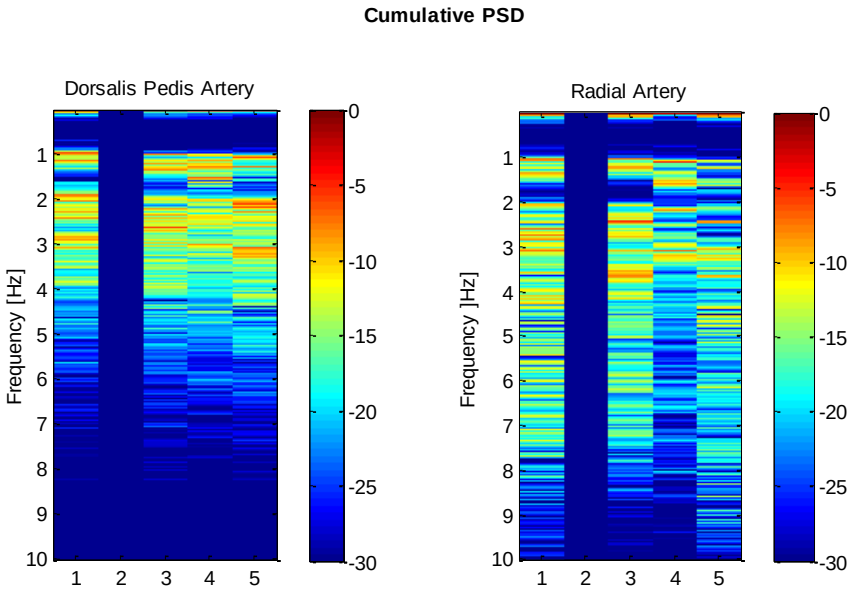

Figure 47: Cumulative Power Spectral Density of dorsalis pedis artery tests (left) and radial artery tests (right). The x-axis indicates the phase in the session.

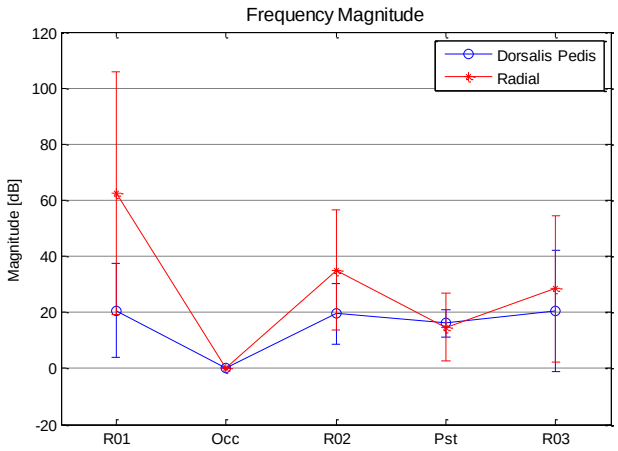

Figure 48: Frequency magnitude from 0-10Hz, for each phase.

CHAPTER 6

DISCUSSION

Vascular responses are in the purview of autonomic regulatory mechanisms. The aim was to develop and implement a capability to profile this response for use in OMT research. The two studies described obtained quantitative measurements at three different locations in the cardiovascular system sites. The Biopac study investigated central activity and skin blood flow, and the spectral Doppler ultrasound project investigated segmental arterial flow. These flow profiles were recorded during an OMT protocol and reactivity tests, and the responses were characterized.

Bilateral Response

The bilateral responses observed across the many analyses presented in this study were confirmed as non-artifact. Rational for bilateral asymmetry in blood flow include metabolic differences between dominant and non-dominant hands, asymmetric drainage lymph flow, or perhaps asymmetric application of treatment. Further analysis would be required to determine the reasons for this, as dominant had of subjects and symmetry of treatment were not recorded. The cumulative PPG results and control groups did not show as distinct of a bilateral response, however, it should be mentioned that the response could be seen within the individual raw data sets. The lack of DC and slow wave components in the PPG signal due to the HPF may have masked the bilateral response in the cumulative results.

Effects of OMT

Time wave Characteristics of Peripheral Flow

To obtain an improved flow blood pressure must increase and systemic resistance must decrease. Blood pressure changes could be a due to parasympathetic activity at the SA node decreasing heart rate, allowing more time for the ventricle to fill during diastole thereby ejecting more blood. It could also be due to increased extent or rate of contractility resulting from sympathetic activation in the ventricle. Sympathetic activation in the blood vessels also reduces systemic resistance. The effects observed during OMT showed that a combination of sympathetic and parasympathetic activation may have occurred in different areas of the heart and sympathetic activity may have occurred in the vascular system.

Table 11
Summary Inc/Dec/NC: Time wave characteristic changes from prior quiescent phase to OMT. Active/peripheral responders/central responders.

	Vessel Diameter (Inverse of Systemic Resistance)	**RBC Velocity** (Blood pressure)	**Volume** (Vessel Diameter*Blood Velocity)	**Heart Rate**
OA-C2	Increase	Increase	Increase	Decrease/ Increase/ Decrease
T1-T4	Decrease/ Increase (Lt only)/ Increase(Lt only)	Decrease/ Increase/ Decrease	Decrease/ Increase/ No Change	Decrease
T8-L2	Increase	Increase	Increase	Increase/ Increase/ Decrease
L5-S	Increase	Decrease/ Increase/ Increase	Decrease/ Increase/ Increase	No Change/ No Change/ Decrease

Frequency Components of Peripheral Flow

The increase in spectral content is due to a combination of AM and FM modulation of the carrier frequency, or HR. Increased spectral content due to increase in sidebands are due to FM modulation, or activity from the SA node. AM modulation is due to myogenic activity, resulting in an increased carrier frequency magnitude and decreased sidebands. AM and FM modulation are additive (Kamal 1989).

In the active group, bandwidth and magnitude increased in the slow wave, fundamental and harmonic components. The peripheral responders had greater spectral content in the 0.5-1.5 Hz range, indicating that treatments resulted in AM modulation, or by local sympathetic induced myogenic activity. Central responders had greater spectral content below 0.5Hz during OMT, indicating that treatments resulted in FM modulation, or parasympathetic influenced SA activity.

The most noticeable changes of all frequency ranges analyzed were in the harmonics. These components were present in the active group and decayed in the control group. In the responder groups the spectral content increased in magnitude during OMT. Per Hsiu et al. (2012), the harmonic components in the PPG PSD are coordinate with blood pressure wave from the radial artery. As blood pressure wave increases, more blood is supplied to the finger pulp, and coordinately, the harmonic content increases. Using this rational, we could say that microvascular blood flow increased during OMT. However, this would need to be validated. The spectral Doppler ultrasound device combined PPG sensor could be used to validate this in a future study.

HR and HRV

The EKG analysis showed that the heart rate did change during OMT. The peripheral responder group had the most elevated initial heart rate, at a mean of 74 BPM. As described earlier, an elevated heart rate indicates somatic dysfunction. Therefore, to the clinician, subjects with greater initial heart rates have the most to gain from therapy. Furthermore, the peripheral responders experienced the greatest decrease in heart rate post session, ending at 70 BPM. For both responder groups, HR decreased during OMT.

Changes were noted in HRV, yet there was no dominant trend. Dominant trends were in noted in the individual LF and HF ranges. The LF magnitudes decreased during OMT and HF magnitudes increased during OMT, excluding T8-L2. Per the literature, this data described a decrease in sympathetic activity and increase in parasympathetic activity (Lewis 2005) (Delaney 2001) (Eur 1996). Such autonomic changes result in decrease in heart rate, which is one goal of OMT. Henley et al. (2008) interpreted a steady HRV (from pre tilt, to tilt to post tilt), as sympathoexitetory inhibition, while Purdy et. al (1996) reviewed both blood flow parameters in coordination with HRV and attributed the trend to parasympathetic excitation. As such, interpretations of the HRV results from this study are not conclusive. We may only note that changes have occurred during OMT.

Spectral Doppler Ultrasound Project

In a proper Trendelenburg position, the table that the subject lies on should be tilted, so that the entire body is tilted at a 15-30 degree angle, with head down and legs above level of heart. The purpose of the position is to use gravitational forces to improve venous return and improve load on the ventricles, thereby

increasing cardiac output and stroke volume. It was originally developed in assisting with abdomen surgery. It was classically used as a first aid in cases of shock and hypotensive patients. Current studies disprove the effectiveness of the Trendelenburg position. In one such study, the subject was inclined at a 6 degree position. The expected hemodynamic effects in normal subjects did not persist beyond five minutes, and venous return was ultimately impeded, attributed to gravitational force on abdomen organs (Summers 2009). In the Doppler ultrasound project, the subject was not tilted, but the legs were inclined at the hip, no bend at the knee. The results from this lower extremity posture change showed changes in systole and diastole. In the dorsalis pedis artery, diastolic peak decreased thereby producing an increased EDV. The systolic peak increased, indicating that the blood ejected from the ventricle increased during posture change. The resulting PP velocity increased, indicating that the contractility of the heart increased, where blood velocity improved. The expected response was a slowing of blood velocity, and a smaller peak to peak value. However, the actual results agree with literature on the Trendelenburg position (Summers 2009). In the radial artery, both systolic and diastolic peaks decreased during posture change. This result can be explained by an increase in systemic resistance due to gravitational forced on the blood in the upper limb. The decreased blood pressure resulted from a decrease in ESV. The PP velocity decreased, indicating that the contractility of the heart was decreased.

Changes in systole and diastole represent autonomic activity of the heart. Heart rate is primarily dependent on changes in diastole (Rhodes). Systole is primarily dependent on ventricular contraction. In light of the reactivity tests performed, it was evident that the radial and dorsalis pedis arteries showed physiological differences, where the dorsalis pedis had a dampened blood velocity as compared to the radial artery.

Limitations

Variability was high in this study, more so in the active group compared to the control group. This variability even persisted in the subset responder groups. This indicates varying subject to subject levels of blood flow and hemodynamics. Also, the effects of OMT in asymptomatic subjects are expected to be subtle, as such, the high amounts of variability may masks the subtleties.

Some aspects of the method were difficult to standardize. For example, intensity of applied therapy required to attain homeostasis per subject differed. In this study the standardization factor was the tenderness rating reported by the subject, which is a subjective measure and not qualitative.

Sensors positioning and fastening was also difficult to standardize. The sensors are highly susceptible to subject movement, sensor position and contact. Care was taken to apply the sensor in a way that would obtain the maximum signal strength. However, this method was not standardized. Gains in the software also varied based up on the subjects measured flow.

Appropriate statistical analysis methods were could be further refined to better assess the trends seen in the frequency domain analysis. The approach taken at this phase of the program was that one of an exploratory study and if assumptions regarding the sample size and normal distribution of data sets were met, the analysis would have been appropriate.

Future Work

As this was a preliminary study, many improvements in experimental design, clinical procedure and data analysis were made evident throughout the study. First, procedural improvements would enhance this study. The hyperthermia wrap was not successful in most trials. A better method of elevating the skin temperature would be needed. Secondly, standardization of test methods and measurements would need to be discussed in full. The inclusion of a sham and touch only procedures are often included in OMT research. Future studies could be designed to understand sham itself, and then subsequently addition of sham to the protocol.

Another area of improvement would be in the data acquisition system. The data acquisition is highly dependent on sensor to skin contact. A standardization of sensor positioning and fastening would strengthen the study. Removal of the HPF on the PPG sensor would add the DC and slow wave components back into the waveform. This may add relevant information on gross changes of blood pooling in the tissue.

Experimental design changes would also serve to improve the study. A larger sample population would increase statistical power. Also, subject selection that included responders only may increase the power of the results. Responders generally had higher heart rates (>70 BPM). Further inclusion criteria for asymptomatic subjects who would be likely responders would need further discussion.

A combined Biopac and spectral Doppler ultrasound technique in a singular study would provide broader vascular profile. Effects on respiration, the right side of the circulatory system, would also increase the cardiovascular profile.

Further areas of improvement include post processing. Spectral estimation techniques could be improved upon. The main spectrum of clinical value is in the very low frequencies (< 0.1 Hz). Lower frequencies contain cardiac activity that may provide more evidence of induced autonomic activity due to OMT. Also, a focus on heart rate variability would be a logical next step in this study. HRV is more and more used in clinical diagnosis and prognosis, and an advanced HRV analysis would certainly add value to understanding cardiovascular response to OMT effects. Also, it would be of interest to examine the correlation between arterial blood pressure and harmonics >2Hz. It is generally accepted that harmonics are of no clinical value (Kamal 1989). However, the blood flow data in this study showed that harmonics persisted during active OMT. Understanding of the harmonics would perhaps provide further information on the filtering, amplification and attenuating effects that the endothelium and precapillary sphincter on blood flow.

Other areas of interest could further focus on the physiologic effects in asymptomatic subjects. For example, the duration of the treatment effect is not well understood. It is thought that the severity and chronicity of a subject's ailment contribute to the efficacy and duration of the effect. It would be interesting to see the duration of the effect after treatment over a group of asymptomatic responders, and then see how the effect duration varies in symptomatic subjects. Figure 1 below shows a subject with increased PPG PP value into the rest phase for almost 1.25 seconds.

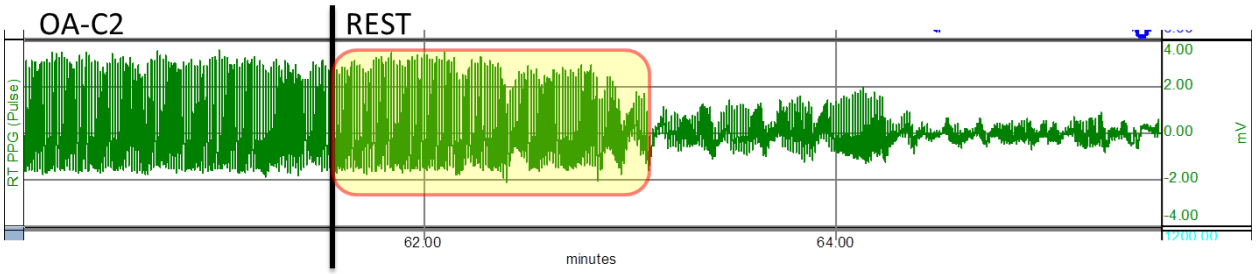

Figure 49: Duration of treatment effect. Subject 14: OA-C2 to Rest phase.

Conclusion

The present study investigated the role of OMT in cardiovascular responses. A clinical study was design for testing these effects. Data analysis was completed for multiple biosignals. Findings suggest that OMT produced significant peripheral flow changes from baseline. Autonomic and non-autonomic effects were not isolated in this study so influences cannot be directly attributed to autonomic balancing. However mechanisms that induce these changes include autonomic mechanisms and suggest that they may be involved.

REFERENCES

[1] Abdollahi, Zahra, Justin P. Phillips, Panayiotis A. Kyriacou (2013). Evaluation of a combined reflectance photoplethysmography and laser Doppler flowmetry surface probe. *35th Annual International Conference of the IEEE EMBS, July 3-7.* Osaka, Japan.

[2] Allen, John, Frame, John R, Murray, Alan (2002). Microvascular blood flow and skin temperature changes in the fingers following a deep inspiratory gasp. *Physiologic Measurement*,23,356-373. (http://iopscience.iop.org/0967-3334/23/2/312)

[3] Allen, John. (2007). Photoplethysmography and its application in clinical physiological measurement. *Physiological Measurement*. 28:R1-R39. doi:10.1088/0967-3334/28/3/R01.

[4] Almond, Nicholas E., Jones, Deric O. (1988). Noninvasive measurement of the human peripheral circulation: Relationship between laser Doppler flowmeter and photoplethysmograph signals from the finger. *Angiology, 39*, 819-829.

[5] Anderson, Gunnar B. J., Lucente, Tracy, Davis, Andrew M., Kappler Robert, E., Lipton, James., Leurgans, Sue (1999). A comparison of osteopathic spinal manipulation with standard care for patients with low back. *The New England Journal of Medicine, 34*(19), 1426-1431.

[6] Askenasy, J.J.M. MD, PhD, N. Askenasy MD, PhD. (1996) Inhibition of muscle sympathetic nerve activity during yawning. *Clinical Autonomic Research*. 6:237-239.

[7] Azhari, H. (2010). *Basics of Biomedical Ultrasound for Engineers.* Wiley-IEEE press. DOI: 10.1002/9780470561478

[8] Beraia, Merab (2010). Arterial pulse impact on blood flow. *Health, 2*(6), 532-540. doi:10.4236/health.2010.26080.

[9] Bergstrand, Sara, Lindberg, Lars, Goran, Ek, Anna-Christina, Linden, Maria, Lindgren, Margareta .(2009). Blood flow measurements at different depths using photoplethysmography and laser Doppler techniques. *Skin Research and Technology*,*15,* 139-147. doi: 10.1111/j.1600-0846.2008.00337.x.

[10] Berntson, Bary G., Bigger, Thomas, Eckberg, Dwain L., Grossman, Paul, Kaugmann, Peter, G., Nagaraja, Haikady, N., Porges, Stephen W., Saul, Phillip J., Stone, Peter H., Van Der Molen, Maurits W. (1997). Heart rate variability: Origins, methods and interpretive caveats. *Psychophysiology 34*, 623-648.

[11] Boron, Walter F., Boulpaep, Emile L.(2012). *Medical Physiology: A Cellular and Molecular Approach.* Philadelphia, PA: Saunders

[12] Bracic, Maja, Stefanovska, Aneta (1998). Wavelet-based analysis of human blood-flow dynamics. *Bulletin of Mathematical Biology, 60,* 919-935.

[13] Brodal, Per (2010). *The Central Nervous System: Structure and Function, 4th edition.* New York, NY: Oxford University Press.

[14] Brolinson, Guunar P., McGinley, Sarah M. G., Kerger Shawn (2008). Osteopathic manipulative medicine and the athlete. *Current Sports Medicine Reports, 7*(1), 49-56.

[15] Celander, E., A.J. Koenig, D.R. Celender PhD. (1968). *Journal of American Osteopathic Association.* 67:1037-1038.

[16] Christen, Samuel, Delachaux, Anne, Dischl, Benoit, Golay Sandrine, Liaudet, Lucas, Feihl, Francios, Waeber, Bernard (2004). *Cardiovascular Pharmacology, 44*(6), 659-664.

[17] Coulon, P., Constans, J., Gosse, P. (2012). Impairment of skin blood flow during post-occlusive reactive hyperemia assessed by laser Doppler flowmetry correlates with renak resistive index. *Journal of Human Hypertension, 26,* 56-63.

[18] Early, Brian E., Luce, Helen (2010). An introduction to clinical research in osteopathic medicine. *Primary Care Clinical Office Practice, 37*, 49-64.

[19] Estrada, Christine, Varas, Grace, Busch, Gregory (2010). Osteopathic manipulative medicine in palliative care. *Journal of Pain and Symptom Management, 39*(2),361-362.

[20] Eun, Hee Chul (1995). Evaluation of skin blood flow by laser Doppler flowmetry. *Clinics in Dermatology, 13*, 337-347.

[21] Fichera, A.P., D.R. Celander. (1969). Effect of osteopathic manipulative therapy on autonomic tone as evidenced by blood pressure changes and activity of the fibrinolytic system. *Journal of American Osteopathic Association.* 68:1036-1038.

[22] Chila, Anthony and the American Osteopathic Association (2010). *Foundations of Osteopathic Medicine.* Philadelphia, PA: Lippincott Williams & Wilkins

[23] Freccero, Carolin, Frank Holmlund, Siv Bornmyr, Jan Castenfors, Anne-Marie Johansson, Goran Sundkvist, Henry Svensson, Per Wollmerb. (2003).

Laser Doppler perfusion monitoring of skin blood flow at different depths in finger and arm upon local heating. *Microvascular research*. 66:183-186.

[24] Fredriksson, Ingemar, Larsson, Marcus, Stromber, Tomas (2009). Measurement depth and volume in laser Doppler flowmetry. *Microvascular Research 78,* 4-13. doi:10.1016/j.mvr.2009.02.008.

[25] Foo, Jong Y. A., Lim, Chy S., Wilson, Stephen J. (2009). Photoplethysmographic assessment of hemodynamic variations using pulsatile tissue blood volume. Angiology, 59(6), 745-752. DOI: 10.1177/0003319708314245

[26] Fullerton, A, Stocker, M, Wilhelm, K. P., Wardell, K., Anderson, C., Fischer, T., Nilsson, G. E., Serup, J. (2002). Guidelines for visualization of cutaneous blood flow by laser Doppler perfusion imaging. *Contact Dermatitis, 46,* 129-140.

[27] Gevitz, Norman (2001). Researched and demonstrated: inquiry and infrastructure at osteopathic institutions. *Journal of the American Osteopathic Association, 101*(3), 174-182.

[28] Gevitz, Norman (2004). *The Dos: Osteopathic Medicine in America*. Baltimore, MD: The Johns Hopkins University Press.

[29] Grim, David, R., Cunningham, Brian M, Burke, Jeanmarie, R. (2005). Autonomic nervous system functions among individuals with acute musculoskeletal injury. *Journal of Manipulative and Physiological Therapeutics, 28*(1), 44-51.

[30] Hall, John E. (2011). Textbook of Medical Physiology. Philadelphia, PA: Saunders Elselvier.

[31] Henley, Charles E., Douglas Ivins, Miriam Mills, Frances K. Wen, Bruce A. Benjamin. (2008). Osteopathic manipulative treatment and its relationship to autonomic nervous system activity as demonstrated by heart rate variability: a repeated measures study. *Osteopathic Medicine and Primary Care.*

[32] Hoi, Yiemeng, Wasserman, Bruce A., Xie, Yuanyuan J., Najjar, Sammer S., Ferruci, Kuigi, Lakatta, Edward G., Gerstenblith, Gary, Steinman, David (2010). Characterization of volumetric flow rate waveforms at the carotid bifurcations of older adults. *Physiological Measurement, 31*, 291-302. doi:10.1088/0967-3334/31/3/002.

[33] Holland, Christy, K., Brown, Janis, M., Scoutt, Leslie, M., Taylor, Keneth J. W. (1998). Lower extremity volumetric arterial blood flow in normal subjects. *Ultrasound in Medicine and Biology, 24*(8), 1079-1086.

[34] Howell, Joel D. (1999). The paradox of osteopathy. *The New England Journal of Medicine.* 341(19):1465-1468.

[35] Hsiu, Hsin, Wei-Chen Hsu, Bo-Hung Chen, Chia-Liang Hsu. Differences in the microcirculatory effects of local skin surface contact pressure stimulation between acupoints and nonacupoints: possible relevance to acupressure. (2010). *Physiological Measurement.* 31:829-841.

[36] Hsiu H., C. L. Hsu, C. T. Chen, W. C. Hsu, H. F. Hu, and F. C. Chen (2012). Correlation of harmonic components between the blood pressure and photoplethysmography waveforms following local-heating stimulation. *International Journal of Bioscience, Biochemistry and Bioinformatics, 2*(4), 248-253.

[37] Humeau, Anne, Benjamin Buard, Guillaume Mah´e, Fran¸cois Chapeau-Blondeau, David Rousseau, Pierre Abraham. (2010). Multifractal analysis of heart rate variability and laser Doppler flowmetry fluctuations: comparison of results from different numerical methods. *Physics in Medicine and Biology.* 55:6279-6297.

[38] Jaff, Micheal R. (2002). Lower extremity arterial disease Diagnostic aspects. *Cadiol Clin 20:* 491-500.

[39] Johnson, Shirley M, Kurtz, Margot E. (2001). Diminished Use of Osteopathic Manipulative Treatment and Its Impact on the Uniqueness of the Osteopathic Profession. *Academic Medicine, 76*(8), 821-828.

[40] Jowsey, Pete, Jo Perry. (2010). Sympathetic Nervous system effects in the hands following a grade III postero-anterior rotator mobilization technique applied to T4: A randomized, placebo-controlled trial. *Manual Therapy.* 30:1-6.

[41] Kamal, A. A. R., Harnes, J. B., Irging, G., Mearns, A. J. (1989). Skin photoplethysmography – a review. *Computer Methods and programs in Biomedicine, 28*, 257-269.

[42] Karason, Agust B., Drysdale, Ian P. (2003). Somatovisceral response following osteopathic HVLAT: A pilot study on the effect of unilateral lumbosacral high-velocity low-amplitude thrust technique on the cutaneous blood flow in the lower limb. *Journal of Manipulative and Physiological Therapeutics, 26* (4), 220-225. doi: 10.1016/S0161-4767(02)54110-5.

[43] Katz, Murray A. (1978). Dissociation of acetylcholine-induced responses of arteriolar resistance vessels and precapillary sphincter-like arterioles. *Microvascular Research, 16*, 133-140.

[44] Kierszenbaum, Abraham L., Tres , Laura L.., (2012). Histology and Cell Biology: An Introduction to Pathology. Philadelphia, PA: Elsevier Saunders.

[45] Kilpatrick, D, Johnston, P. R. (1994). Origin of the electrocardiogram. *IEEE Engineering in Medicine and Biology, August/September Issue*, 479-486.

[46] King, Hollis H. (2002). Osteopathy in the cranial field: Uncovering challenges and potential applications. *Journal of the American Osteopathic Association 107(*7), 367-368.

[47] Knotzer, Hans, Walter R. Hasibeder. (2007). Microcirculatory function monitoring at the bedside – a view from the intensive care. *Physiological Measurement.* 28:R65-R68.

[48] Kvernmo, Hebe Desiree, Stefanovska, Aneta, Kirkeboen, Knut Arvid (1999). Oscillations in human cutaneous blood perfusion signal modified by endothelium-dependent and endothelium-independent vasodilators. *Microvascular Research, 57*, 298-309.

[49] Lefrandt, J.D., E. Bosma, P.H. N. Ooman, J. H. Hoeven, A.M. Room, A.J. Smit, K. Hoogenberg. (2003). Sympathetic mediated vasomotion and skin capillary permeability in diabetic patients with peripheral neuropathy. *Diabetologia*. 46:40-47.

[50] Loukas, Marios, Abel, Nicole, Tubbs, Shane R., Grabska, Joanna, Birungi, Judith, Anderson, Robert H. (2011). The cardiac lymphatic system. *Clinical anatomy 24,* 648-691.

[51] Makin, Inder, Joshua Hope, Deborah Heath(2012). Development and Implementation of a Long-term Multisignal Logging Utility for Peripheral Vascular Flow. Journal of Ultrasound Med. Vol 31. S18-S19.

[52] Mallini, Alberto, Pagani, Massimo, Lombardi, Federico, Cerutti, Sergio (1991). Cardiovascular neural regulation explored in the frequency domain. *Circulation, 84*(2), 482-492. doi: 10.1161/01.CIR.84.2.482.

[53] Miller, Arnold, Evelyn Celander, D.R. Celander, PhD. (1967). Effect of soft tissue manipulative therapy and factors regulating blood pressure. *Journal of American Osteopathic Association.* 66:990-991.

[54] Milnes, Kate, Moran, Robert, W. (2007). Physiological effects of CV4 cranial osteopathic technique on autonomic nervous system function: A preliminary investigation. *International Journal of Osteopathic Medicine, 10*, 8-17.

[55] Moor Instruments (2009). Basic theory and operating principles of laser Doppler blood flow monitoring and imaging (LDF &LDI), Issue 1. Retrieved from www.moor.co.uk.

[56] Murthy, V.S. I, Sripad Ramamoorthy, Narayanan Srinivasan, Sriram Rajagopa, M. Mukunda Rao (2001). Analysis of photoplethysmographic signals of cardiovascular patients. *Proceedings of the 23rd EMBS International Conference, October 25-28,* Istanbul, Turkey.

[57] Nitzan, Meir, Babchenko, Anatoly, Khanokh, Boris, Landau, David (1998). The variability of the photoplethysmographic signal – a potential method for the evaluation of the autonomic nervous system. *Physiological Measurement, 19*, 93-102.

[58] Noll, Donald R., Degenhard, Brian F., Morley, Thomas F., Blais, Francis X., Hortos, Kari A., Hensel, Kendi, Johnson, Jane C., Pasta, David J., Stoll, Scott T. (2010). Efficacy of osteopathic manipulation as an adjunctive treatment for hospitalized patients with pneumonia: a randomized controlled trial. *Osteopathic Medicine and Primary Care, 4, 1-13.*

[59] Northup, George W. (1979). *Osteopathic Medicine: An American Revolution.* Chicago, IL: American Osteopathic Association.

[60] Pagani, Massimo, Lombardi, Federico, Guzzettie, Steano, Rimoldi, Ornella, Furlan, Raffeallo, Pizzenelli, Paolao, Sandrone, Giulia, Malfatto, Gabriella, Dell'Orto, Simonetta, Piccaluga, Emanuela, Turiel, Maurizio, Baselli, Guiseppe, Cerutti, Sergio, Malliani, Alberto (1986). Power spectral analysis of heart rate and arterial pressure variabilities as a marker of sympatho-vagal interaction in man and conscious dog. *Circulation Research, 59*(2), 178-193.

[61] Perry, Jo, Green Ann (2008). An investigation into the effects of a unilaterally applied lumbar mobilization technique on peripheral sympathetic nervous system activity in the lower limbs. *Manual Therapy, 13*, 492-499.

[62] Pizzolorusso, Gianfranco, Turi, Patrizia, Barlafante, Gina, Cerritelli, Francesco, Renzetti, Cinzia, Cozzolino, Vincenzo, D'Orazio, Marianna, Fusilli, Paola, Carinci, Fabrizio, D'Incecco, Carmine (2011). Effect of osteopathic manipulative treatment on gastrointestinal function and length of stay of preterm infants: an exploratory study. *Chiropractic and Manual Therapies, 19*, 1-6.

[63] Purdy, W. Randolph DO, Jesse J. Frank, DO, Brent Oliver, DO, PhD. (1996). Suboccipital dermatomyotomic stimulation and digital blood flow. *Journal of American Osteopathic Association*. 96(5):285-289.

[64] Reaz , M. B. I., M. S. Hussain, F. Mohd-Yasin. (2006). Techniques of EMG signal analysis: detection, processing, classification and applications. *Biological Procedures*. 8(1):11-35.

[65] Rhodes, Rodney, Pflanzer, Richard (1996). *Human Physiology, Third Edition*. Philadelphia, PA: Saunders College Publishing.

[66] Rivers, William Evan, Treffer, Kevin, D., glaros, Alan G., Williams, Charlott L. (2008). Short-term hematologic and hemodynamic effects of osteopathic lymphatic techniques: A pilot crossover trial. *Journal of the American Osteopathic Association, 108*(11), 646-651.

[67] Roberts. V. C. (1982). Photoplethysmography – fundamental aspects of the optical properties of blood in motion. *Transactions of the Institute of Measurement and Control*, *4,* 101-106. DOI: 10.1177/014233128200400205

[68] Robinson, Brian F., Stephen E. Epstein, G. David Beiser, Eugene Braunwald. (1996) Control of heart rate by the autonomic nervous system. *Circulation Research*. 19:400-411.

[69] Rossi, M., Carpi, A., Galetta, F., Franzoni, F., Santoro, G. (2006). The investigation of skin blood flowmotion: a new approach to study the microcirculatory impairment in vascular diseases?. *Biomedicine and Pharmacotherapy, 60*, 437-442.

[70] Rossi, M., A. Carpi, F. Galetta, F. Franzoni, G. Santoro. (2008). Skin vasomotion investigation: a useful tool for clinical evaluation of microvascular endothelial function? *Biomedicine and Pharmacotherapy 62*: 541-545.

[71] Roustit, M., Blaise, S., Milet, C., Cracowski, J. L. (2010). Reliability and methodological issues of skin post-occlusive and thermal hyperemia assessed by the single-point laser Doppler flowmetry. *Microvascular Research, 79,* 102-108.

[72] Roustit, Matthieu, Jean-Luc Cracowski (2013). Assessment of endothelial and neurovascular function in human skin microcirculation. *Trends in Pharmacological Sciences, 34*(7): 373-384.

[73] Shelley, Kirck, H (2007). Photoplethysmography: Beyond the calculation of arterial oxygen saturation and heart rate. *Anesthesia and Analgesia, 105*(6), S31-S36.

[74] Shibasaki, Manabu, Ramussen, Peter, Secher, Niels, Crandall, Craig (2009) Heural and non-neural control of skin blood flow during isometric handgrip exercise in the heat stressed human. *Journal of Physiology, 587.9:* 2101-2107.

[75] Still, Andrew Taylor (1908). *Autobiography of Andrew T. Still – with a history of the discovery and development of the science of osteopathy.* Self-published. Kirksville, Mo.

[76] Su, Yi-Ju, Wan-An Lu, Gau-Yang Chen, Margaret Liu, Hsiang-Tai Chao & Cheng-Deng Kuo (2011). Power spectral analysis of plethysmographic pulse waveform in pregnant women. *Journal of Clinical Monitoring and Computing, 25*(3), 183-191. DOI 10.1007/s10877-011-9291-3.

[77] Tozzi, Paulo (2012) Selected fascial aspects of osteopathic practice. *Journal of Bodywork and Movement Therapies, 16*: 503-519. doi:10.1016/j.jbmt.2012.02.003.

[78] Traikov, Lubomir, I. Antonov, J. Petrova. (2011). Signal processing and wavelet analysis of simultaneously registered blood pressure and laser Doppler flow signals during extremely low frequency electromagnetic field exposure in humans in vivo. *Environmentalist*. 31:187-195.

[79] Voigt, Karen, Liebnitzky, Jan, Burmeister, Ute, Shivonen-Riemenschneider, Henna, Beck Matthias, Voigt, Roger, Bergnamm, Anjte (2011). Efficacy of osteopathic manipulative treatment of female patients with migrane: Results of a randomized controlled trial. *The Journal of alternative and complementary medicine, 17*(3), 225-230.

[80] Walkowski, Stevan, Singh Manindra, Puertas, Juan, Pate, Michelle, Goodrum, Kenneth, Benecia Fabian (2014). Osteopathic manipulative therapy induces early plasma cytokine release and mobilization of a population of blood dendritic cells. *Immune Parameters and Osteopathic Manipulation, 9*(3), 1-12.

[81] Wallin, Gunnar B. (1990). Neural control of human skin blood flow. *Journal of the Autonomic Nervous System, 30,* S185-S190.

[82] Wu, Mingyuan, Bengt Linderoth, Robert D. Foreman. (2008). Putative Mechanisms behind effects of spinal cord stimulation on vascular diseases: A review of experimental studies. *Autonomic Neuroscience: Basic and Clinical.* 138:9-23.

[83] Young, Barbara, O'Dowd, Geraldine, Woodford Phillip (2014). *Wheater's Functional Histology: A Text and Colour Atlas*. Sixth Edition. Philadelphia, PA: Churchill Livingstone.

[84] Zegarra-Parodi ,Rafael, Park ,Peter Yong Soo, Heath, Deborah M., Makin, Inder Raj S., Degenhardt, Brian F., Roustit, Matthieu (2014). Assessment of skin blood flow following spinal manual therapy: A systematic review. *Manual Therapy,XXX*,1-22.

APPENDIX A

IRB APPROVAL

IRB Approval

DATE: September 20, 2010

TO: Deborah M. Heath, DO
Inder Makin, MD, PhD

FROM: ATSU-Mesa IRB Committee

SUBJECT: Research Proposal, IRB tracking #2010-80

Thank you for the opportunity to review the research proposal, *Investigation of Peripheral Blood Flow Response to Provocation Tests Including Osteopathic Digital Pressure on Vertebral Segments.*

After reviewing the proposal, the ATSU-Mesa IRB committee believes that this proposal meets the minimal risk guidelines established by A.T. Still University of Health Sciences. Thank you for your time and attention to detail in completing the IRB proposal submission process. You may now proceed with data collection.

If any changes are made to the protocol following this approval, you must complete and submit the request for changes form located on the IRB website.

If you have any questions, please feel free to call or write.

Respectfully,

Curt Bay, PhD
Chair, ATSU-Mesa Institutional Review Board
Arizona School of Health Sciences
A.T. Still University
5850 East Still Circle
Mesa, AZ 85206
Main: (480) 219-6000
Office: (480) 219-6037
rcbay@atsu.edu

APPENDIX B

OMITTED SESSIONS

Table 12: Table of Experimental Trials: This table shows the active group, control group and provides descriptor on which sessions were omitted from analysis.

Session #	"Subj. #"	Date	Initials	Gender	Age	Subject Set Up	Omission	Experimental Group
1	"5"	5/18/10	AM	M	30	Active provocation	Short Session	NA
2	"6"	5/25/10	MG	F	30	Active provocation	Short Session	NA
3	"7"	6/01/10	DR	F	58	No provocation		C
4	"8"	6/02/10	TH	F	33	Occlusion and Hyperthermia Only	Short Session, broken LDF lead, Systemic stimuli Session only	NA
5	"9"	8/03/10	DR*	F	58	Active provocation	Short Session	NA
6	"10"	8/04/10	MG*	F	30	Active provocation	Short Session, OMT only session	NA
7	"11"	8/10/10	RB	M	28	Active provocation		A
8	"12"	8/11/10	TH*	F	33	No Provocation		C
9	"13"	8/17/10	SW	F	28	Active provocation		A, Rp
10	"14"	8/18/10	KS	F	29	Active provocation		A, Rp, Rc

Session #	"Subj. #"	Date	Initials	Gender	Age	Subject Set Up	Omission	Experimental Group
11	"15"	9/22/10	TH**	F	33	Active provocation	Broken Lead	NA
12	"16"	11/09/10	CN	M	19	Active Provocation		A
13	"17"	02/02/11	"SW*"	F	28	Active Provocation **R "Subj 13"**		A, Rp
14	"18"	02/15/11	"CN*"	M	19	Active Provocation **R "Subj 16"**		A
15	"19"	02/21/11	"KS*"	F	29	Active Provocation **R "Subj 14"**		A, Rp, Rc
16	"20"	05/18/11	JF	F	42	Active Provocation		A, Rc
17	"21"	07/18/11	JF*	F	42	No Provocation		C
18	"22"	08/09/11	JF-N	F	39	Active Provocation		A, Rc
19	"23"	09/21/11	LW	F	39	Active Provocation		A, Rc
20	"24"	09/23/11	TJJr	M	34	Active Provocation		A, Rp
21	"25"	09/26/11	RC	F	24	Active Provocation		A
22	"26"	04/04/12	KH	F	54	Baseline Only		

Session #	"Subj. #"	Date	Initials	Gender	Age	Subject Set Up	Omission	Experimental Group
23	"27"	04/09/12	VD	F	56	Baseline Only	Outlier in hemodynamic response	NA
24	"28"	04/17/12	"LW*"	F	40	Baseline Only **R "Subj 23"**		C
25	"29"	04/24/12	"DH"	F	54	Baseline Only		C
26	"30"	05/11/12	"KH"*	F	54	Active provocation	Noisy data due to sensor and hand positioning	A
27	"31"	10/29/12	"JL"	F	34	Baseline Only		C
28	"32"	11/09/12	"JL*"	F	34	Active Provocation **R "Subj 31"**		A
29	"33"	05/08/13	"BJ"	F	33	Baseline Only		C
30	"34"	05/24/13	"BJ"*	F	33	Active session		A
31	"35"	08/07/13	"JM"	M	41	Baseline Only		C
32	"36"	08/12/13	"JM*"	M	41	**"Simulation" Session**	Sham Session	NA
33	"37"	08/14/13	"JM**"	M	41	Active session		A, Rc

Session #	"Subj. #"	Date	Initials	Gender	Age	Subject Set Up	Omission	Experimental Group
34	"38"	08/17/13	"WM"	F	51	Baseline session		C
35	"39"	08/19/13	"WM*"	F	51	Active session		A
36	"40"	08/21/13	"WM*"	F	51	Baseline session **R "Subj 38"**		C

Table 13: Biopac Sessions recorded and omitted

	Control	Active	**Total**
Sessions Recorded	13	23	**36**
Omitted	2	7	**9**
Total Sessions Used	**11**	**16**	**27**

The Omitted session descriptions are as follows:

Sessions 5, 6, 9 and **10** and were considered "short" sessions by the clinician, while the latter sessions were termed "long" sessions, where the terms "short" and "long" refer to the intensity and duration of the OMT application. Short sessions had lesser in intensity and duration as compared to the longer sessions. The short sessions occurred early on in the study, and after preliminary analysis it was concluded that the "short" sessions yield results similar to the control sessions. In the long sessions the clinician performed the OMT as it would be done on symptomatic subjects, and therefore augmented the results in the raw

data and clinical assessment. This suggests a time dependent threshold, physiologically. For the purpose of this study, the "short" sessions were excluded from the analysis.

Session 8 and **15** were omitted due to broken leads.

Session 30 was omitted because it was too noisy to be utilized in post processing. It was determined that the position of the subjects hands were face down during the session which caused a disturbance with the sensors. In all other sessions the positions of subjects' hands were face up, and therefore this disturbance to the sensors was not present. The disturbances include pressure to the vessels in the finger pulp causing distortion of the signal, or saturated readings where part of the signal is lost due to clipping, and misalignment on the finger pulp causing

Session 10 is an OMP only session, where the first half of the session is baseline only and the last half of the session is the same as the active session, so that only the last four provocations were performed. This study was considered a "short" session and was therefore excluded from analysis. **Session 8** is a non-OMP session, where only the first three systemic provocations were performed, but no OMPs were performed. However, this session had a broken lead and was therefore excluded from analysis.

Subject 27 is an atypical session. All control and active sessions show that the increases in peak to peak value of PPG simultaneously occur with increases in DC value of the LDF signal. And throughout the session for Subject 27, a baseline session, the blood flow and blood volume increased, rather than the decreasing trend found in all other control sessions and some active sessions. Active sessions, specifically responders, did increase if not maintain the signal levels throughout the session. Testing on instrumentation was completed after the session and it was determined that the instrumentation was working appropriately. See sit and standing test in the appendix. Since Subject 27 did not display

the typical behavior it was excluded from the analysis. Further research is required in order to determine the reasons for this atypical behavior. Further subjects are required to determine how common this atypical behavior is.

Subject 27 Outlier Control Session	Subject 07 Typical Control Session
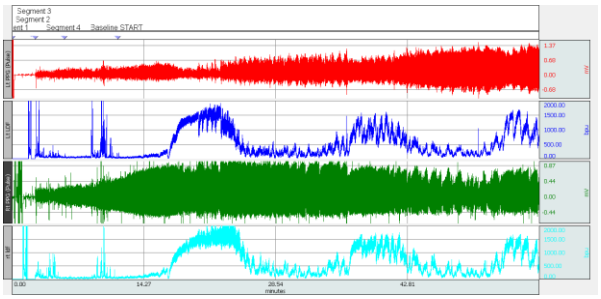	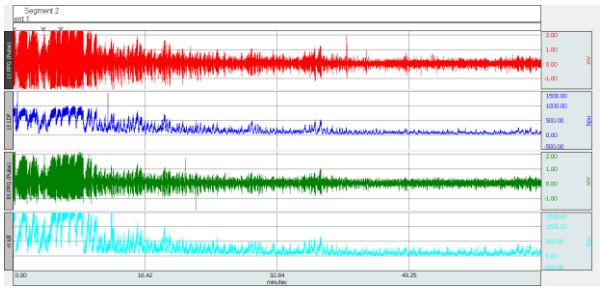

Figure 50: Subject 27 Control Session (left) showing reverse hemodynamics compared to all other control sessions, Subject 07 (right) representative control session. Subject 27 was omitted from the final analysis as it was an outlier in hemodynamic response for control sessions.

APPENDIX C

BIOPAC HARDWARE INSTRUMENTATION AND SOFTWARE SETTINGS

Table 14:
Biopac Hardware and Instrumentation

	Hardware	**Connection**	**Model/Serial No.**
A	3-lead EKG sensor	Master DAQ Box Ch1	SSL2 Electrode 705A1396
B	Room Temp sensor	Master DAQ Box Ch2	SS6L FAST TEMP SN9085138
C	LtPPG sensor	Slave DAQ Box Ch1	SS4LA Pulse SN7054738
D	LtLDF Sensor	LtLDF Signal Conditioner Box	TSD140 SN PR91322
E	Cable from LtLDF Sign al Conditioner to Slave DAQ Box	Analog Channel 1 to Slave DAQ Box Ch 2	BSLCBL14 UIM/IPS-MP35 SN609 0120
F	RtPPG	Slave DAQ Box Ch3	SS4LA Pulse SN7054738
G	RtLDF Sensor	RtLDF Signal Conditioner Box	TSD140 SN PR91302
H	Cable from RtLDF Signal Conditioner Box to Slave DAQ Box	Analog Channel 1 to Slave DAQ Box Ch4	BSLCBL14 UIM/IPS-MP35 SN812 0134
I	Cable Master to Slave DAQ Box	"Analog Output" on Master to "Trigger" BNC input on Slave	OUT2 BNC SN602179
J	Master DAQ Box	Master PC via Biopac MP35 USB cable	MP35 SN MP35A70103726
K	Slave DAQ Box	Slave PC via Biopac MG35 USB cable	MP35 SN MP35A70103715
L	Lt Signal Conditioner Box	NA	LDF100C model IPS100C-1 SN IPS810C0000290
M	Rt Signal Conditioner Box	NA	LDF100C model IPS100C-1 SN IPS810C0000284

Acquisition-Sampling

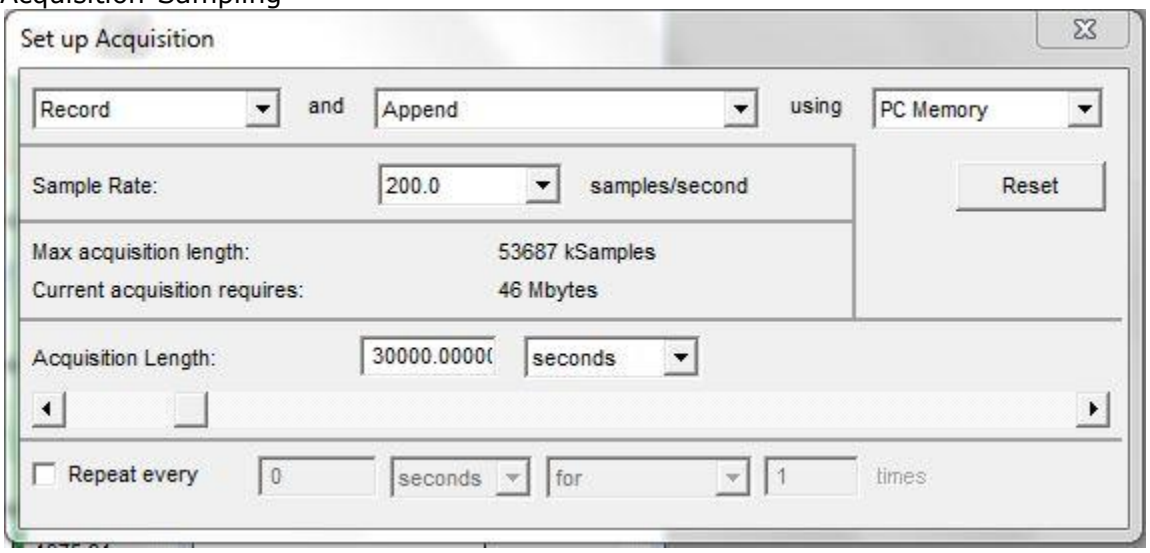

PPF-Filter-HW-Scaling

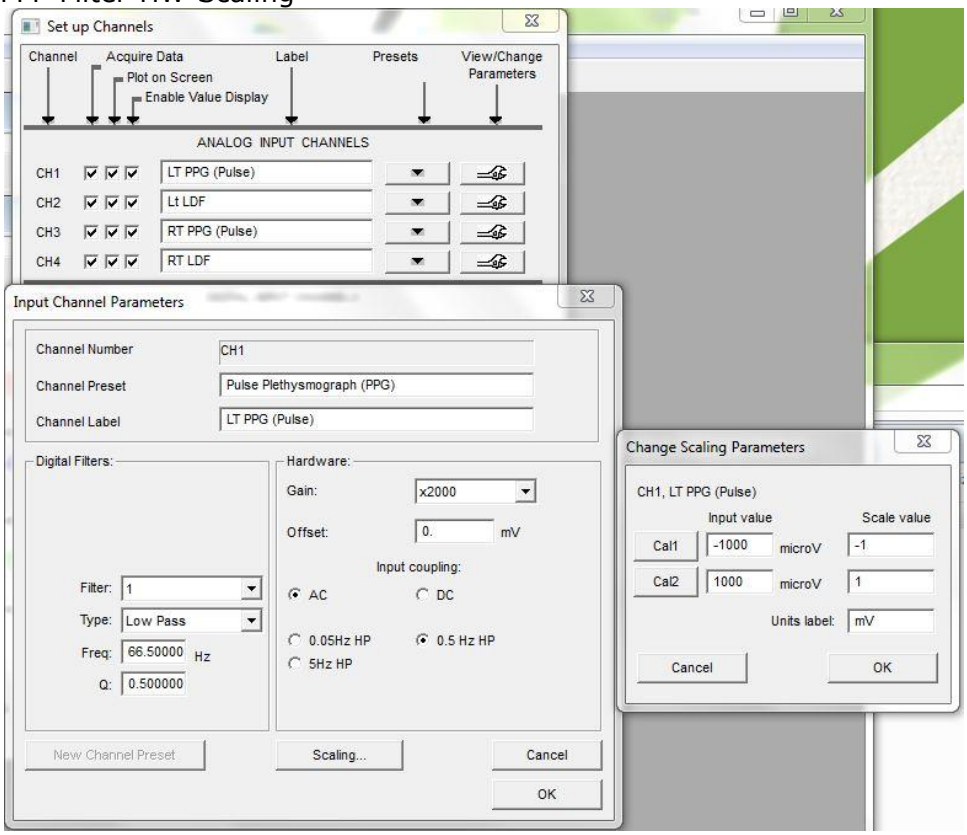

PPG and LDF Filter-HW-Scaling

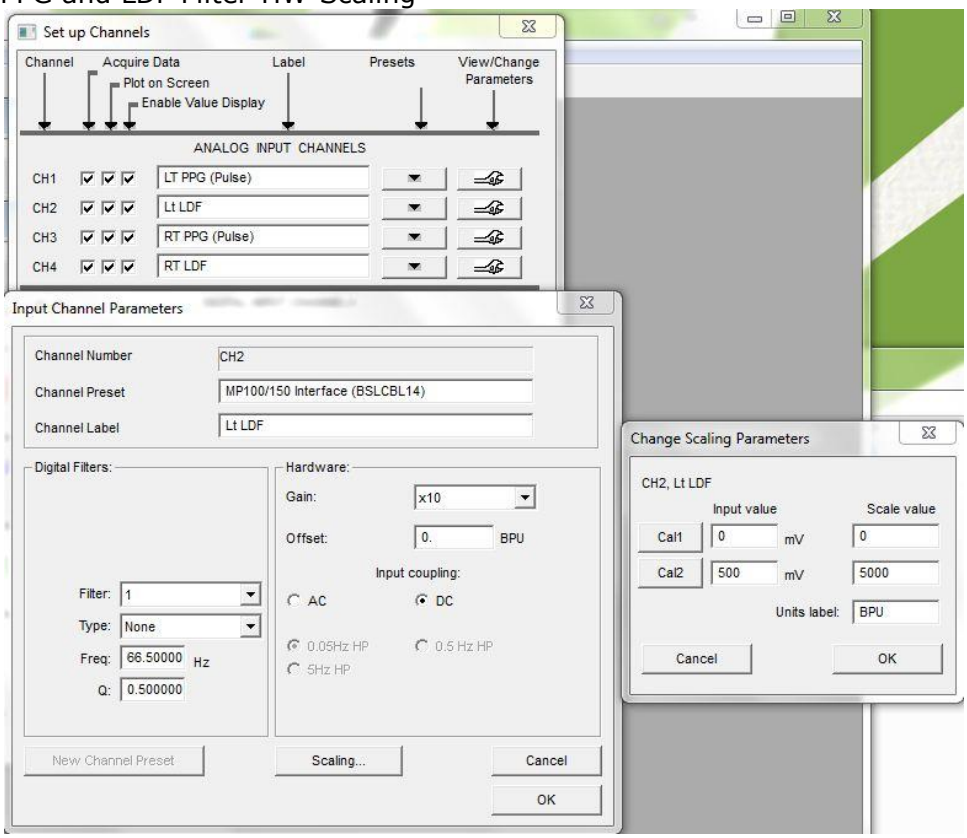

APPENDIX D

BIOPAC SYSTEM TEST FOR HARDWARE VAILDATION

Data Acquisition System Test DATE: 26 September 2011

DAQ system check was performed. The raw data from today's sessions indicated nearly an order of magnitude difference between the right and left side. The first two tests were performed to ensure that the right and left sensors, for both PPG and LDF, were independent. We confirmed that the PPG and LDF signals were independent. The raw data also show a slow wave signal in the LDF data, whereas the PPG data does not have this slow wave. Therefore, the third test conducted was to test the high pass filter on the PPG software setting. The filter was reduced form the default software setting of 0.5 Hz to 0.05Hz. The raw PPG data did show the slow wave after high pass filter setting was reduced.

1. PPG Systemic Check | **Subject: IM**

This test was performed to check if the right and left PPG sensors were appropriately measuring data correctly. The PPG sensors were attached to the index fingers. Data was acquired for approximately two min. Then the channels were swapped and data was acquired again. The channels were swapped back to the original configuration. Each time, data was acquired for approximately 2 min. Regardless of configuration, the left side was always greater in magnitude than the right side. Thus, the sensors were independent.

- Run1: Left finger on Ch1 > Right finger on Ch3
- Run 2: Left finger on Ch3 > Right finger on Ch1
- Run 3: Left finger on Ch1 > Right finger on Ch3

2. LDF Systemic Check | **Subject: IM**

This test was performed similarly to the PPG systemic test described above. The LDF sensors, however, were attached to the middle fingers. NOTE: the PPG sensors were not removed. The raw data will show that all four sensors are activated. Regardless of configuration, the right and left side were within the same range. Thus, the sensors were independent.

- Run 1: Left finger on Ch2 = Right finger on Ch4
- Run 2: Left finger on Ch4 = Right finger on Ch2
- Run3: Left finger on Ch2 = Right finger on Ch4

3. High Pass Filter System Test | **Subject: IM**

Data was first acquired with the default HPF setting. Then it was reduced. Then it was restored to the default setting again. The slow wave was apparent with the reduced filter, and was not apparent with the default. Each acquisition was approximately two minutes.

- Run 1: SW setting on HPF = 0.5Hz : No Slow wave
- Run2: SW setting on HPF = 0.05Hz: Slow wave arises
- Run3: SW setting on HPF = 0.5Hz : No Slow wave

It remains to be determined if the HPF setting will remain at 0.5Hz or reduced to 0.05Hz for subsequent sessions. If the cutoff frequency is reduced, the data can be post processed through a HPF moving the cutoff frequency back to 0.5Hz. In this way the extra low frequency data can be acquired and used for analysis if found to be useful.

APPENDIX E

HEART RATE VARIABILITY SCRIPT VALIDATION

Table 15: Biopac ACQKnowledge Heart Rate Variability Output

1. RR Interval

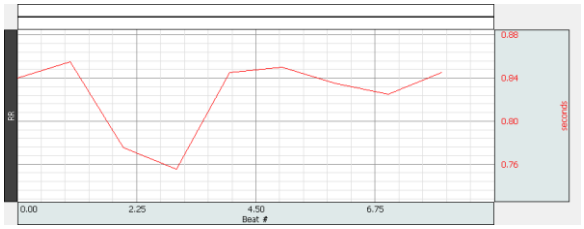

2. Interpolated RR on

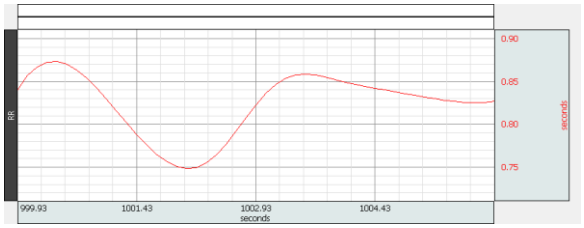

3. Spectrum

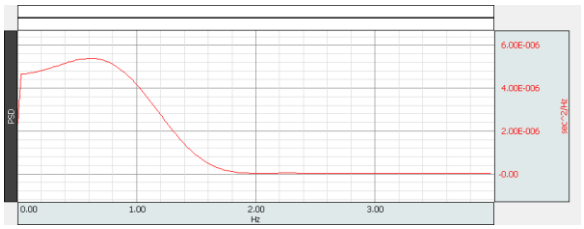

HRV Analysis, CH1, ECG (.5 - 35 Hz)

RR Intervals

0.84

0.855

0.775

0.775

0.845

0.85

0.835

0.825

0.845

Power in the very low frequency band:	1.39E-07	sec^2/Hz
Power in the low frequency band:	5.15E-07	sec^2/Hz
Power in the high frequency band:	1.23E-06	sec^2/Hz
Power in the very high frequency band:	4.42E-06	sec^2/Hz
Sympathetic:	0.295729	
Vagal:	0.704271	
Sympathetic-vagal balance:	0.419907	

APPENDIX F

STATISTICAL ANALYSIS

Mann-Whitney U test

The Mann-Whitney U test using IBM SPSS software was used to test the significance of the data. The Mann-Whitney U test ranks the samples from all groups in order from smallest to large. It then compares the mean rank order from each group. A z-test is then used to determine the if the means of the rank order are significantly different. We cannot reject the null hypothesis if p value is greater than alpha. Alpha is 0.05 or 0.01.

Time Domain statistical analysis was completed for phase by phase comparison across the groups : Data for the analysis are found in the following file: *TimeStats with Summary 2014 10 09 copy for Statistical Analysis.xlsx*

Table 16: Statistical Analysis methods

Analysis	Groupings	Data Set
Between group analysis	Phase 7-15 of: 1) Control to Active 2) Control to Peripheral Responder 3) Control to Central Responder	1) Left PPG RMS 2) Right PPG RMS 3) Left LDF RMS 4) Right LDF RMS 5) Left Volume-Flow RMS 6) Right Volume Flow RMS 7) Heart Rate

Frequency Domain statistical analysis was completed for phase by phase comparison across the groups: Data for the analysis are found in the following file: *FrequencyStats with Summary 2014 10 09 copy for Statistical Analysis.xlsx*

Analysis	Groupings	Data Set
Between group analysis	1) Control to Active 2) Control to Peripheral Responder 3) Control to Central Responder	1) Lt PPG Range 1 [0-0.5Hz] 2) Rt PPG Range 1 [0-0.5Hz] 3) Lt PPG Range 2 [0.5 – 1.5 Hz] 4) Rt PPG Range 2 [0.5-1.5 Hz] 5) Lt PPG Range 3 [1.5 – 3 Hz] 6) Rt PPG Range 3 [1.5-3 Hz] 7) Lt LDF Range 1 [0-0.5Hz] 8) Rt LDF Range 1 [0-0.5Hz] 9) Lt LDF Range 2 [0.5 – 1.5 Hz] 10) Rt LDF Range 2 [0.5-1.5 Hz] 11) Lt LDF Range 3 [1.5 – 3 Hz] 12) Rt LDF Range 3 [1.5-3 Hz]

Null Hypothesis = means are not different, Alternative Hypothesis = means are different.

Statistical Analysis using Parametric Test

Time Domain statistical analysis was completed for mean trend comparison between groups: Data for the analysis are found in the following file: *TimeStats with Summary 2014 10 09 copy for Statistical Analysis.xlsx*

Table 17: Statistical Analysis methods

Analysis	Groupings	Data Set
Between group analysis	Mean Trend of Phase 7-15 of: 1) Control to Active 2) Control to Peripheral Responder 3) Control to Central Responder	1) Left PPG RMS 2) Right PPG RMS 3) Left LDF RMS 4) Right LDF RMS 5) Left Volume-Flow RMS 6) Right Volume Flow RMS 7) Heart Rate

Frequency Domain statistical analysis was completed for mean trend comparison between groups: Data for the analysis are found in the following file:

FrequencyStats with Summary 2014 10 09 copy for Statistical Analysis.xlsx

Analysis	Groupings	Data Set
Between group analysis	Mean Trend of Phase 7-15 of: 1) Control to Active 2) Control to Peripheral Responder 3) Control to Central Responder	1) Lt PPG Range 1 [0-0.5Hz] 2) Rt PPG Range 1 [0-0.5Hz] 3) Lt PPG Range 2 [0.5 – 1.5 Hz] 4) Rt PPG Range 2 [0.5-1.5 Hz] 5) Lt PPG Range 3 [1.5 – 3 Hz] 6) Rt PPG Range 3 [1.5-3 Hz] 7) Lt LDF Range 1 [0-0.5Hz] 8) Rt LDF Range 1 [0-0.5Hz] 9) Lt LDF Range 2 [0.5 – 1.5 Hz] 10) Rt LDF Range 2 [0.5-1.5 Hz] 11) Lt LDF Range 3 [1.5 – 3 Hz] 12) Rt LDF Range 3 [1.5-3 Hz]

APPENDIX G

QUICK ASSESSMENT TOOL

Spectral Doppler ultrasound Quick Assessment Tool

A quick analysis tool was developed using Matlab interactive GUI. This tool was developed for the purpose of providing a quick analysis in a clinical setting. The GUI is shown in Figure 51

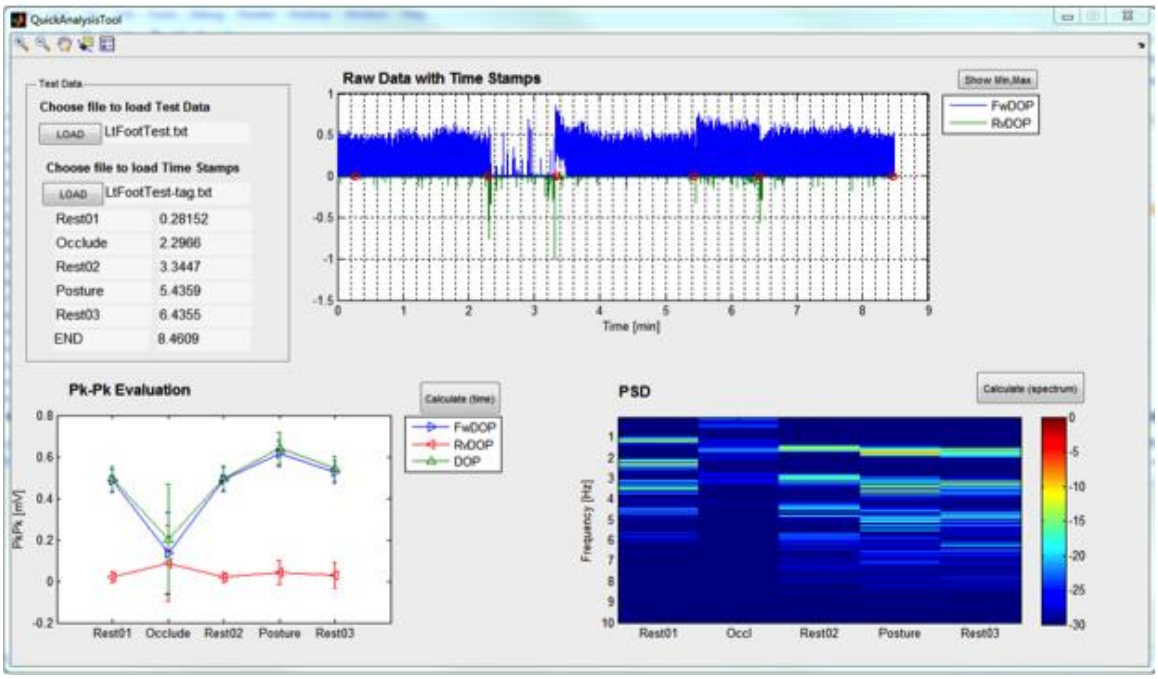

Figure 51: Doppler Project Quick Analysis Took GUI.

APPENDIX H

PERCENT CHANGE TABLES

Percent change Tables

Table 18: Tables of increase and decrease for PPG, LDF, Volume, Left and Right hands

PPG RMS Left

	Control (n=11)			Active (n=16)			P. Resp (n=5)			C. Resp (n=6)		
	Dec	**Inc**	**NC**	**Dec**	**Inc**	**NC**	**Dec**	**Inc**	**NC**	**Dec**	**Inc**	**NC**
Initial to Final	100.0%	0.0 %	0.0 %	100.0 %	0.0 %	0.0 %	100.0 %	0.0%	0.0 %	100.0 %	0.0%	0.0 %
OA-C2	63.6%	27.3 %	9.1 %	31.3 %	56.3 %	12.5 %	20.0 %	80.0 %	0.0 %	33.3 %	50.0 %	16.7 %
T1-T4	63.6%	9.1 %	27.3 %	50.0 %	37.5 %	12.5 %	40.0 %	40.0 %	20.0 %	33.3 %	50.0 %	16.7 %
T8-L2	72.7%	18.2 %	9.1 %	25.0 %	50.0 %	25.0 %	0.0%	100.0 %	0.0 %	16.7 %	66.7 %	16.7 %
L5-S	36.4%	18.2 %	45.5 %	31.3 %	43.8 %	25.0 %	20.0 %	60.0 %	20.0 %	0.0%	66.7 %	33.3 %

PPG RMS Right

	Control (n=11)			Active (n=16)			P. Resp (n=5)			C. Resp (n=6)		
	Dec	**Inc**	**NC**	**Dec**	**Inc**	**NC**	**Dec**	**Inc**	**NC**	**Dec**	**Inc**	**NC**
Initial to Final	100.0 %	0.0 %	0.0 %	81.3 %	12.5 %	6.3 %	40.0 %	40.0 %	20.0 %	66.7 %	16.7 %	16.7 %
OA-C2	54.5 %	18.2 %	27.3 %	50.0 %	43.8 %	6.3 %	40.0 %	60.0 %	0.0 %	33.3 %	50.0 %	16.7 %
T1-T4	54.5 %	18.2 %	27.3 %	50.0 %	31.3 %	18.8 %	40.0 %	40.0 %	20.0 %	50.0 %	50.0 %	0.0 %
T8-L2	54.5 %	18.2 %	27.3 %	25.0 %	56.3 %	18.8 %	0.0%	100.0 %	0.0 %	16.7 %	66.7 %	16.7 %
L5-S	45.5 %	27.3 %	27.3 %	31.3 %	62.5 %	6.3 %	0.0%	80.0 %	20.0 %	0.0%	100.0 %	0.0 %

LDF RMS Left

	Control (n=11)	Active (n=16)	P. Resp (n=5)	C. Resp (n=6)

	Dec	Inc	NC	Dec	Inc	NC	Dec	Inc	NC	Dec	Inc	NC
Initial to Final	100.0 %	0.0 %	0.0 %	81.3 %	12.5 %	6.3 %	60.0 %	20.0 %	20.0 %	83.3 %	0.0%	16.7 %
OA-C2	63.6 %	36.4 %	0.0 %	37.5 %	50.0 %	12.5 %	0.0%	80.0 %	20.0 %	16.7 %	50.0 %	33.3 %
T1-T4	72.7 %	18.2 %	9.1 %	56.3 %	25.0 %	18.8 %	20.0 %	40.0 %	40.0 %	66.7 %	33.3 %	0.0 %
T8-L2	72.7 %	18.2 %	9.1 %	37.5 %	37.5 %	25.0 %	0.0%	100.0 %	0.0 %	50.0 %	33.3 %	16.7 %
L5-S	72.7 %	18.2 %	9.1 %	50.0 %	43.8 %	6.3 %	20.0 %	80.0 %	0.0 %	33.3 %	66.7 %	0.0 %

LDF RMS Right

	Control (n=11)			Active (n=16)			P. Resp (n=5)			C. Resp (n=6)		
	Dec	**Inc**	**NC**	**Dec**	**Inc**	**NC**	**Dec**	**Inc**	**NC**	**Dec**	**Inc**	**NC**
Initial to Final	100.0 %	0.0 %	0.0 %	87.5 %	12.5 %	0.0 %	60.0 %	40.0 %	0.0 %	83.3 %	16.7 %	0.0 %
OA-C2	63.6 %	18.2 %	18.2 %	43.8 %	50.0 %	6.3 %	0.0%	80.0 %	20.0 %	33.3 %	50.0 %	16.7 %
T1-T4	54.5 %	27.3 %	18.2 %	50.0 %	31.3 %	18.8 %	0.0%	60.0 %	40.0 %	50.0 %	33.3 %	16.7 %
T8-L2	45.5 %	27.3 %	27.3 %	37.5 %	50.0 %	12.5 %	0.0%	100.0 %	0.0 %	50.0 %	50.0 %	0.0 %
L5-S	54.5 %	27.3 %	18.2 %	56.3 %	31.3 %	12.5 %	0.0%	80.0 %	20.0 %	50.0 %	33.3 %	16.7 %

Volume RMS -Left

	Control (n=11)			Active (n=16)			P. Resp (n=5)			C. Resp (n=6)		
	Dec	**Inc**	**NC**	**Dec**	**Inc**	**NC**	**Dec**	**Inc**	**NC**	**Dec**	**Inc**	**NC**
Initial to Final	100.0 %	0.0 %	0.0 %	100.0 %	0.0 %	0.0 %	100.0 %	0.0%	0.0 %	100.0 %	0.0%	0.0 %
OA-C2	63.6 %	36.4 %	0.0 %	31.3 %	50.0 %	18.8 %	0.0%	80.0 %	20.0 %	16.7 %	50.0 %	33.3 %
T1-T4	54.5 %	18.2 %	27.3 %	50.0 %	31.3 %	18.8 %	20.0 %	40.0 %	40.0 %	50.0 %	50.0 %	0.0 %

T8-L2	81.8 %	18.2 %	0.0 %	37.5 %	43.8 %	18.8 %	0.0%	100.0 %	0.0 %	33.3 %	50.0 %	16.7 %
L5-S	63.6 %	27.3 %	9.1 %	50.0 %	43.8 %	6.3 %	40.0 %	60.0 %	0.0 %	33.3 %	66.7 %	0.0 %

Volume RMS -Right

	Control (n=11)			Active (n=16)			P. Resp (n=5)			C. Resp (n=6)		
	Dec	**Inc**	**NC**	**Dec**	**Inc**	**NC**	**Dec**	**Inc**	**NC**	**Dec**	**Inc**	**NC**
Initial to Final	100.0 %	0.0 %	0.0 %	81.3 %	18.8 %	0.0 %	40.0 %	60.0 %	0.0 %	66.7 %	33.3 %	0.0 %
OA-C2	81.8 %	18.2 %	0.0 %	50.0 %	43.8 %	6.3 %	20.0 %	60.0 %	20.0 %	50.0 %	50.0 %	0.0 %
T1-T4	63.6 %	18.2 %	18.2 %	50.0 %	31.3 %	18.8 %	20.0 %	40.0 %	40.0 %	50.0 %	50.0 %	0.0 %
T8-L2	54.5 %	18.2 %	27.3 %	43.8 %	50.0 %	6.3 %	0.0%	100.0 %	0.0 %	50.0 %	50.0 %	0.0 %
L5-S	72.7 %	27.3 %	0.0 %	50.0 %	50.0 %	0.0 %	20.0 %	80.0 %	0.0 %	16.7 %	83.3 %	0.0 %